DUPLO Deliverable D4.2

Radio resource management and protocol solutions for full-duplex systems

Project Number:	**316369**
Project Title	**Full-Duplex Radios for Local Access – DUPLO**
Deliverable Type:	**PU**

Contractual Date of Delivery:	**April 30, 2015**
Actual Date of Delivery:	**May 22, 2015**
Editor(s):	**Jawad Seddar (TCS)**
Author(s):	**Ari Pouttu, Ali Cirik, Hirley Alves, Carlos Lima, Kari Rikkinen (UOULU); Mir Ghoraishi, Mohammed Al-Imari (UniS); Hicham Khalife, Jawad Seddar (TCS)**
Workpackage:	**WP4**
Estimated person months:	**38**
Security:	**PU**
Nature:	**Report**
Version:	**1.0**

Abstract: This deliverable provides description of algorithms and protocols for full-duplex operation in small area wireless networks. Different wireless network scenarios are covered, including point-to-point connection, single radio cell, multi-cell network, relaying and mobile ad-hoc network. Developed solutions for hybrid full-duplex and half-duplex operation are also reported.

Keyword list: full-duplex, scheduling, power control, radio resource management, protocols

Executive Summary

This deliverable focuses on system level protocols and algorithms for full-duplex. Several aspects are covered in the eight chapters that compose this deliverable.

Chapter 2 focuses on the single full duplex link case. The achievable rate region is analysed by taking into account the transceiver's non-idealities. Algorithms for rate maximization are derived with either uniform or non-uniform power allocation. A discussion on power allocation policies completes the chapter.

In chapter 3, the discussion focuses on single cell deployments. First, a beamformer design is proposed and algorithms for spectral efficiency maximization are derived. Then, the discussion focuses on scheduling algorithms, power allocation strategies and co-channel interference in full-duplex networks. Hybrid full duplex/half duplex systems as well as full duplex only systems are covered in the studies. The MIMO case with half duplex user equipment is also considered. The chapter ends by considering user selection for device to device communication in cellular networks.

Chapter 4 analyses multi-cell deployment scenarios. This chapter analyses both the SISO and MIMO cases and focuses on full duplex user equipment deployments.

Chapter 5 focuses on relaying in full-duplex. It analyses different relaying schemes such as full duplex dual hop and full duplex joint decoding and derives the outage probabilities in both cases. A network level analysis provides a relay selection algorithm as well as a formulation of the steady state throughput.

Chapter 6 provides an analysis of full duplex in MANETs. In this chapter, a MAC protocol for full duplex MANETs is derived and discussions on routing strategies and control plane design complete the chapter.

Chapter 7 discusses the main results and conclusions, and finally chapter 8 enlists the referred biography.

Authors

Partner	Name	Email
UOULU	Ari Poutttu	apo@ee.oulu.fi
	Ali Cirik	acirik@ee.oulu.fi
	Hirley Alves	halves@ee.oulu.fi
	Carlos Lima	carlosl@ee.oulu.fi
	Kari Rikkinen	krikkine@ee.oulu.fi
UNIS	Mir Ghoraishi	M.Ghoraishi@surrey.ac.uk
	Mohammed Al-Imari	m.al-imari@surrey.ac.uk
TCS	Hicham Khalife	hicham.khalife@thalesgroup.com
	Jawad Seddar	jawad.seddar@thalesgroup.com

Table of Contents

Abbreviations

AWGN	Average White Gaussian Noise
BER	Bit Error Rate
BS	Base Station
CCI	Co-Channel Interference
CDF	Cumulative Distribution Function
CP	Cyclic Prefix
CSI	Channel State Information
CTS	Clear To Send
D2D	Device To Device
DC	Difference of Convex
DL	Downlink
DUPLO	full-DUPlex radios for LOcal access
EVM	Error Vector Magnitude
FD	Full Duplex
FDD	Frequency Division Duplex
FDDH	Full Duplex Dual Hop
FDJD	Full Duplex Joint Decoding
FW	Frank Wolfe algorithm
HD	Half Duplex
IWF	Iterative WaterFilling
KKT	Karush-Kuhn-Tucker
LN	Log Normal
LTE	Long Term Evolution
MAC	Medium Access Control
MAXDET	DETerminant MAXimization
MIMO	Multiple Input Multiple Output
MMSE	Minimum Mean Square Error
MMSE-SIC	Minimum Mean Square Error Successive Interference Cancellation
NAV	Network Allocation Vector
OFDM	Orthogonal Frequency Division Multiplexing
OFDMA	Orthogonal Frequency Division Multiple Access
PDF	Probability Density Function

PPP	Poisson Point Process
QoS	Quality of Service
RF	Radio Frequency
RSA	Relay Selection Algorithm
RTS	Request To Send
RV	Random Variable
SDP	SemiDefinite Program
SDR	SemiDefinite Relaxation
SE	Spectral Efficiency
SEMax	Spectral Efficiency Maximization
SI	Self-Interference
SIC	Self-Interference Cancellation
SINR	Signal to Interference plus Noise Ratio
SIR	Signal to Interference Ratio
SISO	Single Input Single Output
SNR	Signal to Noise Ratio
SPCA	Sequential Parametric Convex Approximation
STA	Standard Tree Algorithm
TCP	Transmission Control Protocol
TDD	Time Division Duplex
UDP	User Datagram Protocol
UE	User Equipment
UL	Uplink
WMMSE	Weighted Minimum Mean Square Error
WSR	Weight Sum Rate

1. INTRODUCTION

Full-duplex (FD) technology offers the opportunity to increase the two-way traffic rate in wireless communications by enabling simultaneous transmission and reception on the same carrier frequency, but it also sets many challenges for implementing wireless transceivers. One of the main challenges regards the self-interference (SI) caused by the full-duplex transceiver communicating on both the uplink and downlink directions simultaneously. Provided that this self-interference can be significantly suppressed, full-duplex transceivers can nearly double their two-way traffic rate in ideal cases.

In order to mitigate the strong self-interference, many recent full-duplex transceiver designs consider hybrid approaches. To begin with, improved antenna isolation reduces the power level of the received self-interference. In addition, feed-forward circuits between the output of the power amplifier at the transmitter-side along with the input of the low noise amplifier (LNA) at the receiver-end further reduce the self-interference so that the LNA is not saturated by the received signal power exceeding its dynamic range. Finally, digital self-interference cancellation at the receiver baseband removes the remaining self-interference and optimizes the detector performance. Motivated by many promising results that have been obtained using these approaches, e.g., [82] and [83], the full-duplex technology is further investigated as a potential candidate for the 5G communication systems in DUPLO project.

This deliverable summarizes our radio resource management and protocol studies in WP4 of the DUPLO project. In the rest of this chapter, we first give a brief overview of the DUPLO project, then review the state-of-the-art literature and identify relevant results to WP4 studies, as well as outline the document structure.

1.1. DUPLO project overview

Different from previous contributions in full-duplex technology development, the DUPLO project focuses not only on the design of full-duplex radios but also on their operation in practical system deployments by considering realistic conditions and constraints. And yet different solutions to obtain an operational validation platform are considered here as well.

In the DUPLO project, there are 5 technical WPs covering different aspects of the full-duplex technology. As the first step of the project, WP1 investigated the application of full duplex in future-oriented mobile wireless communication networks and identified the main design requirements and constraints. Following the recent evolution trend of wireless communication networks, DUPLO identifies small cell and mesh networks as the main areas of interest for the project, which are then further studied within the WP4.

WP2 and WP3 focus on developing the solutions to suppress the self-interference in full-duplex transceivers. In particular, antenna isolation and analog RF cancellation are investigated in WP2, while the digital baseband processing is assessed in WP3. By combining the WP2 and WP3 outputs, a robust implementation for full-duplex transceivers will become viable. In addition, the non-ideality problem of such transceivers will be investigated in WP2, while baseband solutions to compensate for this non-ideality will be developed in WP3.

WP4 focuses on evaluating how full-duplex systems perform with respect to distinct radio resource management solutions. Specifically, we assess the benefits and attainable gains of using full-duplex transceivers at different network nodes, develop interference and radio resource management

strategies and protocols for full-duplex transmissions, as well as design networks deployments where half- and full-duplex nodes coexist and share available resources.

WP5 concentrates mainly on developing the proof-of-concept demonstrator. The demonstrator integrates set of antenna, RF and baseband solutions developed in WP2 and WP3 together into a complete full-duplex transceiver. Furthermore, two full-duplex transceivers can be connected together enabling to study full-duplex operation in practice in short transmission link distances.

1.2. Review of the State of the Art

Full-duplex transmission is a potential air interface technology component for future wireless systems, and it has gained considerable attention from academia and industry recently. Versatile overview of recent advances in in full-duplex transceiver technology and system solutions is presented e.g. in [82] and [86]. In this section, a summary of the state-of-the-art with full-duplex system solutions is given, as relevant for the DUPLO WP4 work. More detailed state-of-the-art discussions follow in the later sections focusing on specific solutions.

Simultaneous uplink and downlink transmission introduced with the full-duplex mode results in additional intra-cell and inter-cell interference. Therefore, to achieve the potential gain of the full-duplex mode, an intelligent scheduler to pair the downlink and uplink users with corresponding transmission powers is necessary. Due to the combinatorial nature of pairing multiple uplink and downlink users on each subcarrier, and also the difficulty of optimal power allocation to each subcarrier, resource allocation in full-duplex systems to maximize the performance of the network is very challenging.

A resource allocation algorithm using matching theory to allocate the subcarriers among uplink and downlink users was proposed in [88]. A cell partitioning algorithm to allocate the frequency resources has been proposed in [89]. Both [88] and [89] consider a single cell full-duplex OFDMA system, and the proposed algorithms in these papers cannot be directly applied for full-duplex multi-cell systems. Moreover, in [89] a user can be allocated to only one subcarrier, and thus the transmission power of the uplink users is fixed, and cannot be adjusted. A suboptimal scheduling algorithm that selects the transmission direction of each user in a multi-cell scenario was proposed in [18]. In this system, interference from the users of neighboring cells is ignored. A hybrid scheduler that can switch between full-duplex and half-duplex mode has been proposed in [17] for the single small-cell scenario. The power allocation has not been considered in both [18] and [17]. A user pairing algorithm has been proposed in [90] for the multi-cell FD system without taking the interference from the neighboring cell users into account, which makes the resource allocation problem easier. Moreover, although the transmission power of the uplink users can ben adjusted, the transmission power of the base-stations is assumed to be fixed in [90].

In the last decade, cooperative diversity re-emerged as a viable solution to increase energy efficiency, reliability and diversity to single antenna devices [69]-[71]. However, most of the research focused on half-duplex (HD) schemes, which are inherently spectrally inefficient. But with the advances on FD transceiver design, FD relaying has received more attention of the academy and industry in the recent years [3]-[5], [11], [40], [72]-[85]. In this context, FD relaying deals not only with multiplexing loss of HD protocols, but at the same time promotes increased link capacity and opens new ways to reuse the spectrum [82],[83].

Differently form the HD case, in FD mode whole process occurs within one single time/frequency slot, and therefore spectrally efficient [69], [71]. In the first phase of FD protocol, namely broadcast phase, the source broadcasts its message to relay and destination. Differently from HD cooperative

schemes, the multiple access phase starts simultaneously with the broadcast phase under the FD mode, in which the relay forwards the received message to the destination [5], [71], [72]-[74].

Performance analysis of distinct FD protocols are also investigated in [5], [72]-[75] as well as in [10]-[11], [40], [76]-[81]. Additionally, [72]-[73] provide an extensive comparison between HD and FD schemes. The authors compare FD decode-and-forward (DF) (where the relay decodes/re-encodes then forward) scheme to the state-of-the-art on HD DF relaying, which are the methods that associate repetition coding with HARQ strategies. Still, [40], [75], [79] deal with FD amplify-and-signal (AF) (relay amplifies the signal and then forwards) relaying, from performance analysis to power allocation and self-interference mitigation. For instance, [40] provides a performance analysis of a gain control scheme, which maximizes the SINR with reduced the transmit power. Then [79] shows that, when the direct link is accounted as a useful source of information rather than interference, performance enhances and that such scheme achieves diversity order of one. We recall that due to self-interference FD relaying suffers from zero diversity order. In order to tackle such issue the authors in [11] propose a hybrid relaying scheme, where the FD relay is able to switch modes from FD to HD given the network constraints. Extending this idea the authors in [80] consider also multiple FD relays under AF protocol, such that the best relay is opportunistically chosen to cooperate in either FD or HD fashion depending on some network constraints. In [81] the authors propose a self-interference cancellation scheme that allows FD relays to achieve diversity order greater than zero due to a block based relaying strategy, which brings time diversity enhancement over independent fading realizations. Furthermore, in [76] and [5] models the residual self-interference through general fading distributions. Both works assess the impact of distinct channel parameters on the performance of a FD cooperative protocol.

Moreover, one common conclusion amongst those works is that it is possible to achieve high performance even in the presence of strong self-interference [3], [10]-[11], [40], [72]-[85], which means that FD communication is feasible. All in all, given that the FD node is able to considerably attenuate the self-interference for (more than 70 dB), FD relaying communication becomes feasible.

When considering MANETs, it is quite hard to find any literature related to FD in these types of networks. This was to anticipate as FD is still in early stages and MANET use cases may have been too high level to study until now. When considering MAC protocols, a few papers address the FD case. In [91] a bidirectional FD MAC protocol is introduced. In this case, only two nodes are involved in the communication which begins in HD mode. In [92] and [93], relay FD MAC protocols are studied. These enable a three node communication setup with the middle node acting as a relay operating in FD mode. In that case, algorithms based on traffic monitoring are used in order to find and schedule FD transmissions based on neighbor tables.

In our work, we chose to base our MANET study on a bidirectional FD MAC protocol and decided to use an alternative solution to the one described in [91].

1.3. The document structure

The description of developed algorithms and protocols for full-duplex transmission is organised in this document according network deployment scenarios, as follows.

Chapter 2 focuses on the single full duplex link case. The achievable rate region is analysed by taking into account the transceiver's non-idealities. Algorithms for rate maximization are derived with either uniform or non-uniform power allocation. A discussion on power allocation policies completes the chapter.

Chapter 3 focuses on single cell deployments. First, a beamformer design is proposed and algorithms for spectral efficiency maximization are derived. Then, the discussion focuses on scheduling algorithms, power allocation strategies and co-channel interference in full-duplex networks. Hybrid full duplex/half duplex systems as well as full duplex only systems are covered in the studies. The MIMO case with half duplex user equipment is also considered. The chapter ends by considering user selection for device to device communication in cellular networks.

Chapter 4 analyses multi-cell deployment scenarios. This chapter analyses both the SISO and MIMO cases and focuses on full duplex user equipment deployments.

Chapter 5 focuses on relaying in full-duplex. It analyses different relaying schemes such as full duplex dual hop and full duplex joint decoding and derives the outage probabilities in both cases. A network level analysis provides a relay selection algorithm as well as a formulation of the steady state throughput.

Chapter 6 provides an analysis of full duplex in MANETs. In this chapter, a MAC protocol for full duplex MANETs is derived and discussions on routing strategies and control plane design complete the chapter.

Chapter 7 discuss the main results and conclusions. Then, references are listed in chapter 8.

2. SINGLE FULL-DUPLEX LINK

2.1. Rate Regions

In this section, we analyze the performance of a full-duplex bi-directional link by taking the transceiver non-ideality into account. We assume that cyclic prefix (CP) assisted OFDM technique has been used by the two-way transmission in our analysis. In practical systems, the non-ideality is usually captured by a measure named as the error vector magnitude (EVM) level. In [48], it was shown that the impact of transceiver non-ideality is similar to the noise added at the transmitter. To simplify the link performance analysis in our study, we take the conclusion of [48] and approximate the non-ideality as a transmitter noise added at the transmitter in a way similar to [49]. The noise has average power proportional to that of the original signal, which is called as the EVM noise in [50] and [51]. Self-interference cancellation is performed in three stages: 1) antenna isolation, 2) RF cancellation, and 3) digital baseband cancellation. In the former two stages the original signal and EVM noise can be suppressed equally but in the third stage the SI due to EVM noise cannot be cancelled any further. Main findings and key results of these papers are summarized D4.1.2.

2.1.1. Error Vector Magnitude Modelling

Practical transceiver implementations suffer from several non-idealities. Such imperfections may result from cascaded effect of signal IQ-imbalances, phase noise of local oscillators, amplifier non-linearities, amplitude distortion, etc. impairments in a realistic hard- and software implementation. All these non-idealities mean that actual signal constellation points deviate from their intended locations. One commonly used metric to quantify such deviation is the error vector magnitude (EVM) level. EVM level limits the achievable signal-to-noise ratio (SNR) of a practical link. Many standards have specified the minimum requirements for EVM. 3GPP has given a requirement that BS should keep the EVM level below 8% for 64-QAM modulation [52]. This corresponds to a SNR about 22 dB. Note that more advanced transceiver designs are required to achieve EVM levels about 30 to 40 dB lower than that of the original signal.

2.1.2. Rate Region With Uniform Power Allocation

The first power allocation strategy allows low complexity design where the same power is allocated on each sub-carrier in each node. When each sub-carrier has uniform power allocation, i.e., consumed energy on sub-carrier is $\varepsilon_i[k] = \varepsilon_i$, the full-duplex link rates can be expressed as

$$r_1(\varepsilon_1,\varepsilon_2)=\sum_{k=1}^{K}\log_2\left(1+\frac{\varepsilon_1\gamma_{\mathrm{E}}\left|h_{21}[k]\right|^2}{\varepsilon_1\left|h_{21}[k]\right|^2+\gamma_{\mathrm{E}}\varepsilon_2\left|h_{22}[k]\beta_2[k]\right|^2+\varepsilon_2\left|h_{22}[k]\right|^2+K(\gamma_{\mathrm{E}}+1)N_2}\right),$$
$$r_2(\varepsilon_1,\varepsilon_2)=\sum_{k=1}^{K}\log_2\left(1+\frac{\varepsilon_1\gamma_{\mathrm{E}}\left|h_{21}[k]\right|^2}{\varepsilon_2\left|h_{12}[k]\right|^2+\gamma_{\mathrm{E}}\varepsilon_1\left|h_{11}[k]\beta_1[k]\right|^2+\varepsilon_1\left|h_{11}[k]\right|^2+K(\gamma_{\mathrm{E}}+1)N_1}\right) \quad (2.1.2.1)$$

where k is the sub-carrier index, $h_{ji}[k]$ is the channel coefficient of the link from node i to node j, γ_{E} is the average SNR due to transmitter EVM limitation, $\beta_i[k]$ is the attenuation factor due to baseband self-interference (SI) cancellation and N_i is the Gaussian noise. So, in the fraction parts of (2.1.2.1) the dividend terms correspond to the desired signals whereas the divisor terms are due to Tx EVM,

signal SI cancellation, EVM SI cancellation and noise, respectively. Similar expressions can be derived for half-duplex link rates as shown in [50] and [51].

Using (2.1.2.1), the following algorithm leads to rate maximization.

ALGORITHM 1. Calculating maximum rate r_2^* under a target rate constraint in full-duplex link.

1: Set $\varepsilon_1^* = E_1/K$, $\varepsilon_2^* = E_2/K$.

2: For given ε_1^*, ε_2^*, calculate r_1, r_2 via (2.1.2.1).

3: If $r_1 = R_1$, set $r_2^* = r_2$ and stop.

4: If $r_1 \leq R_1$, reduce ε_2^* via bisection method until r_1 converges to a value satisfying $r_1 = R_1$. After that, calculate the new r_2^* accordingly and stop.

5: If $r_1 > R_1$, reduce ε_1^* via bisection method until r_1 converges to a value satisfying $r_1 = R_1$. After that, calculate the new r_2^* accordingly and stop.

2.1.3. Rate Region With Non-uniform Power Allocation

To find the rate region for a full-duplex bi-directional link with non-uniform power allocation, we first define a quadratic augmented utility function as $\theta_\mu(r_1,r_2) = r_2 - \mu(r_1 - R_1)^2$, where μ is a negative penalty coefficient. By using this utility function, a new optimization problem can be formulated as

$$\begin{aligned} \underset{\boldsymbol{\varepsilon}_1,\boldsymbol{\varepsilon}_2}{\text{maximize}} \quad & \theta_\mu(r_1,r_2) \\ \text{subject to} \quad & \sum_k \varepsilon_1[k] \leq E_1 \\ & \sum_k \varepsilon_2[k] \leq E_2 \end{aligned} \quad , \qquad (2.1.3.1)$$

where E_1 and E_2 are the maximum energies that can be consumed by nodes 1 and 2, respectively.

Again, the maximum rate calculation is attained with the next algorithm.

ALGORITHM 2. Maximum rate calculation via penalty method in full-duplex link.

1: Initialization: Set the loop index $l = 0$, the penalty factor $\mu = 1$, the step size $\alpha = 1$ and $\varepsilon_1[k] = \varepsilon_2[k] = 0$ for all subcarriers.

2: Solve problem (2.1.3.1) via sub-gradient method until it converges to a locally optimal value.

3: If l is less than a given number, do update $l = l + 1, \mu = 10\mu$, then go to Step 2.

4: Otherwise, stop and give the final output as $\varepsilon_1^*[k], \varepsilon_2^*[k], r_2^*$.

2.2. Power allocation polices

It is considerably important to investigate the accommodation of asymmetric traffic in full-duplex networks. We have done analysis of the full-duplex transmission link and provision of an asymmetric traffic accommodation scheme using the cross-layer approach. The proposed approach exploits the underlying physical layer characteristics, i.e. signal-to-interference-plus-noise ratio (SINR) and network layer transmission buffer. The proposed model takes the advantage of imperfection in the cancellation algorithms to accommodate asymmetric traffic between uplink and downlink in the presence of SI.

In a full-duplex transmission, the assigned frequency resource is fixed for both downlink and uplink. If the traffic increases in the downlink, the base-station cannot allocate more resource even when the uplink resource is sufficiently large for the current uplink traffic volume. To achieve efficient asymmetric traffic accommodation, the system needs to increase the downlink transmission rate. One way to increase the transmission rate without allocating more resources is to increase the power that will result in high SINR, providing an opportunity to transmit more bits per symbol by using a higher modulation scheme. As illustrated in Figure 1, during the full-duplex transmission, the SINR at each node depends not only on the transmit power at the other end of the link, but also the collocated transmitter power. This is because the SI level in the full-duplex receiver is a function of its own transmits power (among other factors). It is noted that a full-duplex receiver employs mechanism to cancel SI as much but still a residual SI remains. The dependency of SINR on the transmit power at both link ends creates the opportunity to adjust the SINR on each node according to the traffic demand, and thereby the transmission rate, at both ends. The proposed scheme exploits the dependency of SINR on the collocated transmitter power to accommodate the asymmetric traffic in the downlink and uplink to maximize the SINR of downlink satisfying minimum quality-of-service (QoS) requirements for uplink. From a link perspective, power control can be seen as a mean to control SINR of both downlink and uplink jointly and to compensate for channel variations. This also depends on the transmission rate requirements of the service in question.

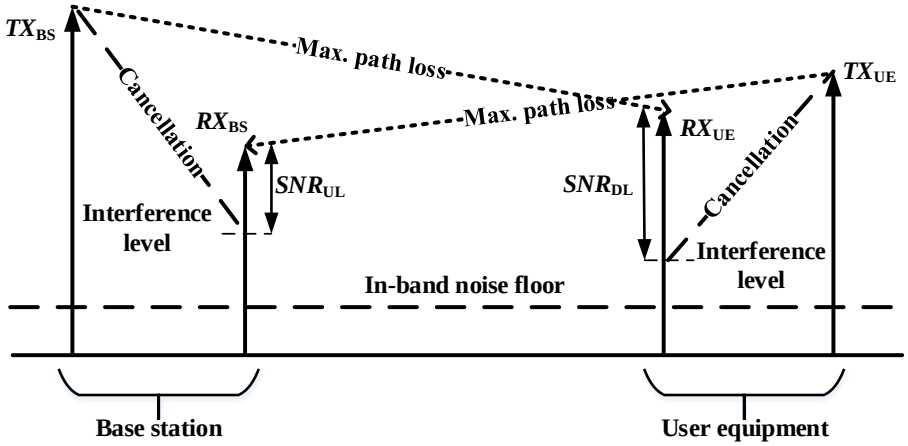

Figure 1: Power level in full-duplex link budget

The objective of the algorithm is to allocate transmit powers to both downlink and uplink. The target is to maximize the downlink SINR, γ_{DL}, with respect to the uplink SINR threshold '*T*'. In this work, a utility function is not only used to adapt the power consumption and service quality efficiently, but also serve as a means of accommodating asymmetric downlink and uplink traffic by minimizing the under-

utilization of resources. Since the full-duplex link uses the same frequency band for downlink and uplink, they mutually interfere with each other.

The base-station and user equipment transmit powers are P_{BS} and P_{UE} respectively. The channel loss at both downlink and uplink is characterized by $g_o > 1$. It is assumed that efficient cancellation is employed to suppress the SI at each link end. The achieved SI cancellation at base-station and user equipment is denoted as SI_{BS} and SI_{UE} respectively. Furthermore, there can be many different QoS constraints depending on the specific applications like voice, video or internet traffic. Thus, depending on the specific application, the proposed algorithm must guarantee the required throughput, latency and fairness.

The objective is to find the appropriate power and rate allocation and the problem can be formulated as:

$$\underset{P_{BS}}{maximize}\ \gamma_{DL} = P_{BS} - g_0 - (P_{UE} - SI_{UE}) \tag{2.2.1}$$

Subject to

$$0 \leq P_{BS} \leq P_{BSmax} \tag{2.2.2}$$

$$0 \leq P_{UE} \leq P_{UEmax} \tag{2.2.3}$$

$$\gamma_{UL} = P_{UE} - g_0 - (P_{BS} - SI_{BS}) \geq \mathrm{T} \tag{2.2.4}$$

The constraints in (2.2.2) and (2.2.3) specify the valid power ranges for base-station and user equipment in the presence of SI cancellation respectively. The constraint in (2.2.4) specifies the minimum uplink SINR, γ_{UL}, required to have an error free communication between user equipment and base-station. The solution of problem in (2.2.1) is called the optimal power allocation. The objective is to find the optimal power allocation that maximizes the downlink SINR subject to the constraints given by the optimization problem. It is a constrained and multivariable problem.

Power Allocation: Let *F* denotes the feasible region, where for each point (*a, b*) in *F*, there exists a corresponding SINR for downlink and uplink satisfying (2.2.1), (2.2.2), (2.2.3) and (2.2.4). Point (*a, b*) represents P_{BS} and P_{UE} respectively. Figure 2 illustrates the geometry of *F* for the utility function given in (2.2.1) and evaluates the optimal solution for different system parameters with the help of simplex method.

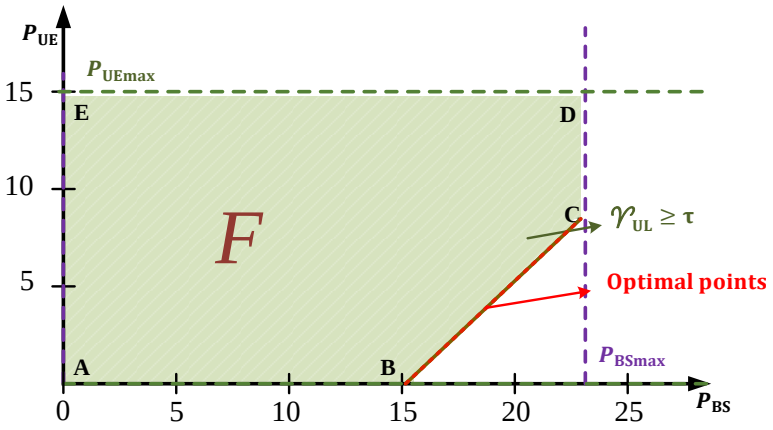

Figure 2: Feasible region 'F': go=70 dB, T =5dB, SIBS=90dB and SIUE=70dB

The simplex method works by finding a feasible initial point, and then moving from that point to any vertex of the feasible set that improves the utility function. Let's choose point A (0, 0) as a starting point, the utility function gives ϒUL= 20 dB and ϒDL = 0 dB. From this point, we can either move to point B (15, 0) or point E (0, 15). At Point B (15, 0) the utility function decrease for ϒUL = 5 dB and increase for ϒDL = 15 dB, while point E (0, 15) increases ϒUL = 35 dB and decrease ϒDL = 15 dB. Since point B provides an improvement, we will select it as our first iteration. At this point, the value of ϒDL increases from 0 dB to 15 dB, while ϒUL = 5 dB remains within the threshold constraint.

From point B, we check whether a move to point C (23, 8) is advantageous, we know that moving back to A is not. At Point C (23, 8) the utility function gives ϒUL = 5 dB and ϒDL = 15 dB, which is same as point B. Now from point C, we again have two options either to move back to Point B or move forward to point D (23, 15). Let's move to Point D and check if there is any more improvement in ϒDL. At Point D, the utility function for ϒDL increases to 12 dB and ϒUL drops to 8 dB. Thus utility function maximizes on the boundary of the feasible region. This means that downlink SINR maximize when the uplink is on lower bound. Thus the optimal solutions exist on the lower boundary of the feasible region.

After the power control converges, the appropriate constellation sizes is chosen according to the SINR value of uplink and downlink which results in maximization of data rates. Table 1 shows the minimum required SINR corresponding to various BER during full-duplex operation based on our results. The detailed analysis is presented in simulation results.

Table 1: Required SINR to achieve BER threshold

BER	Required SINR (dB)
10-1	4.5
10-2	6.5
10-3	7.1

3. RADIO RESOURCE MANAGEMENT IN SINGLE CELL DEPLOYMENTS

This chapter introduces methods and algorithms enabling full-duplex transmission in wireless networks. The focus is in single cell deployment, thus the inter-cell interference management is excluded from these analysis. Firstly, a beamformer design solution for spectral efficiency maximization is introduced. Then, discussion focuses on scheduling algorithms, co-channel interference and power control solutions in single cell full-duplex network. Potential solutions for multiple antenna and device-to-device scenarios are also investigated. The considered operation scenarios follow the target scenarios identified in D1.1 [53].

3.1. Spectral Efficiency and Beamformer Design

Following the generic scenario illustrated in Figure 3, full-duplex capable base station (BS) is assumed to operate with multiple half-duplex users on the same system resources. The main challenges in the design are the self-interference (SI) due to FD and co-channel interference (CCI) due to multiple users transmitting at the same time. In FD systems SI and CCI problem between up- and downlink is coupled. Therefore, the best solution is to optimize both link directions jointly. Thus, the main objective here is to propose a joint beamformer design approach, which accounts for the downlink and uplink simultaneously. The problem of interest is to maximize total system spectral efficiency (SE) under some power constraints. Dirty paper coding is known to be optimal downlink transmission strategy [54] but it has high complexity. As a result we adopt lower complexity linear beamforming technique for downlink design. For the uplink we adopt minimum mean square error and successive interference cancellation (MMSE-SIC) that is optimal nonlinear multi-user scheme [54][21]. Figure 3 below depicts the assumed system model in the study. The number of transmit and receive antennas at the BS are N_T and N_R, respectively.

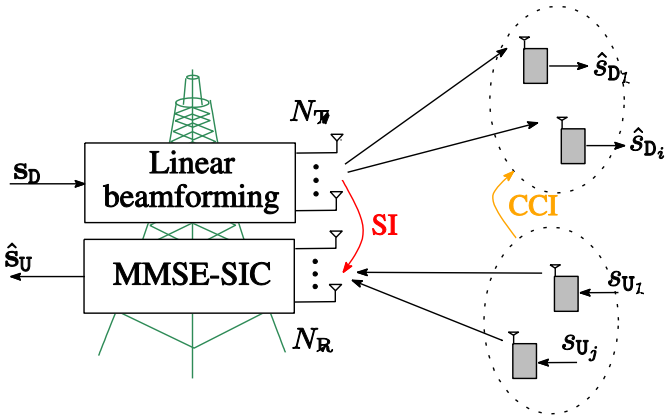

Figure 3: Illustration of the multi-user small cell scenario in full-duplex wireless systems.

Total spectral efficiency maximization (SEMax) problem is first formulated as a rank-constrained optimization. In general, it is difficult to find globally optimal solution for such a problem. The standard method of rank relaxation can then be applied but the problem still remains non-convex. After solving the relaxed problem, the randomization technique presented in [55] is applied to find the beamformers for the original design problem. We note that the rank relaxation technique, commonly known as semidefinite relaxation (SDR) method under various contexts, is widely used to solve the problem of linear precoder design in MIMO downlink channels, e.g., in [55]–[60]. Very often, the relaxed problems in those cases are convex and general convex program solvers can be employed to find the solutions. Moreover, in some special cases, the rank relaxation is proved to be tight [61], [58], and [60]. Unfortunately, the same property is not applicable to the case under consideration here.

To resolve the nonconvexity of the relaxed problem, we resort to two iterative local optimization algorithms. The first one is a direct result of exploiting the "difference of convex" (DC) structure of the relaxed problem. More specifically, by utilizing the idea of the Frank-Wolfe (FW) algorithm [62], a determinant maximization (MAXDET) program at each iteration can be formulated. The second approach involves some transformations before invoking the framework of sequential parametric convex approximation (SPCA) method [63], which has proved to be an effective tool for numerical solutions of nonconvex optimization problems [63]–[65]. In particular, we are able to approximate the relaxed problem as a semidefinite program (SDP) at each iteration of the second iterative algorithm. While the first design algorithm sticks to MAXDET problem solvers, the second one offers more flexibility in choosing optimization software and can take advantage of many state-of-the-art SDP solvers. Additionally, since there is no (even rough) way to estimate beforehand which algorithm is better than the other for a given set of channel realizations, the two iterative algorithms can be implemented in a concurrent manner and a solution is obtained when one of them terminates. Alternatively, we run the two algorithms in parallel until they converge, and then select the better solution.

Full-duplex transmission, if successfully implemented, is clearly expected to improve the spectral efficiency of the wireless communications systems. However, a quantitative answer on how much the potential gains are for some particular scenarios is still missing. For this purpose, the proposed algorithms are used to evaluate the performance of the full-duplex system of consideration under the 3GPP LTE specifications for a small cell system. The numerical experiments in D4.1.2 [68] demonstrate that small cell full-duplex transmissions are superior to the conventional half-duplex one as the self-interference power is efficiently cancelled.

3.1.1. Proposed algorithms

This section describes the two investigated algorithms toward FD system spectral efficiency maximization. Only the main optimization problems and the related steps carried out in the proposed algorithms are shown and the remaining technical details can be found from [67].

The optimization problem can be formulated as

$$\underset{\{\mathbf{Q}_{\mathrm{D}_i}\},\{q_{\mathrm{U}_j}\}}{\text{maximize}} \quad R_{\mathrm{D}} + R_{\mathrm{U}} \tag{3.1.1.1}$$

$$\text{subject to} \quad 0 \le q_{\mathrm{U}_j} \le \bar{q}_{\mathrm{U}_j}, \forall j = 1,\ldots,K_{\mathrm{U}}, \tag{3.1.1.2}$$

$$\sum_{i=1}^{K_{\mathrm{D}}} \mathrm{Tr}\left(\mathbf{Q}_{\mathrm{D}_i}\right) \le P_{\mathrm{BS}}, \tag{3.1.1.3}$$

$$\mathbf{Q}_{\mathrm{D}_i} \succeq 0, \forall i = 1,\ldots,K_{\mathrm{D}}, \tag{3.1.1.4}$$

$$\mathrm{rank}\left(\mathbf{Q}_{\mathrm{D}_i}\right) = 1, \forall i = 1,\ldots K_{\mathrm{D}}, \tag{3.1.1.5}$$

where downlink SE R_{D} and uplink SE R_{U} are defined as

$$R_D = \sum_{i=1}^{K_{\mathrm{D}}} \log\left(1+\gamma_{\mathrm{D}_i}\right) = \sum_{i=1}^{K_{\mathrm{D}}} \log\left(\frac{\sigma_n^2 + \sum_{k=1}^{K_{\mathrm{D}}} \mathbf{h}_{\mathrm{D}_i}^H \mathbf{Q}_{\mathrm{D}_k} \mathbf{h}_{\mathrm{D}_i} + \sum_{j=1}^{K_{\mathrm{U}}} q_{\mathrm{U}_j} \left|g_{ji}\right|^2}{\sigma_n^2 + \sum_{k\neq i}^{K_{\mathrm{D}}} \mathbf{h}_{\mathrm{D}_i}^H \mathbf{Q}_{\mathrm{D}_k} \mathbf{h}_{\mathrm{D}_i} + \sum_{j=1}^{K_{\mathrm{U}}} q_{\mathrm{U}_j} \left|g_{ji}\right|^2}\right) \quad (3.1.1.6)$$

and

$$R_{\mathrm{U}} = \sum_{j=1}^{K_{\mathrm{U}}} \log\left(1+\gamma_{\mathrm{U}_j}\right) = \sum_{j=1}^{K_{\mathrm{U}}} \log\left(1+ q_{\mathrm{U}_j} h_{U_j}^H \left(\sigma_n^2 \mathbf{I} + \sum_{m>j}^{K_{\mathrm{U}}} q_{\mathrm{U}_m} \mathbf{h}_{\mathrm{U}_m} \mathbf{h}_{\mathrm{U}_m}^H + \sum_{i=1}^{K_{\mathrm{D}}} \mathbf{H}_{\mathrm{SI}} \mathbf{Q}_{\mathrm{D}_i} \mathbf{H}_{\mathrm{SI}}^H\right)^{-1} \mathbf{h}_{\mathrm{U}_j}\right) \quad (3.1.1.7)$$

$$= \log \frac{\left|\sigma_n^2 \mathbf{I} + \sum_{i=1}^{K_{\mathrm{D}}} \mathbf{H}_{\mathrm{SI}} \mathbf{Q}_{\mathrm{D}_i} \mathbf{H}_{\mathrm{SI}}^H + \sum_{j=1}^{K_{\mathrm{U}}} q_{\mathrm{U}_j} \mathbf{h}_{\mathrm{U}_j} \mathbf{h}_{\mathrm{U}_j}^H\right|}{\left|\sigma_n^2 \mathbf{I} + \sum_{i=1}^{K_{\mathrm{D}}} \mathbf{H}_{\mathrm{SI}} \mathbf{Q}_{\mathrm{D}_i} \mathbf{H}_{\mathrm{SI}}^H\right|}.$$

Iterative MAXDET-based algorithm

The original optimization problem can be approximated at iteration n+1 as

$$\underset{\mathbf{Q},\mathbf{q}}{\text{maximize}} \quad h(\mathbf{Q},\mathbf{q}) - g^{(n)}(\mathbf{Q},\mathbf{q}) \quad (3.1.1.8)$$

$$\text{Subject to (3.1.1.2), (3.1.1.3), (3.1.1.4)} \quad (3.1.1.9)$$

where $h(\mathbf{Q},\mathbf{q})$ and $g(\mathbf{Q},\mathbf{q})$ are defined as follows

$$h(\mathbf{Q},\mathbf{q}) \overset{\Delta}{=} \log\left|\sigma_n^2 \mathbf{I} + \sum_{i=1}^{K_{\mathrm{D}}} \mathbf{H}_{\mathrm{SI}} \mathbf{Q}_{\mathrm{D}_i} \mathbf{H}_{\mathrm{SI}}^H + \sum_{j=1}^{K_{\mathrm{U}}} q_{\mathrm{U}_j} \mathbf{h}_{\mathrm{U}_j} \mathbf{h}_{\mathrm{U}_j}^H\right| + \sum_{i=1}^{K_{\mathrm{D}}} \log\left(\sigma_n^2 + \sum_{k=1}^{K_{\mathrm{D}}} \mathbf{h}_{\mathrm{D}_i}^H \mathbf{Q}_{\mathrm{D}_i} \mathbf{h}_{\mathrm{D}_i} + \sum_{j=1}^{K_{\mathrm{U}}} q_{\mathrm{U}_j} \left|g_{ji}\right|^2\right), \quad (3.1.1.10)$$

$$g(\mathbf{Q},\mathbf{q}) \overset{\Delta}{=} \sum_{i=1}^{K_{\mathrm{D}}} \log\left(\sigma_n^2 + \sum_{k\neq 1}^{K_{\mathrm{D}}} \mathbf{h}_{\mathrm{D}_i}^H \mathbf{Q}_{\mathrm{D}_i} \mathbf{h}_{\mathrm{D}_i} + \sum_{j=1}^{K_{\mathrm{U}}} q_{\mathrm{U}_j} \left|g_{ji}\right|^2\right) + \log\left|\sigma_n^2 \mathbf{I} + \sum_{i=1}^{K_{\mathrm{D}}} \mathbf{H}_{\mathrm{SI}} \mathbf{Q}_{\mathrm{D}_i} \mathbf{H}_{\mathrm{SI}}^H\right|, \quad (3.1.1.11)$$

$g^{(n)}(\mathbf{Q},\mathbf{q})$ is an affine majorization of $g(\mathbf{Q},\mathbf{q})$, $\bar{q}_{\mathrm{U}_j}$ is the power constraint at each user in the uplink channel, K_{U} is the number of single-antenna uplink users, K_{D} is the number of single-antenna downlink users and P_{BS} is the maximum transmission power of the small cell BS. Note that $h(\mathbf{Q},\mathbf{q})$ and $g(\mathbf{Q},\mathbf{q})$ are jointly concave functions with respect to $\mathbf{Q}$ and $\mathbf{q}$ (that are symbolic notations denoting the set of design variables $\{\mathbf{Q}_{\mathrm{D}_i}\}$ and $\{q_{\mathrm{U}_j}\}$, respectively).

This optimization problem is then applied in the following algorithm.

ALGORITHM 3. Iterative MAXDET-based algorithm.

Initialization:

1: Generate initial values for $\mathbf{Q}_{\mathrm{D}_i}^{(0)}$ for i = 1, 2, …, K_{D} and $q_{\mathrm{U}_j}^{(0)}$ for i = 1, 2, …, K_{U}.

2: Set $n := 0$.

Iterative procedure:

3: **repeat**

4: Solve (3.1.1.8)-(3.1.1.9) and denote the optimal solutions as $(\mathbf{Q}^*, \mathbf{q}^*)$.

5: Update: $\mathbf{Q}_{\mathrm{D}_i}^{(n+1)} := \mathbf{Q}_{\mathrm{D}_i}^*$; and $q_{\mathrm{U}_j}^{(n+1)} := q_{\mathrm{U}_j}^*$.

6: Set $n := n + 1$.

7: **until** Convergence.

Finalization:

8: Perform randomization to extract a rank-1 solution if required.

Iterative SDP-based algorithm

Since the solvers for MAXDET programs are quite limited we would next resort to iterative semidefinite program (SDP) based approach. The SDP-based algorithm tackles the convex approximate problem at iteration n+1 by following this mathematical formulation

$$\underset{\mathbf{Q},\mathbf{q},\mathbf{t}_{\mathrm{D}},\mathbf{t}_{\mathrm{U}},\beta_{\mathrm{D}},\mathbf{x}_{\mathrm{U}}}{\text{maximize}} \quad \prod_{i=1}^{K_{\mathrm{D}}} t_{\mathrm{D}_i} \prod_{j=1}^{K_{\mathrm{U}}} t_{\mathrm{U}_j} \tag{3.1.1.12}$$

$$\text{subject to} \quad F\left(t_{\mathrm{D}_i}, \beta_{\mathrm{D}_i}, \psi_{\mathrm{D}_i}^{(n)}\right) \le \sigma_n^2 + \sum_{k=1}^{K_{\mathrm{D}}} \mathbf{h}_{\mathrm{D}_i}^H \mathbf{Q}_{\mathrm{D}_k} \mathbf{h}_{\mathrm{D}_i} + \sum_{j=1}^{K_{\mathrm{U}}} q_{\mathrm{U}_j} \left|g_{ji}\right|^2, \forall i = 1,\ldots K_{\mathrm{D}}, \tag{3.1.1.13}$$

$$G\left(x_{\mathrm{U}_j}, \mathbf{Q}, \mathbf{q}, x_{\mathrm{U}_j}^{(n)}, \mathbf{Q}^{(n)}, \mathbf{q}^{(n)}\right) \le 1 - t_{\mathrm{U}_j}, \forall j = 1,\ldots K_{\mathrm{U}}, \tag{3.1.1.14}$$

$$\sigma_n^2 + \sum_{k\neq 1}^{K_{\mathrm{D}}} \mathbf{h}_{\mathrm{D}_i}^H \mathbf{Q}_{\mathrm{D}_k} \mathbf{h}_{\mathrm{D}_i} + \sum_{j=1}^{K_{\mathrm{U}}} q_{\mathrm{U}_j} \left|g_{ji}\right|^2 \le \beta_{\mathrm{D}_i}, \forall i = 1,\ldots, K_{\mathrm{D}}, \tag{3.1.1.15}$$

$$q_{\mathrm{U}_j} \ge x_{\mathrm{U}_j}^2, \forall j = 1,\ldots, K_{\mathrm{U}}, \tag{3.1.1.16}$$

$$0 \le q_{\mathrm{U}_j} \le \bar{q}_{\mathrm{U}_j}, \forall j = 1,\ldots, K_{\mathrm{U}}, \tag{3.1.1.17}$$

$$\sum_{i=1}^{K_{\mathrm{D}}} \mathrm{Tr}\left(\mathbf{Q}_{\mathrm{D}_i}\right) \le P_{\mathrm{BS}}, \tag{3.1.1.18}$$

$$\mathbf{Q}_{\mathrm{D}_i} \succeq 0, \forall i = 1,\ldots, K_{\mathrm{D}}, \tag{3.1.1.19}$$

$$t_{\mathrm{D}_i} \geq 1, \forall i = 1, \ldots, K_{\mathrm{D}}; t_{\mathrm{U}_j} \geq 1, \forall j = 1, \ldots, K_{\mathrm{U}}. \quad (3.1.1.20)$$

The previous optimization problem results from reformulating the original SE maximization through some intermediate steps that utilize epigraph representation, constraint relaxation and some other mathematical manipulations known from the literature, e.g., [87].

The algorithm below then shows how this iterative optimization progresses toward converged solution.

ALGORITHM 4. Iterative SDP-based algorithm.

Initialization:

1: Generate initial points for $\psi_{\mathrm{D}_i}^{(0)}$ and $\mathbf{Q}_{\mathrm{D}_i}^{(0)}$ for i = 1, 2, …, K_{D}; and $q_{\mathrm{U}_j}^{(0)}$ and $x_{\mathrm{U}_j}^{(0)}$ for j = 1, 2, …, K_{U}.

2: Set $n := 0$.

Iterative procedure:

3: **repeat**

4: Solve (3.1.1.12)-(3.1.1.20) to find optimal solutions $\mathbf{Q}_{\mathrm{D}_i}^*$, $t_{\mathrm{D}_i}^*$, and $\beta_{\mathrm{D}_i}^*$ for i = 1, 2, …, K_{D}, and $q_{\mathrm{U}_j}^*$, and $x_{\mathrm{U}_j}^*$ for j = 1, 2, …, K_{U}.

5: Set $n := n + 1$.

6: Update: $\psi_{\mathrm{D}_i}^{(n)} := t_{\mathrm{D}_i}^* / \beta_{\mathrm{D}_i}^*$; $x_{\mathrm{U}_j}^{(n)} := x_{\mathrm{U}_j}^*$; $\mathbf{Q}_{\mathrm{D}_i}^{(n)} := \mathbf{Q}_{\mathrm{D}_i}^*$; $q_{\mathrm{U}_j}^{(n)} := q_{\mathrm{U}_j}^*$.

7: **until** Convergence.

Finalization:

8: Perform randomization to extract a rank-1 solution as in ALGORITHM 3.

3.2. Scheduling Methods for FD Single Cells

Next generation wireless communication systems dynamically schedule users, and allocate subcarriers and power among them in order to meet the quality of service (QoS) requirements of each user, and to utilize the limited resources efficiently. The scheduling issue of the full-duplex cellular networks, where a full-duplex mode base station communicates with half-duplex mode users, was considered in [16]-[17]. In particular, a sub-optimal scheduling algorithm to maximize the system throughput is proposed in [17], and a hybrid scheduler that can switch between full-duplex and half-duplex modes to maximize the system throughput as well as to ensure fairness is proposed in [16], but these works have not considered the power allocation.

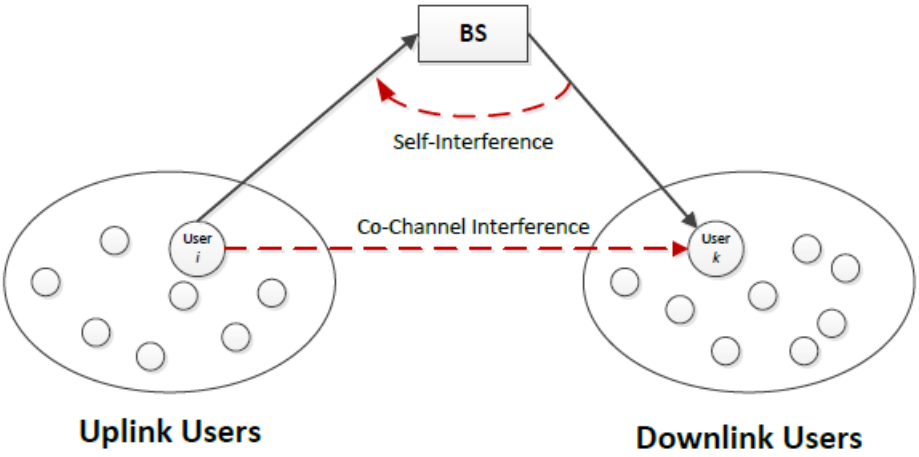

Figure 4: The system model of the FD wireless network.

In this section, we evaluate the performance of three resource allocation algorithms discussed in [18]-[20] which consider both the subcarrier and power allocation for an OFDMA system having a full-duplex base-station with randomly distributed half-duplex uplink and downlink users given in Figure 4. A simple three-step algorithm is proposed in [18] to maximize the sum-rate of full-duplex system subject to predefined target rate constraints at the uplink and downlink users, and transmit power constraints at the base-station and uplink users. Depending on the locations of the mobile users, propagation channels, the self-interference cancellation capability of the base-station, transmission power of the mobile users and base-station, etc, it might be better to switch to half-duplex mode. Therefore, a dynamic hybrid scheduler that can switch between half-duplex uplink, half-duplex downlink and full-duplex mode opportunistically to maximize the sum-rate has been designed in [19]. The algorithms in [18] and [19] assume perfect channel state information (CSI) at the transmitting nodes which may be unrealistic because of user mobility, feedback/processing delay and small channel coherence time. Therefore, a subcarrier and rate allocation for full-duplex OFDMA systems under imperfect CSI has been studied in [20][20].

We consider a single-cell single-input single-output (SISO) OFDMA system having a full-duplex base-station in the center with randomly distributed half-duplex uplink and downlink users. Let us denote I^{UL}, K^{DL} and N as the sets associated with uplink users, downlink users, and subcarriers, respectively. As shown in Figure 4, the base-station simultaneously receives signal from one of its uplink user and transmits signal to one of its downlink user. The received signals at the uplink and downlink channels of the base-station serving *i*-th uplink user, and *k*-th downlink user on the *n*-th subcarrier simultaneously are given, respectively, as

$$y_{ik,n}^{UL} = \sqrt{p_{i,n}^{UL}} h_{i,n}^{UL} s_{i,n}^{UL} + \sqrt{\frac{p_{k,n}^{DL}}{C_{SI}}} s_{k,n}^{DL} + w_{0,n},$$
$$y_{ki,n}^{DL} = \sqrt{p_{k,n}^{DL}} h_{k,n}^{DL} s_{k,n}^{DL} + \sqrt{p_{i,n}^{UL}} h_{ki,n} s_{i,n}^{UL} + w_{k,n}, \quad (3.2.1)$$

where $p_{i,n}^{UL}$ and $p_{k,n}^{DL}$ denote the transmit power of the *i*-th uplink user and the transmit power of the base-station serving downlink user *k* on the nth subcarrier, respectively. $s_{i,n}^{UL}$ and $s_{k,n}^{DL}$ are the data streams of the *i*-th uplink and *k*-th downlink user with unit powers, respectively. $h_{i,n}^{UL}$ and $h_{k,n}^{DL}$ denote

the channel from the *i*-th uplink user to the base-station and the channel from base-station to the *k*-th downlink user on the *n*-th subcarrier, respectively. $h_{ki,n}$ denote the co-channel interference from the *i*-th uplink user to the *k*-th downlink user on the *n*-th subcarrier. $w_{0,n}$ and $w_{k,n}$ denote the additive white Gaussian noise (AWGN) at the base-station and *k*-th downlink user on the *n*-th subcarrier, respectively. C_{SI} denotes the self-interference cancellation value at the base-station. In particular, $\frac{p_{k,n}^{DL}}{C_{SI}}$ represents the residual self-interference power at the base-station on the *n*-th subcarrier.

Three Step Algorithm:

We will first start with evaluation of the algorithm proposed in [18]. The optimal scheduling algorithm to maximize the sum-rate of the full-duplex system is formulated as

$$
\begin{aligned}
\max_{\mathbf{W},\ \mathbf{P}^{UL},\ \mathbf{P}^{DL}} \quad & \sum_{n=1}^{N} \sum_{i\in\mathcal{I}^{UL}} \sum_{k\in\mathcal{K}^{DL}} w_{nik}\left(R_{ik,n}^{UL} + R_{ki,n}^{DL}\right) \\
\text{s.t.} \quad & \sum_{n=1}^{N} \sum_{k\in\mathcal{K}^{DL}} p_{k,n}^{DL} \le P_T, \\
& \sum_{n=1}^{N} p_{i,n}^{UL} \le P_i,\ i \in \mathcal{I}^{UL}, \\
& \sum_{n=1}^{N} \sum_{k\in\mathcal{K}^{DL}} w_{nik} R_{ik,n}^{UL} \ge R_t^{UL},\ i \in \mathcal{I}^{UL} \\
& \sum_{n=1}^{N} \sum_{i\in\mathcal{I}^{UL}} w_{nik} R_{ki,n}^{DL} \ge R_t^{DL}, k \in \mathcal{K}^{DL} \\
& \sum_{i\in\mathcal{I}^{UL}} \sum_{k\in\mathcal{K}^{DL}} w_{nik} = 1,\ n = 1,\ldots,N, \\
& p_{k,n}^{DL} \ge 0,\ k \in \mathcal{K}^{DL},\ n = 1,\ldots,N, \\
& p_{i,n}^{UL} \ge 0,\ i \in \mathcal{I}^{UL},\ n = 1,\ldots,N, \quad (
\end{aligned}
\tag{3.2.2}
$$

where P_T and P_i are the transmit power constraints at the base-station and *i*-th uplink user, respectively. R_t^{UL} and R_t^{DL} are the minimum required target rates at the uplink and downlink users, respectively. When a user experiences deep fading, its instantaneous achievable rate becomes extremely low, and thus its quality-of-service (QoS) requirement may not be satisfied. The minimum required target rate constraints try to achieve certain instantaneous rate for each user to guarantee the fairness among different users. w_{nik} is an indicator variable which is equal to 1 if subcarrier *n* is allocated to *i*-th uplink user and *k*-th downlink user. The design variables $\mathbf{W}, \mathbf{P}^{UL}$, and $\mathbf{P}^{DL}$ are matrices obtained by stacking all w_{nik}, $p_{i,n}^{UL}$, and $p_{k,n}^{DL}$, respectively. Note that each subcarrier can be allocated to at most one uplink and one downlink user. This optimization problem is a combinatorial problem due to the indicator variable w_{nik}, which requires high-complexity algorithms and exhaustive

search to solve. Therefore, we introduce a heuristic subcarrier and power allocation algorithm to solve this optimization problem.

1) Proposed Scheduling Algorithm: The proposed algorithm has three steps. In the initial subcarrier allocation, subcarriers are sequentially assigned to two users (one downlink and one uplink) whose rates are below the target rate and will increase the sum-rate on this subcarrier the most with this additional assignment. This step ends when the rates of all uplink or downlink users reach the target rate, or when all the subcarriers are assigned. At this stage, to reduce the computation complexity and to make the problem tractable, the transmit power of each user is assumed to be equally distributed over the assigned subcarriers. In the residual subcarrier allocation step, the rest of the subcarriers, which are not allocated in the first step are assigned to users to further increase the sum-rate. If all uplink (downlink) users reach the target rate in the first step, then in the residual subcarrier allocation step, the uplink (downlink) users are chosen among all the uplink (downlink) users, and downlink (uplink) users are chosen among the users which have not reached the target rate. If both uplink and downlink users reach the target rate, and there are still available subcarriers, then the downlink and uplink users are chosen among all users. After the subcarriers are assigned, power allocation based on the iterative-water-filling (IWF) is performed in the last step. In particular, each uplink (downlink) user applies the single-user waterfilling algorithm given that the interference from the downlink (uplink) users over the assigned subcarriers are fixed.

Let us denote S_i^{UL} and S_k^{DL} as the subcarrier set assigned to *i*-th uplink user and *k*-th downlink user, respectively. Moreover, U^{UL} and U^{DL} denote the indices of uplink and downlink users whose rates are below target rate, respectively. Defining $R_i^{UL}\left(S_i^{UL}\right)$ and $R_k^{DL}\left(S_k^{DL}\right)$ as the uplink and downlink rates under equal power allocation among subcarriers, respectively, the detailed algorithm is given in Table 2.

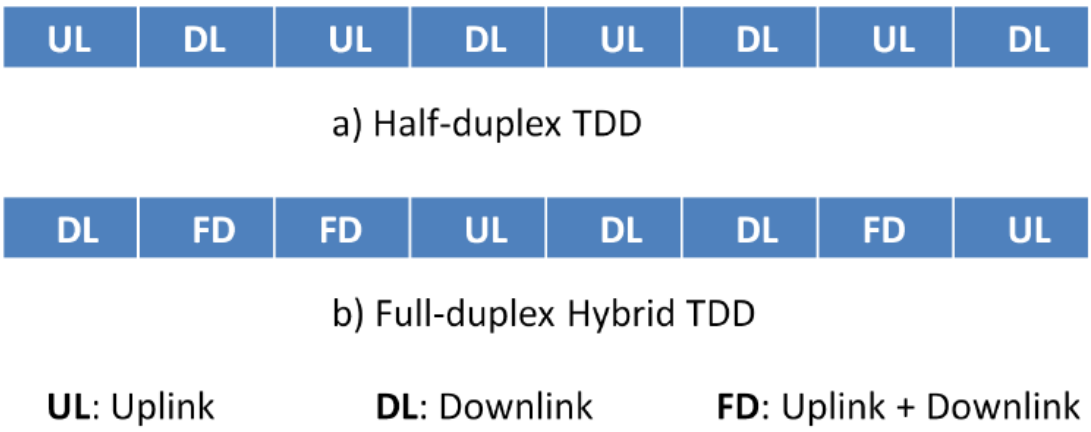

Figure 5: a) Half-duplex TDD scheduling, b) Hybrid scheduling

Hybrid Algorithm: Even though full-duplex is a promising path to performance gains, the majority of devices in existing networks operate in half-duplex mode. It is important to develop schemes to support the coexistence of the two technologies and to support the adaptation of transmission between half-duplex and full-duplex operation depending on the network topology. In half-duplex time-division-duplex (HD-TDD) systems shown in Figure 5.a, all time slots operate in the same frequency band alternating between uplink and downlink transmission, and thus there is no interference between uplink and downlink channels. In full-duplex scheduling, all time slots can be allocated to

simultaneous uplink and downlink transmissions, since full-duplex transmission has a potential to double the capacity. But as discussed in [16], depending on the locations of the mobile users, propagation channels, the self-interference cancellation capability of the base-station, transmission power of the mobile users and base-station, etc., it might be better to dedicate a time slot to only half-duplex uplink or half-duplex downlink transmission. Therefore, a dynamic hybrid scheduler that can switch between half-duplex uplink, half-duplex downlink and full-duplex mode opportunistically should be designed as shown in Figure 5.b. To implement the hybrid scheduling, at each decision epoch, the scheduler runs the proposed algorithm for full-duplex, half-duplex downlink and half-duplex uplink, and selects the mode which yields the largest value to maximize the throughput.

In this subsection, we present a hybrid scheduler proposed in [19] that can switch between full-duplex, half-duplex uplink and half-duplex downlink mode at each time slot to maximize the sum-rate in full-duplex OFDMA systems, where the base station and uplink users have transmission power constraints. The scheduling algorithm to maximize the sum-rate of the full-duplex system is formulated as:

$$
\begin{aligned}
\max_{\mathbf{W},\ \mathbf{P}^{UL},\ \mathbf{P}^{DL}} \quad & \sum_{n=1}^{N} \sum_{i \in \mathcal{I}^{UL}} \sum_{k \in \mathcal{K}^{DL}} w_{nik} \left(R_{ik,n}^{UL} + R_{ki,n}^{DL} \right) \\
\text{s.t.} \quad & \sum_{n=1}^{N} \sum_{k \in \mathcal{K}^{DL}} p_{k,n}^{DL} \leq P_T, \\
& \sum_{n=1}^{N} p_{i,n}^{UL} \leq P_i, \ i \in \mathcal{I}^{UL}, \\
& \sum_{i \in \mathcal{I}^{UL}} \sum_{k \in \mathcal{K}^{DL}} w_{nik} = 1, \ n = 1, \ldots, N, \\
& p_{k,n}^{DL} \geq 0, \ k \in \mathcal{K}^{DL}, \ n = 1, \ldots, N, \\
& p_{i,n}^{UL} \geq 0, \ i \in \mathcal{I}^{UL}, \ n = 1, \ldots, N, \\
& w_{nik} \in \{0, 1\}, \ \forall (n, i, k),
\end{aligned}
\tag{3.2.3}
$$

Using Karush-Kuhn-Tucker (KKT) conditions associated with sum-rate maximization problem, a greedy subcarrier allocation, and a power allocation based on IWF algorithm is proposed in [19] , and the summary of the algorithm is provided in Table 3. In particular, in the proposed algorithm, subcarriers are sequentially assigned to two users (one downlink and one uplink) which maximizes the sum-rate on each subcarrier. The required powers to compute the uplink rate and downlink rate are obtained through the power allocation algorithm based on the IWF. This process repeats until all subcarriers have been assigned.

Table 2: PROPOSED SCHEDULING ALGORITHM

Initialization: $\mathcal{S}_i^{UL} = \phi,\ \mathcal{S}_k^{DL} = \phi,\ \bar{n} = 0$
$\mathcal{U}^{UL} = \mathcal{I}^{UL}$, and $\mathcal{U}^{DL} = \mathcal{K}^{DL}$.

Step 1: Initial subcarrier allocation.

while $\mathcal{U}^{UL}$ or $\mathcal{U}^{DL}$ or $\mathcal{N}$ is not empty

1) $\bar{n} = \bar{n} + 1,\ \tilde{\mathcal{S}}_i^{UL} = \mathcal{S}_i^{UL} \bigcup \bar{n},\ \tilde{\mathcal{S}}_k^{DL} = \mathcal{S}_k^{DL} \bigcup \bar{n}.$

2) $\Delta_{ik} = R_i^{UL}\left(\tilde{\mathcal{S}}_i^{UL}\right) + R_k^{DL}\left(\tilde{\mathcal{S}}_k^{DL}\right) - R_i^{UL}\left(\mathcal{S}_i^{UL}\right) - R_k^{DL}\left(\mathcal{S}_k^{DL}\right),\ i \in \mathcal{U}^{UL},\ k \in \mathcal{U}^{DL}.$

3) $(i^*, k^*) = \arg\max_{i \in \mathcal{U}^{UL},\ k \in \mathcal{U}^{DL}} \Delta_{ik}.$

4) $w_{\bar{n}i^*k^*} = 1,\ \mathcal{S}_{i^*}^{UL} = \mathcal{S}_{i^*}^{UL} \bigcup \bar{n},\ \mathcal{S}_{k^*}^{DL} = \mathcal{S}_{k^*}^{DL} \bigcup \bar{n}.$

5) Update $R_{i^*}\left(\mathcal{S}_{i^*}^{UL}\right)$ and $R_{k^*}\left(\mathcal{S}_{k^*}^{DL}\right)$.

6) **if** $R_{i^*}\left(\mathcal{S}_{i^*}^{UL}\right) \geq R_t^{UL}, \mathcal{U}^{UL}/\{i^*\}$ **end if**

7) **if** $R_{k^*}\left(\mathcal{S}_{k^*}^{DL}\right) \geq R_t^{DL}, \mathcal{U}^{DL}/\{k^*\}$ **end if**

8) $\mathcal{N} = \mathcal{N}/\{\bar{n}\}.$

end loop

Step 2: Residual subcarrier allocation.

Residual subcarrier allocation is almost the same as Step 1.

The only difference is that line 3 must be replaced by:

if $\mathcal{U}^{UL} = \phi$ and $\mathcal{U}^{DL} \neq \phi$

9) $(i^*, k^*) = \arg\max_{i \in \mathcal{I}^{UL},\ k \in \mathcal{U}^{DL}} \Delta_{ik}.$

else if $\mathcal{U}^{DL} = \phi$ and $\mathcal{U}^{UL} \neq \phi$

10) $(i^*, k^*) = \arg\max_{i \in \mathcal{U}^{UL},\ k \in \mathcal{K}^{DL}} \Delta_{ik}.$

else

11) $(i^*, k^*) = \arg\max_{i \in \mathcal{I}^{UL},\ k \in \mathcal{K}^{DL}} \Delta_{ik}.$

end if

Step 3: Sequential Iterative Water-Filling.

for $l = 1$: Max-iteration

for $m \in \left(\mathcal{I}^{UL} \bigcup \mathcal{K}^{DL}\right)$

if $m \in \mathcal{I}^{UL}$

12) $p_{m,n}^{UL} = \left[\mu_m - \frac{N_{0,n} + \frac{p_{\bar{m},n}^{DL}}{C_{SI}}}{\left|h_{m,n}^{UL}\right|^2}\right]^+,\ \sum_{n \in \mathcal{S}_m^{UL}} p_{m,n}^{UL} = P_m,$

else

13) $p_{m,n}^{DL} = \left[\mu_m - \frac{N_{m,n} + p_{\bar{m},n}^{UL}\left|h_{m\bar{n},n}\right|^2}{\left|h_{m,n}^{DL}\right|^2}\right]^+,$

$$\sum_{n \in \mathcal{S}_m^{DL}} p_{m,n}^{DL} = \frac{\left|\mathcal{S}_m^{DL}\right| P_T}{N}.$$

end if

end loop

end loop

Table 3: PROPOSED HYBRID SCHEDULING ALGORITHM

Initialization: $\mathcal{S}_i^{UL} = \phi,\ \mathcal{S}_k^{DL} = \phi.$

for $n = 1 : N$

for $i \in \mathcal{I}^{UL},\ k \in \mathcal{K}^{DL}$

1) $\tilde{\mathcal{S}}_i^{UL} = \mathcal{S}_i^{UL} \bigcup n,\ \tilde{\mathcal{S}}_k^{DL} = \mathcal{S}_k^{DL} \bigcup n.$
$\tilde{\mathcal{S}}_j^{UL} = \mathcal{S}_j^{UL},\ j \neq i, \quad \tilde{\mathcal{S}}_l^{DL} = \mathcal{S}_l^{DL},\ l \neq k.$

2) Apply **IWF Algorithm** given below to compute $p_{i,n}^{UL}$ and $p_{k,n}^{DL}$ assuming that nth subcarrier is assigned to ith uplink and kth downlink user (as shown in Step 1).

3) $\Delta_{ik} = R_{ik,n}^{UL} + R_{ki,n}^{DL},\ i \in \mathcal{I}^{UL},\ k \in \mathcal{K}^{DL}.$

end loop

4) $(i^*, k^*) = \arg\max_{i \in \mathcal{I}^{UL},\ k \in \mathcal{K}^{DL}} \Delta_{ik}.$

5) $w_{ni^*k^*} = 1,\ \mathcal{S}_{i^*}^{UL} = \mathcal{S}_{i^*}^{UL} \bigcup n,\ \mathcal{S}_{k^*}^{DL} = \mathcal{S}_{k^*}^{DL} \bigcup n.$

end loop

Iterative Water-Filling (IWF) Algorithm

for $l = 1$: Max-iteration

for $m \in \left(\mathcal{I}^{UL} \bigcup \mathcal{K}^{DL}\right)$

if $m \in \mathcal{I}^{UL}$

$$p_{m,n}^{UL} = \left[\mu_m - \frac{N_{0,n} + \frac{p_{\bar{m},n}^{DL}}{C_{SI}}}{\left|h_{m,n}^{UL}\right|^2}\right]^+, \quad \sum_{n \in \mathcal{S}_m^{UL}} p_{m,n}^{UL} = P_m,$$

else

$$p_{m,n}^{DL} = \left[\mu_m - \frac{N_{m,n} + p_{\bar{m},n}^{UL}\left|h_{m\bar{m},n}\right|^2}{\left|h_{m,n}^{DL}\right|^2}\right]^+,$$

$$\sum_{n \in \mathcal{S}_m^{DL}} p_{m,n}^{DL} = \frac{\left|\mathcal{S}_m^{DL}\right| P_T}{N}.$$

end if

end loop

end loop

Extension to Imperfect Channels:

The algorithms in [18]-[19] discussed in the previous two subsections assume perfect CSI at the transmitting nodes which results in non-zero outage probability, since the transmitting nodes encode data at rate higher than the rates actual channel can support. In this subsection, we present a scheduler that exploits the partial CSI to maximize the system's successfully transmitted rate, referred as goodput in full-duplex OFDMA systems, where the base station and uplink users have

transmission power constraints. Using the KKT conditions associated with sum-goodput maximization problem, a computationally efficient algorithm for subcarrier and rate allocation is proposed.

The partial CSI at the transmitters is modeled as the channel estimation that is treated as a deterministic mean plus an error term with known probability density function (pdf) to account for various sources of uncertainty. The relation between the estimated and actual channel gains of each user is given by

$$h_{i,n}^{UL} = \tilde{h}_{i,n}^{UL} + e_{i,n}^{UL},\ i \in \mathcal{I}^{UL}, \quad n \in \mathcal{N}, \tag{3.2.4}$$

$$h_{k,n}^{DL} = \tilde{h}_{k,n}^{DL} + e_{k,n}^{DL},\ k \in \mathcal{K}^{DL}, \quad n \in \mathcal{N}. \tag{3.2.5}$$

The statistical conditional pdf of the channel estimation can be assumed as Gaussian, and is expressed as

$$\begin{aligned} p\left(h_{i,n}^{UL} | \tilde{h}_{i,n}^{UL}\right) &\sim \mathcal{CN}\left(\tilde{h}_{i,n}^{UL},\ \sigma_{ul,in}^2\right), \\ p\left(h_{k,n}^{DL} | \tilde{h}_{k,n}^{DL}\right) &\sim \mathcal{CN}\left(\tilde{h}_{k,n}^{DL},\ \sigma_{dl,kn}^2\right), \end{aligned} \tag{3.2.6}$$

where $s_{ul,in}^2\left(s_{dl,kn}^2\right)$denotes the channel estimation variance in the uplink (downlink) channel, and depends on the accuracy of channel estimation and delay in feedback/processing, Doppler spread, and quantization errors. Based on the partial CSI, *i*-th uplink user transmits at a rate of $r_{ik,n}^{UL}$ on the *n*-th subcarrier that the actual channel cannot support resulting in non-zero outage probability, i.e., $P_{out}^{UL}\left(R_{ik,n}^{UL}\right)@\Pr\left\{r_{ik,n}^{UL} > R_{ik,n}^{UL} \middle| \tilde{h}_{i,n}^{UL}\right\}$, where $R_{ik,n}^{UL}$ is the uplink instantaneous rates. Note that the outage probability for the downlink case can be found similarly. In this case a meaningful performance measure is the average rate of data in bits/s/Hz correctly received, or the so-called goodput [21]. This is defined as the product between the spectral efficiency and the corresponding probability of successful communication, i.e.,

$$G_{ik,n}^{UL} = r_{ik,n}^{UL}\left(1 - P_{out}^{UL}\left(r_{ik,n}^{UL}\right)\right) \tag{3.2.7}$$

The subcarrier and rate allocation algorithm to maximize the sum-goodput of the FD system is formulated as

$$
\begin{aligned}
\max_{\mathbf{R},\,\mathbf{W},\,\mathbf{P}} \quad & \sum_{n=1}^{N} \sum_{i\in\mathcal{I}^{UL}} \sum_{k\in\mathcal{K}^{DL}} w_{nik}\left(G_{ik,n}^{UL}+G_{k,n}^{DL}\right) \\
\text{s.t.} \quad & \sum_{n=1}^{N} \sum_{k\in\mathcal{K}^{DL}} p_{k,n}^{DL} \le P_T, \\
& \sum_{n=1}^{N} p_{i,n}^{UL} \le P_i,\ i\in\mathcal{I}^{UL}, \\
& \sum_{i\in\mathcal{I}^{UL}} \sum_{k\in\mathcal{K}^{DL}} w_{nik} \le 1,\ n=1,\ldots,N, \\
& p_{k,n}^{DL} \ge 0,\ k\in\mathcal{K}^{DL},\ n=1,\ldots,N, \\
& p_{i,n}^{UL} \ge 0,\ i\in\mathcal{I}^{UL},\ n=1,\ldots,N, \\
& w_{nik} \ge 0,\ \forall\,(n,i,k)\,, \\
& r_{ik,n}^{UL} \ge 0,\ r_{k,n}^{DL} \ge 0,\ \forall\,(n,i,k)\,,
\end{aligned}
\tag{3.2.8}
$$

This optimization problem is again a combinatorial problem which requires high-complexity algorithms and exhaustive search to solve. A similar approach to the hybrid scheduling discussed in the previous subsection can be applied to solve this problem.

3.3. Correlated co-channel interference from UL to DL

Herein, we investigate how hybrid half- and full-duplex networks perform under the correlated shadowing assumption, since there is a considerable performance gap between results with independent and correlated shadowing. In the FD context, we look at the Uplink (UL) to Downlink (DL) interference, which is particularly challenging because users are randomly scattered within serving cell coverage area. Based on accurate channel measurements, serving Base Stations (BSs) can schedule users so as to minimize intra-cell interference, though too much overhead may be incurred.

The common sense is that only users located farther way can transmit simultaneously. However, this approach limits the scheduling flexibility and may cause performance degradation. Bearing this in mind, we analyze the impact of the correlation between Half-Duplex (HD) User Equipments (UEs) associated to a common FD BS is investigated, as depicted in Figure 6. Our investigations are carried out in a single cell deployment wherein multiple UEs are randomly scattered. The user of interest is degraded by simultaneous transmission of other interfering UE transmitting in their vicinity. The resulting Co-Channel Interference (CCI) is affected by shadowing correlation as a function of the disposition of concurrent UEs in UL and DL. Thus, our focus is on the issue of co-channel interference of nearby users simultaneously communicating with a FD serving BS.

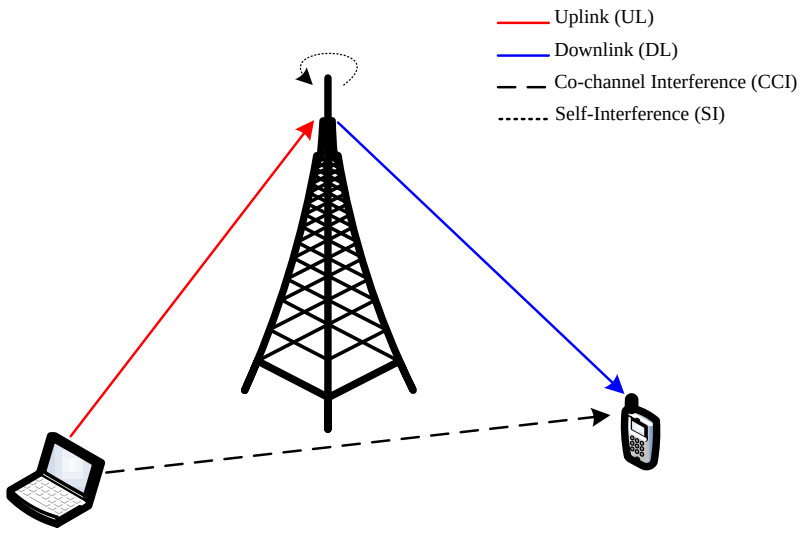

Figure 6: General single cell deployment: FD BS communicating to multiple HD UEs. Note that the nodes in DL suffer CCI from nodes in UL, and FD BS suffers from self-interference.

We assess the performance of interference networks operating in hybrid FD/HD modes and under composite fading channel, namely correlated Log-Normal (LN) shadowing and Nakagami-m fading. Moreover, we consider a small cell deployment scenario with low transmission power BSs. In every transmission interval, the serving BS independently schedules users that share the available spectrum on the UL and DL simultaneously. All communicating nodes have antennas with omni-directional radiation pattern. BSs and UEs are also assumed to operate with full buffer and exhibit symmetric traffic patterns. Neighboring BSs are assumed to carry out inter-cell interference coordination, so that other cell interference is negligible.

Consider that a FD BS serves two HD UEs on the UL and DL simultaneously which share the available radio resources and communicate over the same set of frequency bands. We consider a DL interference profile herein the serving BS (b_0) transmits with p_0 to the user of interest u_0 which is interfered by a random co-site user u transmitting on the UL direction with pi towards b_0. The user u_0 is the DL UE who is taken as the reference to compute the CCI and performance metrics. UEs are randomly scattered over the network deployment area according to a homogeneous Poisson Point Process (PPP) with density λ (UE/m2) [1]. A signal strength decay function $r^{-\alpha}$, where α is the path loss exponent, describes the path loss attenuation, while the squared-envelop due to multipath fading and shadowing is represented by a random variable (RV) X. An arbitrary transmitter degrades the communication of u_0 with a component given by $Y = p\, r^{-\alpha}\, x$, where p represents the transmit power. In order to evaluate such scenarios we introduce an analytical framework that uses stochastic geometry to model random network deployments, and higher order statistics in order to recover both the distributions of the received power Y_0 and the CCI Y at the u_0 [1]-[2] .This framework is described in details in [16]-[17], while **Procedure 1** summarizes its main steps as follows:

Procedure 1. Analytical framework: Log-Normal Composite channel model
6: Determine the LogNormal parameters of the composite fading channels as $\mu_{dB} = \xi\,[\psi(m) - \ln(m)] + \mu_{\Omega_p}$ and $\sigma_{dB} = \xi^2 \zeta(2, m) + \sigma^2_{\Omega_p}$,

where $\psi(m)$is the Euler Psi function, $\zeta(2,m)$is the Zeta Riemann function and m is the Nakagami-m fading figure, while $\mu_{\Omega_p}$and $\sigma^2_{\Omega_p}$ are the given shadowing parameters.

7: Determine the characteristic function of the received signal

$$\Psi_Y(\omega) = E[e^{j\omega Y}],$$

where $j = \sqrt{-1}$ and Y be a RV representing the CCI generated by a interfering user u.

8: Determine the n-th cumulant as

$$\kappa_n(Y) = \frac{1}{j^n}\left[\frac{\partial^n}{\partial \omega^n}\ln(\Psi_Y(\omega))\right]_{\omega=0}$$

9: Determine the parameters of the approximated distribution as a function of the first and second cumulants as

$$\mu = \ln\frac{\kappa_1^2}{\sqrt{\kappa_1^2+\kappa_2}} \text{ and}$$

$$\sigma^2 = \ln 1 + \frac{\kappa_2}{\kappa_1^2},$$

which are, respectively, the mean and standard deviation of the distribution $Normal(\mu,\sigma^2)$ in the logarithmic scale.

10: If necessary, determine the cross-correlation coefficient between two received signals as

$$\rho_{ij} = \frac{E[(Y_i-\mu_i)(Y_j-\mu_j)]}{\sigma_i\sigma_j}$$

Given the network setup introduced above, we attain the characteristic function of a RV Y which described the received power at the user of interest from an annular region varying from R_m to R_M [1] as $\Psi_Y(\omega) = \frac{2}{R_M^2-R_m^2}E[R(\omega)]$, where $E[x]$ represents the expectation of a RV X, and $R(\omega) = \int_{R_m}^{R_M} e^{j\omega p r^{-\alpha_x}} r\, dr$.

Bearing this in mind, the cumulants are obtained in [1] and then following the steps of **Procedure 1** we can attain the parameters of the approximated distribution, namely V_0, which is a Normal RVs (in logarithmic scale) representing the power received from the desired transmitter and V the CCI at the user of interest. Then the SIR can be represented as $\Gamma \sim Normal\left(\mu_{V_0}-\mu_V, \sigma^2_{V_0}+\sigma^2_V-2\rho_{V_0V}\sigma_{V_0}\sigma_V\right) \sim Normal(\mu_\Gamma,\sigma_\Gamma)$, which lead us to the an outage probability given as $Pr[\Gamma < \gamma_{th}] = Q\left[\frac{\mu_\Gamma-\gamma_{th}}{\sigma_\Gamma}\right]$. Further discussions and results are introduced in Deliverable D.4.1.2.

3.4. Power Allocation Strategies for FD Single Cells

3.4.1. Analytical Results

Some analytical insights are required about the self-interference cancelation and power control that will make rate gains in FD comparing to HD. Two HD users scenario, one uplink-UE and one downlink-UE, with FD base-station, as shown in Figure 7, will be considered. Flat fading over the subcarriers is assumed, however, the analysis is applicable for frequency-selective channel with 1-2 dB correction.

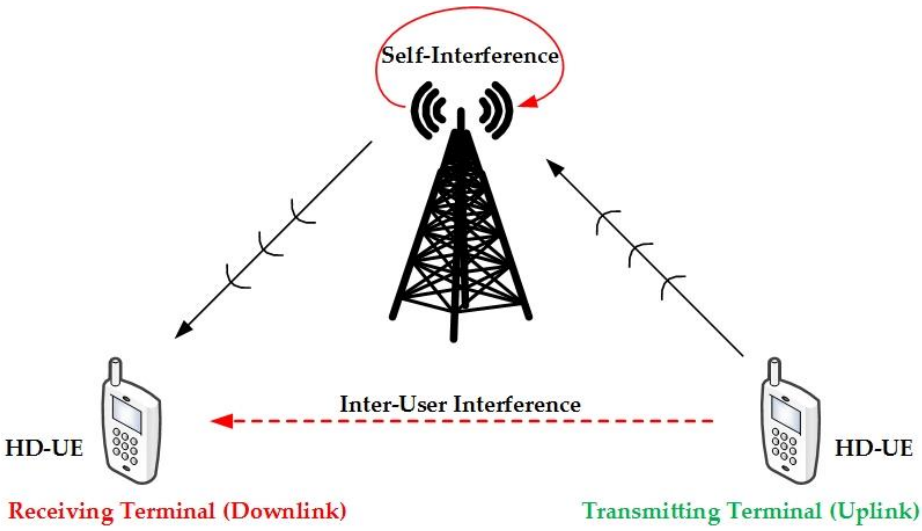

Figure 7: Two HD users and FD base-station scenario

Here we assume that the traffic is asymmetric in the sense that there is more traffic demand on the downlink comparing to uplink. Thus, the uplink power transmission will be adapted and the downlink transmission power is maintained at the maximum level to achieve rate gain in the FD downlink. The downlink rate R_{DL}^{F} in FD system is given by

$$\begin{aligned} R_{DL}^{F} &= \sum_{n=1}^{N} \log_2 \left(1 + \frac{\frac{P^b}{N\theta_{dl}}}{z_u + \frac{\tilde{P}_u}{N\theta_{u2u}}} \right) \\ &= N \log_2 \left(1 + \frac{\frac{P^b}{\theta_{dl}}}{N z_u + \frac{\tilde{P}_u}{\theta_{u2u}}} \right) \end{aligned} \tag{3.4.1.1}$$

where, N is the number of subcarriers, θ_{dl} is the pathloss between the base-station and the downlink user, θ_{u2u} is the pathloss between the downlink and the uplin users, P^b is the base-station total transmit power, $\tilde{P}_u$ is the uplink user total transmission power and z_u is the noise power at the user equipement. On the other hand, the downlink rate R_{DL}^{H} for the HD scenario will be

$$\begin{aligned} R_{DL}^{H} &= \sum_{n=1}^{N/2} \log_2 \left(1 + \frac{\frac{2P^b}{N\theta_{dl}}}{z_u} \right) \\ &= \frac{N}{2} \log_2 \left(1 + \frac{2P^b}{N z_u \theta_{dl}} \right) \end{aligned} \tag{3.4.1.2}$$

Hence, a gain in FD over HD is achieved in the downlink if the following is true

$$\begin{aligned} R_{DL}^{F} &> R_{DL}^{H} \\ N\log_2\left(1+\frac{\frac{P^b}{\theta_{dl}}}{Nz_u+\frac{\tilde{P}_u}{\theta_{u2u}}}\right) &> \frac{N}{2}\log_2\left(1+\frac{2P^b}{Nz_u\theta_{dl}}\right) \end{aligned} \tag{3.4.1.3}$$

After some mathematical manipulations we obtain

$$\theta_{u2u}^2 P^b N z_u - \theta_{u2u} 2\tilde{P}_u \theta_{dl} N z_u - 2\theta_{dl}\tilde{P}_u^2 > 0 \tag{3.4.1.4}$$

And solving for $\tilde{P}_u$ we can find the required user uplink power to achieve gain in the downlink as follows

$$\tilde{P}_u = \min\left[P_u^{max}, \frac{\theta_{u2u} N z_u}{2}\left(\sqrt{1+\frac{2P^b}{\theta_{dl} N z_u}}-1\right)\right] \tag{3.4.1.5}$$

where P_u^{max} is the user maximum transmission power. Using the uplink power from the previous equation, the uplink rate R_{UL}^{F} for FD scenario will be

$$R_{UL}^{F} = N\log_2\left(1+\frac{\frac{\tilde{P}_u}{\theta_{ul}}}{Nz_b+\frac{P^b}{\theta_s}}\right) \tag{3.4.1.6}$$

where θ_{ul} is the pathloss between the uplink user and the base-station, θ_s is the self-interference cancelation factor and z_b is the noise power at the base-station. The uplink rate R_{UL}^{H} for HD scenario is given by

$$R_{UL}^{H} = \frac{N}{2}\log_2\left(1+\frac{2P_u^{max}}{Nz_b\theta_{ul}}\right) \tag{3.4.1.7}$$

Thus, the uplink FD will have gain over uplink HD when the following holds

$$\begin{aligned} R_{UL}^{F} &> R_{UL}^{H} \\ N\log_2\left(1+\frac{\frac{\tilde{P}_u}{\theta_{ul}}}{Nz_b+\frac{P^b}{\theta_s}}\right) &> \frac{N}{2}\log_2\left(1+\frac{2P_u^{max}}{Nz_b\theta_{ul}}\right) \end{aligned} \tag{3.4.1.8}$$

It can been shown that this inequality holds if the self-interference cancelation factor is greater than the following threshold

$$\theta_s > P_b \frac{2P_u^{max} - \tilde{P}_u + \tilde{P}_u\sqrt{1+\frac{2P_u^{max}}{\theta_{ul}Nz_b}}}{\frac{\tilde{P}_u^2}{\theta_{ul}} - 2Nz_b(P_u^{max}-\tilde{P}_u)} \tag{3.4.1.9}$$

This condition insures that FD will outperform HD in both directions; uplink and downlink. It can be observed from this equation that when the denominator approaches zero, the required self-interference cancelation factor will go to infinity. Thus, the maximum uplink pathloss that allow gain in the uplink FD can be given by

$$\theta_{ul}^{max} = \frac{\tilde{P}_u^2}{2Nz_b(P_u^{max}-\tilde{P}_u)} \tag{3.4.1.10}$$

In other word, if the uplink pathloss is greater than θ_{ul}^{max}, no gain can be achieved in uplink FD comparing to uplink HD regardless the self-interference cancelation factor, given the power uplink control to improve the downlink rate. Also, when $\tilde{P}_u = P_u^{max}$ the equation will be

$$\theta_s > \frac{P^b}{P_u^{max}}\theta_{ul}\left(1+\sqrt{1+\frac{2P_u^{max}}{\theta_{ul}Nz_b}}\right) \tag{3.4.1.11}$$

3.4.2. Radio resource allocation HD-UEs & FD-BS

Due to the effect of interference, radio resource allocation plays an important role in optimizing the full-duplex system performance. Current radio resource allocation algorithms are designed for half-duplex systems [30], [31], where the uplink and downlink channels are orthogonal to each other, hence, can be optimized independently. On the contrary, the uplink and downlink resource allocation problem is coupled in full-duplex, and has to be optimized jointly. Thus, it is not possible to apply the conventional half-duplex resource allocation algorithms to full-duplex systems in a straightforward manner. In this section, we address the joint radio resource allocation problem for uplink and downlink channels in a single-cell full-duplex system, with the objective of sum-rate maximization. As the problem is non-convex, we model the problem as a non-cooperative game between the uplink and downlink channels, and propose an iterative algorithm to achieve the Nash equilibrium. The simulation results show that the proposed algorithm achieves fast convergence rate and the full-duplex significantly outperforms half-duplex performance.

We consider a single-cell with a full-duplex base-station that communicates with half-duplex users' terminals through multicarrier orthogonal channels, such as Orthogonal Frequency-Division Multiplexing (OFDM). The available bandwidth is divided into a set of subcarriers $\mathcal{N} = \{1, \dots, N\}$. The base-station uses the available subcarriers to transmit to the *downlink* users. In the same time, the *uplink* users can use the same subcarriers to transmit to the base-station. At the base-station, the downlink transmitted signal will leak into its own receiver RF chain (which is referred to as self-interference) and mixed with the received signals from the uplink channel. Advanced analog and digital self-interference cancellation techniques are able to suppress significant amount of this interference. Similarly, at the user terminal, the downlink channel will suffer from the inter-user interference due to the uplink transmission from other users. However, unlike the self-interference, there is no cancellation implemented for the inter-user interference. Let $\mathcal{K} = \{1, \dots, K\}$ be the set of users that transmit in the uplink, and $\mathcal{J} = \{1, \dots, J\}$ be the set of users that receive in the downlink. Using Shannon's formula for Gaussian channel, the user's rate on a subcarrier in the downlink channel is given by

$$R_{j,n} = x_{j,n}\log_2\left(1+\frac{p_n h_{j,n}}{\sigma_e^2 + I_{j,n}}\right), \quad \forall j \in \mathcal{J}, n \in \mathcal{N}, \tag{3.4.2.1}$$

where $I_{j,n}$ is the inter-user interference from the uplink users to the *j*th downlink user on the *n*th subcarrier, and it's given by

$$I_{j,n} = \sum_{k\in\mathcal{K}} p_{k,n} g_{k,j}. \tag{3.4.2.2}$$

Here, p_n is the power transmitted by the base-station on the *n*th subcarrier, and $h_{j,n}$ is the downlink channel gain between the *j*th user and the base-station on the *n*th subcarrier. $p_{k,n}$ is the power transmitted by the *k*th user on the *n*th subcarrier in uplink. $g_{k,j}$ is the channel gain between the *k*th and *j*th users, and σ_e^2 is the additive white Gaussian noise (AWGN) power per subcarrier at the user equipment. $x_{j,n}$ is the subcarrier allocation binary indicator where $x_{j,n}$ equals to 1 if subcarrier *n* is allocated to user *j*, and 0 otherwise. In the downlink, each subcarrier is allocated to one user only. For uplink channel, the users' rate on each subcarrier will be

$$R_{k,n} = \log_2\left(1 + \frac{p_{k,n}h_{k,n}}{\sigma_b^2 + I_{k,n} + p_n\beta}\right), \quad \forall k \in \mathcal{K}, n \in \mathcal{N} \tag{3.4.2.3}$$

where β represents the self-interference cancellation factor at the base-station, i.e., $p_n\beta$ will be the residual self-interference on the *n*th subcarrier. $h_{k,n}$ is the uplink channel gain between the *k*th user and the base-station on the *n*th subcarrier, and σ_b^2 is the AWGN power per subcarrier at the base-station. $I_{k,n}$ is the interference the *k*th user sees from other uplink users on the *n*th subcarrier. Assuming that the users are decoded in an increasing order of their indices, the first user to be decoded, *k=1*, will see interference from all the other users k=2, …, K, and the second user to be decoded will see interference from the users k=3, …, K, and so on. Thus, the interference $I_{k,n}$ each user experience on each subcarrier with this decoding order will be

$$I_{k,n} = \sum_{j=k+1}^{K} p_{j,n}h_{j,n}, \quad k = 1, \cdots, K-1. \tag{3.4.2.4}$$

It is worth mentioning that the decoding order does not affect the sum-rate, and any arbitrary decoding order can be assumed. It is clear from (3.4.2.1) and (3.4.2.3) that the power allocation is coupled between downlink and uplink channels due to the self-interference and inter-user interference. Thus, a joint downlink and uplink power allocation need to be implemented to optimize the system performance in both transmission directions. With the knowledge of channel state information, the subcarrier and power allocation problem that maximizes the system spectral efficiency can be formulated as follows

$$\max_{x_{j,n}, p_n, p_{k,n}} \sum_{j\in\mathcal{J}}\sum_{n\in\mathcal{N}} R_{j,n} + \sum_{k\in\mathcal{K}}\sum_{n\in\mathcal{N}} R_{k,n} \tag{3.4.2.5}$$

subject to

$$\sum_{j\in\mathcal{J}} x_{j,n} \le 1, \quad x_{j,n} \in \{0,1\}, \quad \forall n \in \mathcal{N}, \forall j \in \mathcal{J}, \tag{3.4.2.6}$$

$$\sum_{n\in\mathcal{N}} p_n \le P_T, \tag{3.4.2.7}$$

$$\sum_{n\in\mathcal{N}} p_{k,n} \le P_k, \quad \forall k \in \mathcal{K}, \tag{3.4.2.8}$$

where P_k and P_T are the maximum transmit powers of the kth user and the base-station, respectively. Unfortunately, the problem ((3.4.2.5)-(3.4.2.8)) cannot be expressed as a convex optimization problem because the objective functions (3.4.2.1) and (3.4.2.3) are non-convex functions due to the interference terms. Finding the optimal solution is computationally difficult and intractable for systems with large number of users (J and K) and subcarriers (N). Consequently, instead of seeking the global

optimal, we will solve the problem for competitively optimal power allocation by modelling the problem as a non-cooperative game.

Initially, we consider the two users case, i.e. one uplink user (u) and one downlink (d) user, and extend the solution to more generic scenario later. A utility function (or pay-off function) needs to be defined to construct a game based on it. The users' data rates can be considered as the reward obtained by transmitting power. The rates of the two users will be

$$R^u = \sum_{n\in\mathcal{N}} \log_2\left(1+\frac{p_{u,n}h_{u,n}}{\sigma_b^2+p_n\beta}\right), \tag{3.4.2.9}$$

$$R^d = \sum_{n\in\mathcal{N}} \log_2\left(1+\frac{p_n h_{d,n}}{\sigma_e^2+p_{u,n}g_{u,d}}\right). \tag{3.4.2.10}$$

It can be noticed that when each transmitter (uplink or downlink) increases its power, it will increase its data rate, however, at the same time it will increase the interference on the other channel direction. This can be modelled as non-cooperative game between the uplink and downlink channels. In this sitting, each user attempts to maximise its performance regardless of the other user performance. This process can be done continuously, and if there is an equilibrium point it will converge. This equilibrium is referred to as Nash equilibrium, which is defined as a strategy set in which each user strategy is an optimal response to the other user's strategy. The following theorem shows the condition under which a Nash equilibrium will exists for the full-duplex two users non-cooperative game.

Theorem 1: *At least one Nash equilibrium strategy exists in the two user's full-duplex game, if the following condition is satisfied*

$$\beta < \min_{n\in\mathcal{N}}\left(\frac{h_{u,n}h_{d,n}}{g_{u,d}}\right). \tag{3.4.2.11}$$

Proof: The two users' rate can be reformulated as follows

$$R^u = \sum_{n\in\mathcal{N}} \log_2\left(1+\frac{p_{u,n}}{z_{u,n}+\alpha_{u,n}p_n}\right), \tag{3.4.2.12}$$

$$R^d = \sum_{n\in\mathcal{N}} \log_2\left(1+\frac{p_n}{z_{d,n}+\alpha_{d,n}p_{u,n}}\right), \tag{3.4.2.13}$$

where

$$z_{u,n} = \frac{\sigma_b^2}{h_{u,n}}, \quad \alpha_{u,n} = \frac{\beta}{h_{u,n}}, \tag{3.4.2.14}$$

$$z_{d,n} = \frac{\sigma_u^2}{h_{d,n}}, \quad \alpha_{d,n} = \frac{g_{u,d}}{h_{d,n}}. \tag{3.4.2.15}$$

It has been shown that for (3.4.2.12) and (3.4.2.13), if $\alpha_{u,n}\alpha_{d,n} < 1\ \forall\, n \in \mathcal{N}$, there exists at least one Nash equilibrium strategy in the two users scenario [32]. With some algebraic manipulation, it can be shown that this condition is satisfied when

$$\beta < \min_{n\in\mathcal{N}}\left(\frac{h_{u,n}h_{d,n}}{g_{u,d}}\right).$$

Considering the large-scale channel effect, i.e. the pathloss which is function of the users' distance from the base-station, the required self-interference cancellation β will be proportional to the users' pathloss and inversely proportional to the distance between the two users. The farther the users from the base-station, the more self-interference cancellation is required (i.e. lower β), also, the more distance between the users, the less self-interference cancellation needed (i.e. higher β). For practical scenarios, it can be shown that this condition is generally satisfied. The largest pathloss values will occur when both users are at the cell-edge, i.e. for a base-station communication range up to 200m, this means at the worst case scenario both users are 200m from the base-station. Figure 8 shows an example of the required self-interference cancellation, β, to satisfy the condition (3.4.2.11) versus the distance between the two users, for the worst case scenario (200m) and more moderate case (100m). It can be noticed that even for the worst case scenario, the Nash equilibrium existence condition (3.4.2.11) can be satisfied with the current reported self-interference cancellation values. Note that a base-station's communication range is usually less than 100m in a small cell. Clearly, considering the interference from the other user as noise, the optimal power allocation strategy for each user is water-filling. Consequently, the Nash equilibrium can be reached by iteratively performing water-filling considering the interference from the other user. When the condition (3.4.2.11) satisfied, the iterative water-filling is guaranteed to reach to an equilibrium from any starting point.

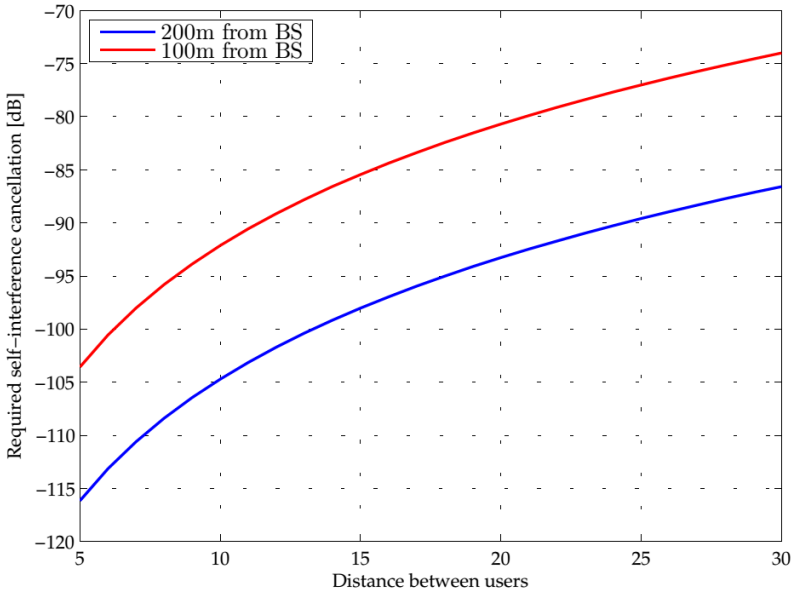

Figure 8: Required self-interference cancellation for different users' distances.

We now extend the non-cooperative game to the multiuser scenario. For a given uplink power allocation, the downlink subcarrier and power allocation can be formulated as follows

$$\max_{x_{j,n},p_n} \sum_{j\in\mathcal{J}} \sum_{n\in\mathcal{N}} x_{j,n} \log_2 \left(1 + \frac{p_n h_{j,n}}{\sigma_e^2 + I_{j,n}}\right), \tag{3.4.2.16}$$

subject to equations (3.4.2.6) and (3.4.2.7). The optimal solution for this problem can be found by allocating each subcarrier to the user that has the maximum unit power Signal to Interference-plus-Noise Ratio (SINR), i.e.

$$j_n^\star = \arg\max_{j\in\mathcal{J}} \left(\frac{h_{j,n}}{\sigma_e^2 + I_{j,n}}\right), \quad \forall \in \mathcal{N}. \tag{3.4.2.17}$$

Then, the base-station power is distributed over the subcarriers through water-filling policy. Thus, the downlink rate will be

$$R_{DL} = \sum_{n \in \mathcal{N}} \log_2 \left(1 + p_n \tilde{h}_n^{dl}\right), \tag{3.4.2.18}$$

where

$$\tilde{h}_n^{dl} = \max_{j \in \mathcal{J}} \left(\frac{h_{j,n}}{\sigma_e^2 + \sum_{k \in \mathcal{K}} p_{k,n} g_{k,j}} \right). \tag{3.4.2.19}$$

The downlink power allocation will be

$$p_n = \left[\frac{1}{\lambda} - \frac{1}{\tilde{h}_n^{dl}} \right]^+ \tag{3.4.2.20}$$

where $[x]^+ = \max(0, x)$ and λ is known as the water-level that should satisfy the power constraint in Eq. (3.4.2.7). It can be noticed that the multiuser downlink channel after optimal subcarrier allocation Eq. (3.4.2.17) can be represented by an *effective* single user with channel gains given by Eq. (3.4.2.19). Now, for a given downlink power allocation, the uplink power allocation is the solution for the following problem

$$\max_{p_{k,n}} \sum_{k \in \mathcal{K}} \sum_{n \in \mathcal{N}} \log_2 \left(1 + \frac{p_{k,n} h_{k,n}}{\sigma_b^2 + I_{k,n} + p_n \beta}\right), \tag{3.4.2.21}$$

Subject to Eq. (3.4.2.8), where the objective function Eq. (3.4.2.21) can be reformulated as

$$\max_{p_{k,n}} \sum_{n \in \mathcal{N}} \log_2 \left(1 + \frac{\sum_{k \in \mathcal{K}} p_{k,n} h_{k,n}}{\sigma_b^2 + p_n \beta}\right). \tag{3.4.2.22}$$

This problem represents a classical multicarrier multiple access channel, and the global optimal power allocation can be found by iterative water-filling [33]. Hence, there is optimal power allocation strategy for the uplink users given the downlink subcarrier and power allocation, and there is optimal subcarrier and power allocation strategy for the downlink users given the uplink power allocation. Therefore, the multiuser resource allocation can be formulated as non-cooperative game between the uplink and the downlink channels, where the downlink channel represented by an *effective* user with channel gains given Eq. (3.4.2.19) and water-filling as the optimal power allocation in response to the uplink power allocation. The uplink channel is also represented by *effective* user with iterative water-filling as the optimal power allocation in response to the downlink power allocation. Consequently, by iteratively implementing the optimal resource allocation in the uplink and downlink, an equilibrium can be reached. The detailed algorithm is listed in ALGORITHM 5.

Initialization: Set $p_n = 0,\ \forall n \in \mathcal{N}$ and $p_{k,n} = 0,\ \forall k \in \mathcal{K},\ n \in \mathcal{N}$.
repeat
1) ***Optimal uplink power allocation:***
for $k = 1$ to K **do**
Perform water-filling over $(\sigma_b^2 + p_n\beta + \sum_{i \in \mathcal{K} \setminus k} p_{i,n} h_{i,n})$
end for
2) ***Optimal downlink subcarrier and power allocation:***
Find the maximum SINR for each subcarrier:
$\tilde{h}_n^{dl} = \max_{j \in \mathcal{J}} \left(\frac{h_{j,n}}{\sigma_e^2 + \sum_{k \in \mathcal{K}} p_{k,n} g_{k,j}} \right)$
Perform water-filling for the downlink over $\tilde{h}_n^{dl}$
until Stopping criterion is reached.

ALGORITHM 5. Iterative radio resource allocation.

3.4.3. Radio resource allocation FD-UEs & FD-BS

In this section, we consider the radio resource allocation for single-cell with a full-duplex base-station that communicates with full-duplex users' terminals through multicarrier orthogonal channels, as shown in Figure 9. The subcarriers are exclusively allocated to the users to ensure orthogonality among the users and, thus, eliminate the inter-user interference. In this setting, each user is allocated a set of subcarriers used for uplink and downlink transmissions simultaneously.

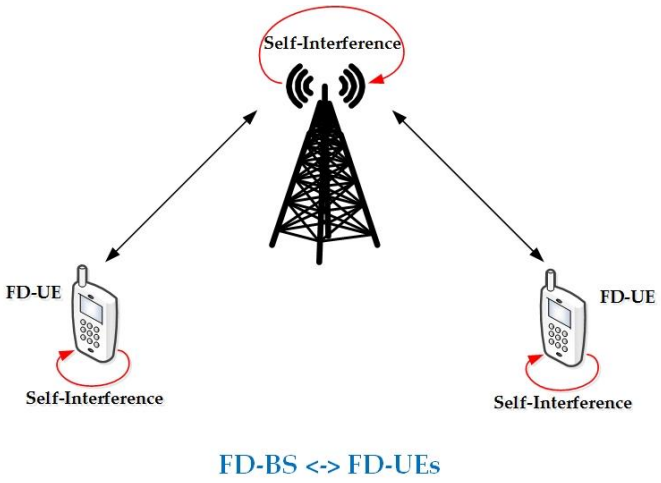

Figure 9: Full-duplex users and Full-duplex base-station scenario

The *k*th user rate on the nth subcarrier in the downlink channel is given by

$$R_{k,n}^{DL} = \log_2 \left(1 + \frac{p_n h_{k,n}}{\sigma_e^2 + p_{k,n}\alpha} \right), \tag{3.4.3.1}$$

where α represents the self-interference cancellation factor at the user equipment. Similarly, for the uplink channel, the users' rate on each subcarrier will be

$$R_{k,n}^{UL} = \log_2\left(1 + \frac{p_{k,n}h_{k,n}}{\sigma_b^2 + p_n\beta}\right), \tag{3.4.3.2}$$

Our proposed algorithm consists of two steps. At the first step, the subcarrier allocation problem is addressed. In the second step, the power allocation for uplink and downlink channels is considered. For subcarrier allocation, it can be noticed from (3.4.3.1) and (3.4.3.2) that the channel gain affects the user rate in uplink and downlink. Thus, to maximize the system sum-rate, greedy subcarrier allocation algorithm is considered, where each subcarrier is allocated to the user with the best channel condition on that subcarrier as follows

$$x_{k,n} = 1, \ \text{if}, \ k = \arg\max_{k\in\mathcal{K}}(h_{k,n}) \tag{3.4.3.3}$$

For a given subcarrier allocation, the power allocation problem is formulated as

$$\max_{p_n,p_{k,n}} \sum_{n\in\mathcal{N}} \log_2\left(1+\frac{p_n\tilde{h}_n}{\sigma_e^2 + p_{k,n}\alpha}\right) + \log_2\left(1+\frac{p_{k,n}\tilde{h}_n}{\sigma_b^2 + p_n\beta}\right), \tag{3.4.3.4}$$

subject to (3.4.2.7) and (3.4.2.8), where

$$\tilde{h}_n = \{h_{k,n} : x_{k,n} = 1\}. \tag{3.4.3.5}$$

It can be noticed that when each transmitter (uplink or downlink) increases its power, it will increase its data rate, however, at the same time it will increase the interference on the other game between the uplink and downlink channels. In this game, each transmitter attempts to maximise its performance regardless of the other transmitter performance. This process can be done continuously, and it will converge if there is an equilibrium point. This equilibrium is referred to as Nash equilibrium, which is defined as a strategy set in which each transmitter strategy is an optimal response to the other transmitter's strategy.

It can be noticed that the multiuser downlink channel after subcarrier allocation can be represented by an effective single user with channel gains given by (3.4.3.5). Thus, for a given uplink power allocation, the downlink power allocation can be formulated as follows

$$\max_{p_n} \sum_{n\in\mathcal{N}} \log_2\left(1 + \frac{p_n\tilde{h}_n}{\sigma_e^2 + p_{k,n}\alpha}\right), \tag{3.4.3.6}$$

subject to (3.4.2.7). This problem represents a classical multi-carrier single user channel, and the global optimal power allocation can be found by water-filling. For a given downlink power allocation, the uplink power allocation can be decomposed into K power allocation sub-problems, each for a single-user. Again, the optimal power allocation can be obtained by single-user water-filling.

Hence, there is optimal power allocation strategy for the uplink transmission given the downlink power allocation, and there is optimal power allocation strategy for the downlink transmission given the uplink power allocation. Therefore, the multiuser power allocation can be formulated as non-cooperative game between the uplink and the downlink channels, where the downlink channel represented by an effective user with the channel gain given by (3.4.3.5) and water-filling as the optimal power allocation in response to the uplink power allocation. The uplink channel is also represented by effective user with water-filling as the optimal power allocation in response to the downlink power allocation. Consequently, the Nash equilibrium can be reached by iteratively performing the optimal water-filling in the uplink and downlink considering the interference from the other transmission direction. The detailed algorithm is listed in ALGORITHM 6.

Initialization: Set $p_{k,n} = 0,\ \forall k \in \mathcal{K},\ n \in \mathcal{N}$.
1) ***Subcarriers allocation:*** $\tilde{h}_n = \max_{k \in \mathcal{K}}(h_{k,n})$.
repeat
  1) *Optimal downlink power allocation:*
  Perform water-filling for the downlink
  2) *Optimal uplink power allocation:*
  for $k = 1$ to K **do**
    Perform water-filling over for the kth user
  end for
until Stopping criterion is reached.

ALGORITHM 6. Iterative radio resource allocation for FD-UEs and FD-BS.

3.5. Multiple MIMO HD UEs per FD BS

In this section, we consider a full-duplex cellular system, in which a full-duplex base-station communicates with *K* uplink and *J* downlink users operating in half-duplex mode, simultaneously as seen in Figure 10. The number of data streams transmitted from the *k*-th uplink user (to the *j*-th downlink user) is denoted by d_k^{UL} $\left(d_j^{DL}\right)$. In addition to self-interference channel at the base-station, the co-channel interference (CCI) caused by the uplink users to downlink users is also taken into account, which increases the difficulty of the optimization problem further. Full-duplex multi-user systems has been investigated in [25]-[27]. However the CCI is not taken into account in [26], and single-antenna users are assumed in [25]. Moreover, [25]-[27] ignores several fundamental impediments of FD systems, i.e. transmitter and receiver distortion caused by non-ideal amplifiers, oscillators, ADCs/DACs, etc., i.e., several system parameters were ideally assumed. These practical considerations are carefully examined in our works in [22]-[24].

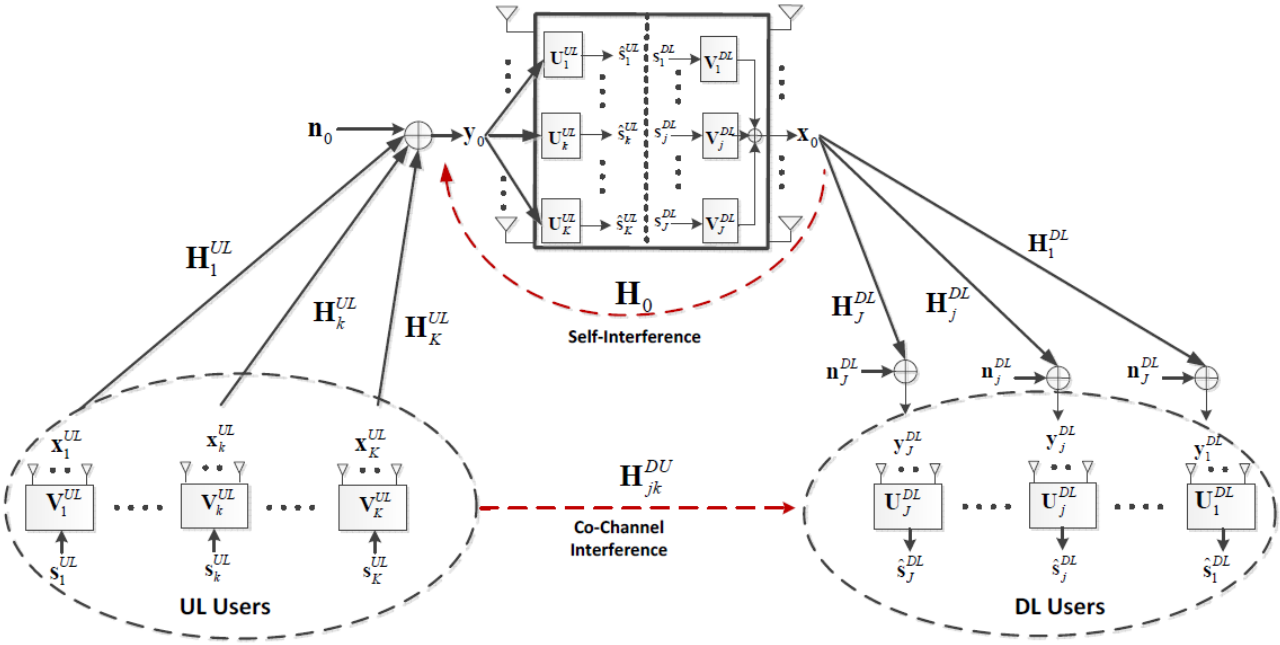

Figure 10: Full-duplex multi-user MIMO system model

The weighted-sum-rate maximization (WSR) problem can be formulated as:

$$\begin{aligned}
\max_{\substack{\mathbf{v}_{k,m}^{UL},\mathbf{u}_{k,m}^{UL}\\ \mathbf{v}_{j,m}^{DL},\mathbf{u}_{j,m}^{DL}}} \quad & \sum_{k=1}^{K}\mu_k^{UL}\sum_{m=1}^{d_k^{UL}}\log_2\left(1+\gamma_{k,m}^{UL}\right) \\
& \quad +\sum_{j=1}^{J}\mu_j^{DL}\sum_{m=1}^{d_j^{DL}}\log_2\left(1+\gamma_{j,m}^{DL}\right) \\
\text{s.t.} \quad & \sum_{m=1}^{d_k^{UL}}\left(\mathbf{v}_{k,m}^{UL}\right)^H\mathbf{v}_{k,m}^{UL}\le P_k,\ \ k\in\mathcal{S}^{UL}, \\
& \sum_{j=1}^{J}\sum_{m=1}^{d_j^{DL}}\left(\mathbf{v}_{j,m}^{DL}\right)^H\mathbf{v}_{j,m}^{DL}\le P_0,
\end{aligned} \tag{3.5.1}$$

where $\mathbf{v}_{k,m}^{UL}$ and $\mathbf{u}_{k,m}^{UL}$ are the precoding and receive matrices for the *m*-th stream of the *k*-th uplink user, respectively, and $\mathbf{v}_{j,m}^{DL}$ and $\mathbf{u}_{j,m}^{DL}$ are the precoding and receive matrices for the *m*-th stream of the *j*-th downlink user. P_k is the transmit power constraint at the *k*-th uplink user, P_0 is the total power constraint at the base-station, and $m_k^{UL}\left(m_j^{DL}\right)$ is the weight at the *k*-th (*j*-th) uplink (downlink) user. Here, $g_{k,m}^{UL}$ and $g_{j,m}^{DL}$ are the SINR of the *m*-th stream of *k*-th uplink and *j*-th downlink user given as:

$$\gamma_{k,m}^{UL}=\frac{\left|\left(\mathbf{u}_{k,m}^{UL}\right)^H\mathbf{H}_k^{UL}\mathbf{v}_{k,m}^{UL}\right|^2}{\left(\mathbf{u}_{k,m}^{UL}\right)^H\boldsymbol{\Sigma}_k^{UL}\mathbf{u}_{k,m}^{UL}+\sum_{n\neq m}^{d_k^{UL}}\left|\left(\mathbf{u}_{k,m}^{UL}\right)^H\mathbf{H}_k^{UL}\mathbf{v}_{k,n}^{UL}\right|^2},$$

$$\gamma_{j,m}^{DL}=\frac{\left|\left(\mathbf{u}_{j,m}^{DL}\right)^H\mathbf{H}_j^{DL}\mathbf{v}_{j,m}^{DL}\right|^2}{\left(\mathbf{u}_{j,m}^{DL}\right)^H\boldsymbol{\Sigma}_j^{DL}\mathbf{u}_{j,m}^{DL}+\sum_{n\neq m}^{d_j^{DL}}\left|\left(\mathbf{u}_{j,m}^{DL}\right)^H\mathbf{H}_j^{DL}\mathbf{v}_{j,n}^{DL}\right|^2}. \tag{3.5.2}$$

Here, $\mathbf{H}_k^{UL}$ and $\mathbf{H}_j^{DL}$ represent the *k*-th uplink channel and the *j*-th downlink channel, respectively, and $\boldsymbol{\Sigma}_k^{UL}\left(\boldsymbol{\Sigma}_j^{DL}\right)$ is the aggregate interference-plus-noise terms at the *k*-th uplink (*j*-th downlink) user.

Note that this optimization problem is not jointly convex over transmit precoding matrices and receiving filter matrices, but is component-wise convex. Since it is not jointly convex, we cannot apply the standard convex optimization methods to obtain the optimal solution. Therefore, we will employ an iterative algorithm that finds the efficient solutions. Under fixed transmit precoding matrices, the optimum receive filters are computed as minimum-mean-squared-error (MMSE) filters, and to compute the optimum precoding matrices under the fixed receiving filters, we exploit the relationship between WSR and Weighted Minimum-Mean-Squared-Error (WMMSE) [28] problems for full-duplex MIMO cellular systems, and an alternating iterative algorithm to find a local WSR optimum is proposed.

3.6. Optimum User Selection for Hybrid-Duplex Device-to-Device in Cellular Networks

3.6.1. Introduction

Device-to-device (D2D) communications has been considered as a key technique in 5th generation (5G) communications because of its several advantages, i.e., throughput enhancement, user equipment power savings, and instantaneous data rate increase [34]. For D2D underlay cellular networks, D2D users send data signals to each other over a direct link by reusing cellular resources, similar to the secondary user scenario introduced in cognitive radio systems [35]. However, the major differences between the D2D and cognitive radio systems is the radio resource usage can be controlled in cooperation with cellular networks in the D2D underlay scenario, whereas the secondary user in cognitive radio systems is not controlled by the primary user networks [36].

Furthermore, current wireless communication networks usually employ half-duplex model. Most existing work has been targeted at half duplex device-to-device (HD-D2D) networks including resource allocation [37], and power optimization [38]. However half-duplex transmission incurs 50% loss in spectral efficiency. In order to improve spectral efficiency, full duplex transmission, which was previously considered impractical due to the associated self-interference (SI), has been considered recently because of the advances in SI cancelation approaches (e.g. [39] and [40]). Furthermore, [41] and [42] have combined the concepts of full duplex and D2D to improve the system sum-rate, because it can harvest the advantages of both technologies to improve the spectral efficiency of wireless communications. Most previous works implied Doppler's mechanism [36] in which the base station (BS) controls the maximum transmit power of the D2D transmitter which can efficiently manage the D2D interference to BS in upper link. However the interference from cellular user to D2D receiver has not been considered in aforementioned works.

In this chapter, we consider cellular user selection scheme in hybrid-duplex D2D cellular networks with uplink underlaying policy, where one BS, one D2D pair and K available cellular users. We not only consider efficient interference coordination to prevent harmful interference to BS, but also achieve throughput enhancement of D2D systems by proper design of the cellular user selection scheme. We can also switch the hybrid-duplex between half and full duplex according to residual SI to improve the throughput of D2D link. Moreover, satisfying these conditions makes it very hard to obtain the distribution of the SINR and the related outage probability at the D2D node. The main contribution of this paper, therefore, is to derive an integral-form expression of the outage probability for the cellular user selection in hybrid-duplex D2D cellular networks. The analysis not only provides a deep insight into understanding cellular user selection in an interference limited D2D cellular system, but also suggestion an interesting way for analysing similar systems.

3.6.2. System Model

A cellular network with hybrid-duplex D2D is shown in **Error! Reference source not found.**, where there is one cellular base station and K available users (The available users means the users that can be guaranteed a reliable communicate with BS) from S_1 to S_K and a hybrid-duplex D2D pair. We assume the BS and each user are half-duplex devices and D2D pair can switch between half-duplex and full-duplex modes. The channels S_i to BS, D_1 to BS, D_2 to BS, S_i to D_1, S_i to D_2, D_1 to $D_1$and D_2 to D_2, which are denoted as h_{s_ib}, h_{d_1b}, h_{d_2b}, $h_{s_id_1}$, $h_{s_id_2}$, $h_{d_1d_1}$ and $h_{d_2d_2}$, respectively, are independently Rayleigh flat fading, and keep unchanged within one packet but may vary from one packet to another have been assumed. Therefore, the corresponding channel gains, obtained as $\gamma_j = |h_j|^2$~(j $\in\{ s_ib, d_1b, d_2b, s_id_1, s_id_2, d_1d_1, d_2d_2\}$) respectively, are independently exponentially distributed with mean of λ_j, respectively. We assume the channel information between each user and full-duplex device-to-device (FD-D2D) pair can be obtained by the BS (The CSI is usually estimated through pilots and feedback (e.g. [43]), and the CSI estimation without feedback may also be applied (e.g. [44]), which are beyond the scope of this paper). In the cellular cell, the K available users attempt to transmit signals to the base station BS by using uplink resource. In order to enhance the throughput of D2D link, the best user will be selected by BS and share same uplink resources (i.e., time slot and frequency bin) with current D2D user.

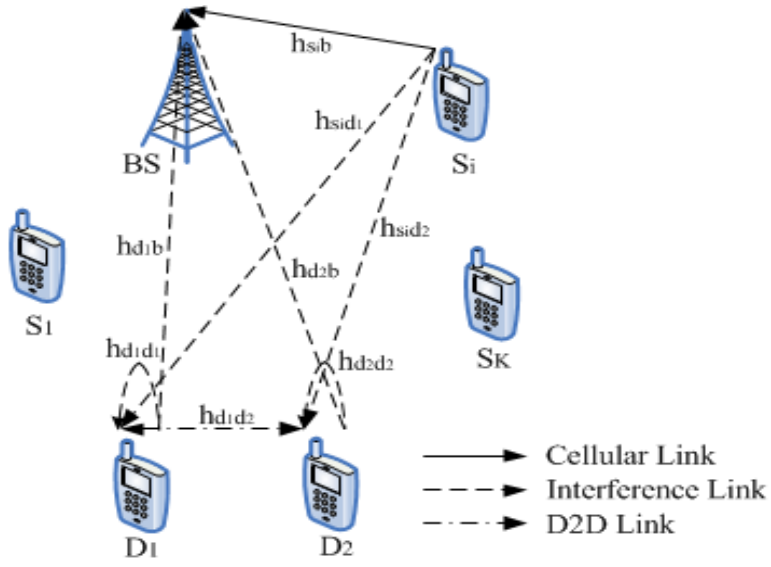

Figure 11: A cellular network with a hybrid-duplex D2D pair and K available cellular users with three different links.

In our proposed system, the maximum power of D2D transmitter is strictly limited so as not to generate any harmful interference to BS, and can be defined

$$P_{d_1} \le \min\left(\frac{I_{th}}{\gamma_{d_1b}}, \overline{P}\right) \quad \text{and} \quad P_{d_2} \le \min\left(\frac{I_{th}}{\gamma_{d_2b}}, \overline{P}\right) \tag{3.6.2.1}$$

where I_{th} is the interference threshold, and $\bar{P}$ is the maximum transmission power as in [39]. All noises are additive white Gaussian noise. Without losing generality, the noise variances and

transmission power P_s for the each cellular user are all normalized to unity. In the next section, we will analyze the cellular user selection for half duplex D2D transmission.

3.6.3. Cellular user selection in half duplex D2D networks

For half duplex D2D system, D_1 transmits signal to D_2 sharing uplink radio resource with the selected user. Therefore, the received signal according to different time slots at the D_2 is given by

$$\mathbf{y}_{d_2,i}^H = \sqrt{P_{d_1}}\mathbf{x}_{d_1}h_{d_1d_2} + \sqrt{P_s}\mathbf{x}_s h_{s_id_2} + \mathbf{n}_{d_2}, \tag{3.6.3.1}$$

where $\mathbf{x}_{d_1}$and$\mathbf{x}_s$are transmission vectors from $D_1$and S_i, respectively, and $\mathbf{n}_{d_2}$is the noise vector at D_2 with zero mean and covariance matrix of $\sigma_{d_2}^2\boldsymbol{I}$, where $\boldsymbol{I}$ is an identity matrix. According to (3.6.2.1) and (3.6.3.1), at high SNRs, the instantaneous SINR from D_1 to D_2 can be obtained as

$$\gamma_{d_2,i}^H = \frac{P_{d_1}|h_{d_1d_2}|^2}{P_s|h_{s_id_2}|^2 + \sigma_{d_2}^2} \simeq \frac{\min\left(\frac{I_{th}}{\gamma_{d_1b}}, \overline{P}\right)\gamma_{d_1d_2}}{\gamma_{s_id_2}} \tag{3.6.3.2}$$

where $\gamma_{d_1d_2}$and $\gamma_{s_id_2}$are channel gains between D_1 and D_2 and between $S_i$and D_2, respectively. In this work, the SINR of D2D link can be enhanced by the optimum cellular user selection as

$$\gamma_{d_2}^H = \max_{i\in K}\{\gamma_{d_2,i}^H\} = \frac{\min\left(\frac{I_{th}}{\gamma_{d_1b}}, \overline{P}\right)\gamma_{d_1d_2}}{\min\limits_{i\in K}\{\gamma_{s_id_2}\}} \tag{3.6.3.3}$$

Next, we first derive expressions for the probability density function (PDF) and cumulative distribution function (CDF) of the SINR in (3.6.3.3), and then obtain the outage probability for the D2D pair. For better exposition, we let $x = \gamma_{d_1b}$, $y = \gamma_{d_1d_2}$ and $w = \min\limits_{i\in K}\{\gamma_{s_id_2}\}$and the PDF of y is $f_Y(y) = 1/\lambda_{d_1d_2}e^{-y/\lambda_{d_1d_2}}$ and the CDF of ω can be obtained as

$$F_W(w) = e^{-\frac{K}{\lambda_{sd_2}w}}. \tag{3.6.3.4}$$

The CDF of t = yw can thus be derived as

$$F_T(t) = \int_0^\infty f_Y(y)F_W(t/y)dy = \frac{\lambda_{sd_2}t}{K\lambda_{d_1d_2} + \lambda_{sd_2}t}. \tag{3.6.3.5}$$

Next we can obtain the CDF of $\gamma_{d_2} = \min\left(\frac{I_{th}}{x}, \overline{P}\right)t$ as

$$F_{\gamma_{d_2}^H}(\gamma) = \int_{I_{th}/\overline{P}}^\infty \int_0^{\gamma x/I_{th}} f_X(x)f_T(t)dtdx + \int_0^{I_{th}/\overline{P}} \int_0^{\gamma/\overline{P}} f_X(x)f_T(t)dtdx \tag{3.6.3.6}$$

$$= \frac{\lambda_{sd_1}\gamma + K\overline{P}\lambda_{d_1d_2}e^{-\frac{I_{th}}{\overline{P}\lambda_{d1b}}}}{K\overline{P}\lambda_{d_1d_2} + \lambda_{sd_2}\gamma} - \alpha e^{\varphi}\mathrm{Ei}(1, \varphi + \frac{1}{\overline{P}\lambda_{d_1b}})$$

where $\varphi = \frac{I_{th}K\lambda_{d_1d_2}}{\lambda_{sd_2}\gamma\lambda_{d_1b}}$ and Ei(1,a) is an exponential integral as $\mathrm{Ei}(1,a) = \int_1^\infty \frac{\exp(-ta)}{a}dt, a > 0$

The outage event occurs when the SINR at the D2D pair falls below a certain target level. From (3.6.3.6), the outage probability for the proposed relay selection system is given by

$$P_{out}^{H} = \int_{0}^{\alpha} f_{\gamma_{d_2}^{H}}(\gamma) d\gamma = F_{\gamma_{d_2}^{H}}(\alpha), \tag{3.6.3.7}$$

where α is the pre-defined target SINR which is $2^{R_T} - 1$. In this work we consider the delay-limited transmission mode, where the average throughput can be calculated by the outage probability of the system at a fixed transmission rate R_T b/s/Hz. In the HD-D2D scenario, the throughput can be calculated as

$$T_H = R_T(1 - P_{out}^{H}). \tag{3.6.3.8}$$

In the next section, the FD-D2D scenario will be analysed.

3.6.4. Cellular user selection in full duplex D2D networks

For FD-D2D systems, the best cellular user will be selected from K available users to share the same uplink radio resources with a FD-D2D pair, and D_1 and D_2 transmit signals to each other enabled by SI cancellation. As we mention earlier, with the current state-of-the-art technology, the SI can be nearly cancelled to noise level [39] and [40]. Therefore, the received signal according to different time slots at the D_2 is given by

$$\mathbf{y}_{d_2,i}^{F} = \sqrt{P_{d_1}}\mathbf{x}_{d_1} h_{d_1 d_2} + \sqrt{P_{d_2}}\mathbf{x}_{d_2} h_{d_2 d_2} + \sqrt{P_s}\mathbf{x}_s h_{s_i d_2} + \mathbf{n}_{d_2}, \tag{3.6.4.1}$$

where $\mathbf{x}_{d_2}$ is transmission vectors from D_2. According to (3.6.2.1) and (3.6.3.8), at high SNRs, the instantaneous SINR at D_2 can be obtained as

$$\gamma_{d_2,i}^{F} = \frac{P_{d_1}|h_{d_1 d_2}|^2}{P_{d_2}|h_{d_2 d_2}|^2 + P_s|h_{s_i d_2}|^2 + \sigma_{d_2}^2} \simeq \frac{\min\left(\frac{I_{th}}{\gamma_{d_1 b}}, \overline{P}\right)\gamma_{d_1 d_2}}{\min\left(\frac{I_{th}}{\gamma_{d_2 b}}, \overline{P}\right)\gamma_{d_2 d_2} + \gamma_{s_i d_2}}. \tag{3.6.4.2}$$

The maximum capacity of FD-D2D link can be obtained by the optimum cellular user selection as

$$\gamma_{d_2}^{F} = \max_{i \in K}\left\{\gamma_{d_2,i}^{F}\right\} = \frac{\min\left(\frac{I_{th}}{\gamma_{d_1 b}}, \overline{P}\right)\gamma_{d_1 d_2}}{\min\left(\frac{I_{th}}{\gamma_{d_2 b}}, \overline{P}\right)\gamma_{d_2 d_2} + \min\limits_{i \in K}\left\{\gamma_{s_i d_2}\right\}}. \tag{3.6.4.3}$$

Next, we derive expressions for the PDF and CDF of the SINR in (3.6.4.3), and then obtain the outage probability for the overall system. For better exposition, we let $z = \gamma_{d_2 b}$, the PDF of z is $f_Z(z) = 1/\lambda_{d_2 b} e^{-z/\lambda_{d_2 b}}$.Therefore, by using the same calculation as (3.6.3.6), the CDF and PDF of $A = \min\left(\frac{I_{th}}{\gamma_{d_1 b}}, \overline{P}\right)\gamma_{d_1 d_2}$ can be derived as

$$F_A(a) = 1 - e^{-\frac{a}{\overline{P}\lambda_{d_1 d_2}}} + \frac{\lambda_{d_1 b} a}{I_{th}\lambda_{d_1 d_2} + \lambda_{d_1 b} a} e^{-\frac{I_{th}\lambda_{d_1 d_2} + \lambda_{d_1 b} a}{\overline{P}\lambda_{d_1 d_2}\lambda_{d_1 b}}}, \tag{3.6.4.4}$$

$$f_A(a) = \frac{e^{-\frac{a}{\overline{P}\lambda_{d_1 d_2}}}}{\overline{P}\lambda_{d_1 d_2}} + \frac{\lambda_{d_1 b}(I_{th}\lambda_{d_1 d_2}^2\overline{P} - \lambda_{d_1 b} a - I_{th}\lambda_{d_1 d_2}^2 a)}{(I_{th}\lambda_{d_1 d_2} + \lambda_{d_1 b} a)^2 \lambda_{d_1 d_2}\overline{P}} e^{-\frac{I_{th}\lambda_{d_1 d_2} + \lambda_{d_1 b} a}{\overline{P}\lambda_{d_1 d_2}\lambda_{d_1 b}}}, \tag{3.6.4.5}$$

respectively, and the CDF of $B = \min\left(\frac{I_{th}}{\gamma_{d_2 b}}, \overline{P}\right)\gamma_{d_2 d_2}$ an be obtained as

$$F_B(b) = 1 - e^{-\frac{b}{\overline{P}\lambda_{d_2d_2}}} + \frac{\lambda_{d_2b}b}{I_{th}\lambda_{d_2d_2} + \lambda_{d_2b}b} e^{-\frac{I_{th}\lambda_{d_2d_2}+\lambda_{d_2b}b}{\overline{P}\lambda_{d_2d_2}\lambda_{d_2b}}}. \tag{3.6.4.6}$$

Then the CDF of D = B+w is obtained as

$$\begin{aligned} F_D(d) &= \int_0^d \int_0^{d-w} f_B(b) f_W(w) dbdw \\ &= -\frac{1}{\lambda_{d_2b}\lambda_{sd_2}(K)\overline{P}}[I_{th}K^2\overline{P}\lambda_{d_2d_2}^2\nu(Ei(1,\theta) \\ &- \mathrm{Ei}(1,\mu)) - K\overline{P}\lambda_{d_2b}\lambda_{d_2d_2}\lambda_{sd_2}(1 - e^{-\frac{d}{\overline{P}\lambda_{d_2d_2}}}) \\ &- I_{th}K\overline{P}\lambda_{d_2d_2}\lambda_{sd_2}\nu(\mathrm{Ei}(1,\theta) - \mathrm{Ei}(1,\mu)) \\ &- K\overline{P}\lambda_{d_2d_2}\lambda_{sd_2}\lambda_{d_2b}(e^{-\frac{I_{th}\lambda_{d_2d_2}+d\lambda_{d_2b}}{\overline{P}\lambda_{d_2b}\lambda_{d_2d_2}}} \\ &- e^{-\frac{I_{th}\lambda_{sd_2}+dK\overline{P}\lambda_{d_2b}}{\overline{P}\lambda_{d_2b}\lambda_{sd_2}}}) + \lambda_{d_2b}\lambda_{sd_2}^2(1 - e^{-\frac{Kd}{\lambda_{sd_2}}})], \end{aligned} \tag{3.6.4.7}$$

where $\theta = -\frac{I_{th}(K\overline{P}\lambda_{d_2d_2}-\lambda_{sd_2})}{\overline{P}\lambda_{d_2b}\lambda_{sd_2}}$, $\mu = -\frac{I_{th}K\overline{P}\lambda_{d_2d_2}^2+K\overline{P}d\lambda_{d_2b}\lambda_{d_2d_2}+I_{th}\lambda_{sd_2}\lambda_{d_2d_2}-d\lambda_{sd_2}\lambda_{d_2b}}{\overline{P}\lambda_{sd_2}\lambda_{d_2b}\lambda_{d_2d_2}}$ and $\nu = e^{-\frac{(I_{th}\lambda_{d_2d_2}+d\lambda_{d_2b})K}{\lambda_{d_2b}\lambda_{sd_2}}}$.

Finally, according to (3.6.4.4) and (3.6.4.7), the CDF of γ_{d2}^F can be obtained as

$$F_{\gamma_{d2}^F}(\gamma) = \int_0^\infty f_A(a) F_D(a/\gamma) da \tag{3.6.4.8}$$

While (3.6.4.8) is in an integral form, it can be easily evaluated numerically with, for example Matlab or Maple [45]. We can derive the outage probability from D_1 to D_2 as $P_{out}^{F_1}$ by using the same method as (3.6.3.8). Furthermore, in the delay-limited transmission mode, the average throughput can be calculated by the outage probability of the system at a fixed transmission rate. The throughput of FD-D2D scenario can be calculated as

$$T_F = R_T(1 - P_{out}^{F_1}) + R_T(1 - P_{out}^{F_2}), \tag{3.6.4.9}$$

where $P_{out}^{F_2}$ is the outage probability from D_2 to D_1 which can be calculated by the same method with $P_{out}^{F_1}$.

4. RADIO RESOURCE MANAGEMENT IN MULTI CELL DEPLOYMENTS

4.1. Multiple FD UEs per FD BS

4.1.1. Network Model and Assumptions

Consider an interference-limited scenarios where all nodes operate in FD fashion, as shown in Figure 12. Figure 13 illustrates a realization of the random topology where UEs and small cell BSs are uniformly scattered over network area. Moreover, devices that transmit and receive simultaneously are exposed to strong self-interference, and all nodes have separated antennas for transmission and reception. Even though advanced interference cancellation and antenna attenuation techniques are utilized, there still exists a residual self-interference level [2]-[6], which can be modelled as a composite fading model that one can emulate various (non) line-of-sight configurations [3]. We assume that all channel coefficients are quasi-static and follow a composite fading channel distribution, which combines Log-Normal (LN) shadowing and Nakagami-m fading.

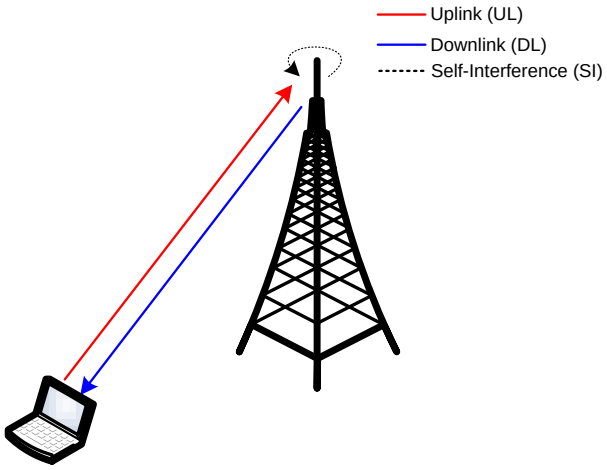

Figure 12: System model: FD UE communicating to FD BS.

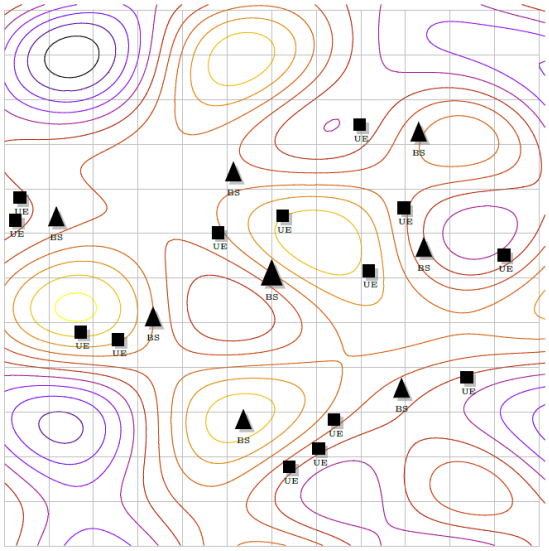

Figure 13: Illustration of a random deployment of small cells and user terminals over an arbitrary network area. Shaded squares represent user terminals, while shaded up-triangles depict small cell base stations. A heat map represents the corresponding random composite fading channel where the fading intensity varies from red/strong to dark blue/weak.

The DL of a traditional HD network constitutes our benchmark scenario wherein the user of interest is interfered by surrounding small cells. BSs independently schedule a random user in every transmission interval. All communicating nodes are equipped with omni-directional antennas. BSs and UEs are also assumed to have full buffer and symmetric traffic patterns. We resort to the analytical framework introduced in [1]-[2] to carry our investigations.

Following the steps 1 to 4 from **Procedure 1** we can determine the statistics of the perceived CCI at the user of interest, and then the corresponding SIR. We define the CCI at tagged FD receiver as

$$Z_0^{FD} = \delta\, p_{00} x_{00} + \sum_{(\varphi_i, x_i) \in \tilde{\Phi}_{BS}} Y_{i0} + \sum_{(\varphi_i, x_i) \in \tilde{\Phi}_{UE}} Y_{j0} \tag{4.1.1}$$

where p_{00} and δ represent the self-interference component and the respective attenuation factor, respectively. To account for the aggregate CCI from multiple interfering tiers we employ the cumulants additivity property. Since BSs and UEs are assumed to be independently deployed, the resulting process from each such tier is also independent. Note that the tagged receiver perceives, not only the interference from the neighboring BSs (first summand in Z_0^{FD}), but also the interference for the neighboring UEs (second summand in Z_0^{FD}), and self-interference.

4.1.2. Performance Metrics

We first analyze the spectral efficiency of such deployment. We recall that as discussed in [7] the aggregate interference perceived by the tagged receiver has non-Gaussian nature, and the Shannon formula is used as a lower bound for the ergodic rate. Bearing this in mind and assuming that all users are allocated on the same bandwidth W, we first recover the SIR distribution of the tagged receiver, and then compute the respective capacity. Thereby, the spectral efficiency in bits/s/Hz of the tagged receiver is

$$\frac{\bar{C}}{W} = \sum_{k=0}^{K} \frac{\omega_k}{\sqrt{\pi}} \log_2 \left[1 + e^{\frac{\eta_k \sqrt{2}\,\sigma + \mu}{\xi}} \right], \quad (4.1.2.1)$$

where K is the order of the Gauss-Hermite quadrature (degree of the Hermite polynomial), and $\eta = \left((\xi \ln \gamma - \mu) / \sqrt{2}\,\sigma \right)$ [8].

Next, we assess the performance of such networks by means of the resulting outage probability with regard to the tagged receiver. Note that the scenarios under consideration are interference limited and hence the thermal noise is negligible in comparison to the resulting aggregate CCI [9]. The outage probability is given by $\Pr[\Gamma < \gamma_{th}]$ where the RV Γ represents the SIR at the tagged receiver, and γ_{th} the corresponding SIR threshold. Then, by following the steps 1 until 4 from Procedure 1 we attain the parameters of the approximated distribution, namely V_0, which is a Normal RVs (in logarithmic scale) representing the power received from the desired transmitter and V the CCI at the user of interest.

With those results at hand, we can then determine the SIR at the receiver, which can be represented as $\Gamma \sim \text{Normal}\left(\mu_{V_0} - \mu_V, \sigma_{V_0}^2 + \sigma_V^2\right) \sim \text{Normal}(\mu_\Gamma, \sigma_\Gamma)$, which lead us to the an outage probability given as

$$\Pr[\Gamma < \gamma_{th}] = Q\left[\frac{\mu_\Gamma - \gamma_{th}}{\sigma_\Gamma}\right]. \quad (4.1.2.2)$$

The SIR distribution is given by the quotient of two independent LN RVs, namely, e^{V_0} which is the received power from the target transmitter, and e^{V} which corresponds to an equivalent LN RV of the aggregate CCI at the tagged receiver. Hence, the multiplicative reproductive property of LN RVs is applied to obtain the SIR distribution [8]. As discussed in [7] the aggregate interference perceived by the tagged receiver has non-Gaussian nature, and the Shannon formula is used as a lower bound for the ergodic rate.

Further discussions and results are introduced in Deliverable D.4.1.2.

4.2. MIMO FD BS with FD or HD UEs

In this subsection, we consider a multi-cell system consisting of full-duplex base-stations and full-duplex users. In addition to well-known interference sources in traditional multi-cell half-duplex systems, i.e., from uplink users to base-stations and from base-stations to downlink users, incorporating full-duplex empowered base-stations and users to traditional half-duplex cellular systems introduces new sources of interference due to simultaneous transmission and reception at all nodes in the system, 1) the self-interference at each full-duplex base-stations and users, 2) the interference among adjacent base-stations, i.e., inter-base-station interference, 3) CCI among all the users in all cells. The system model of a full-duplex multi-cell multi-user MIMO system is seen in Figure 14. We consider a *K* cell full-duplex system, where base-station *k* serves I_k users in cell *k*. We denote i_k to be the *i*-th user in cell *k.*

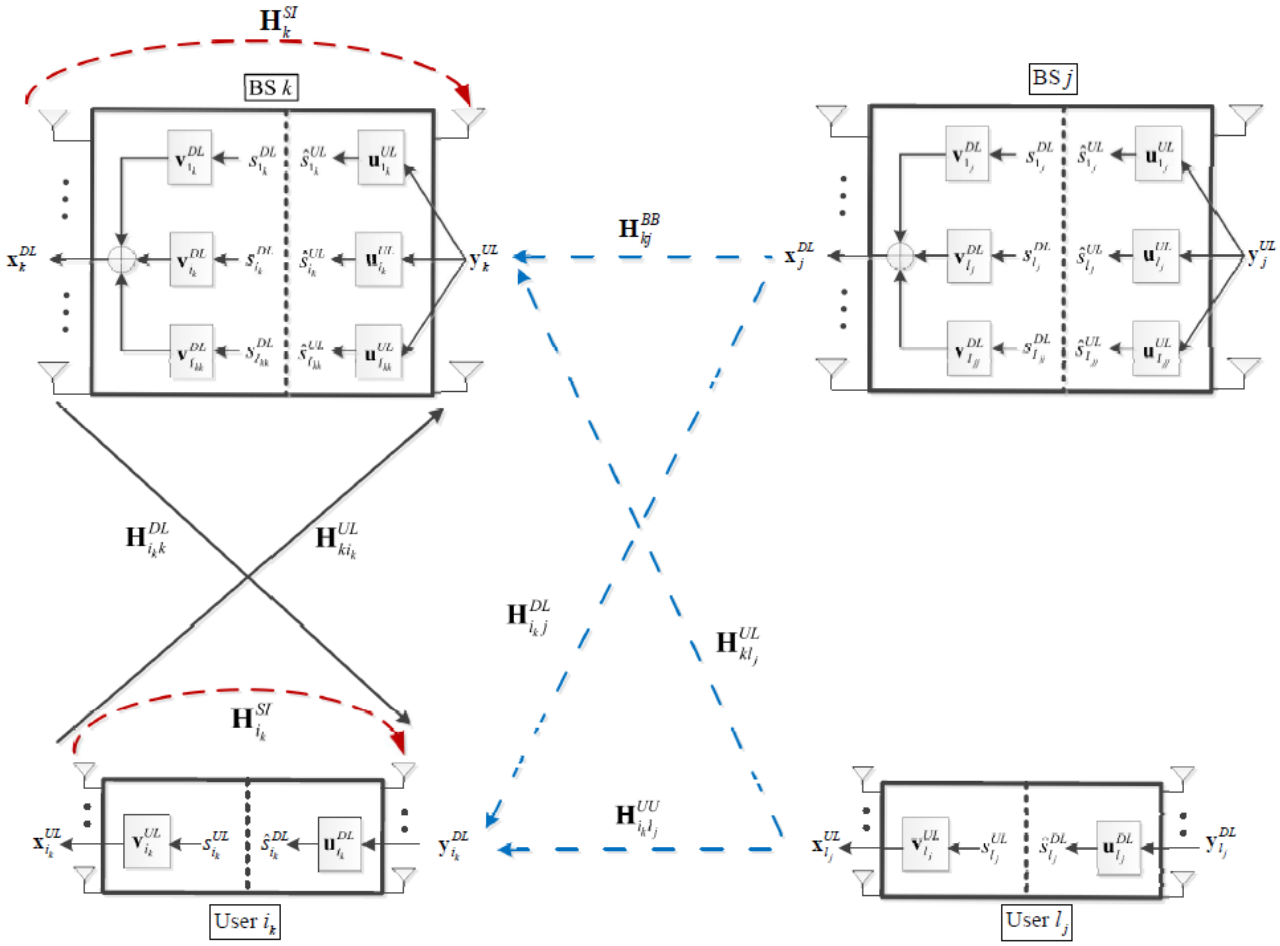

Figure 14: Full-duplex MIMO multi-cell system

The weighted sum-rate maximization problem to compute the optimum precoding vector $\mathbf{v}_{i_k}^{UL}\left(\mathbf{v}_{i_k}^{DL}\right)$ and the receiving vector $\mathbf{u}_{i_k}^{UL}\left(\mathbf{u}_{i_k}^{DL}\right)$ for the i_k-th user in the uplink (downlink) channel, can be formulated as:

$$\begin{aligned}
\max_{\substack{\mathbf{v}_{i_k}^{UL},\mathbf{u}_{i_k}^{UL} \\ \mathbf{v}_{i_k}^{DL},\mathbf{u}_{i_k}^{DL}}} \quad & \sum_{k=1}^{K}\sum_{i=1}^{I_k} \log_2\left(1+\gamma_{i_k}^{UL}\right) \\
& + \sum_{k=1}^{K}\sum_{i=1}^{I_k} \log_2\left(1+\gamma_{i_k}^{DL}\right) \\
\text{s.t.} \quad & \left(\mathbf{v}_{i_k}^{UL}\right)^H \mathbf{v}_{i_k}^{UL} \le P_{i_k},\ i_k \in \mathcal{I}, \\
& \sum_{i=1}^{I_k} \left(\mathbf{v}_{i_k}^{DL}\right)^H \mathbf{v}_{i_k}^{DL} \le P_k,\ k \in \mathcal{K},
\end{aligned} \tag{4.2.1}$$

where P_{i_k} is the transmit power constraint at the user i_k, P_k is the total power constraint at the *k*-th base-station, and $l_{i_k}^{UL}\left(l_{i_k}^{DL}\right)$is the SINR of user i_k in the uplink (downlink) channel given as

$$\begin{aligned}
\gamma_{i_k}^{UL} &= \frac{\left|\left(\mathbf{u}_{i_k}^{UL}\right)^H \mathbf{H}_{ki_k}^{UL}\mathbf{v}_{i_k}^{UL}\right|^2}{\left(\mathbf{u}_{i_k}^{UL}\right)^H \mathbf{\Sigma}_{i_k}^{UL}\mathbf{u}_{i_k,m}^{UL}}, \\
\gamma_{i_k}^{DL} &= \frac{\left|\left(\mathbf{u}_{i_k}^{DL}\right)^H \mathbf{H}_{i_k k}^{DL}\mathbf{v}_{i_k}^{DL}\right|^2}{\left(\mathbf{u}_{i_k}^{DL}\right)^H \mathbf{\Sigma}_{i_k}^{DL}\mathbf{u}_{i_k,m}^{DL}}.
\end{aligned} \tag{4.2.2}$$

Here, $\mathbf{H}_{ki_k}^{UL}$ and $\mathbf{H}_{i_k k}^{DL}$ represent the channel between user i_k and base-station *k* in the uplink and downlink channel, respectively. å $_{i_k}^{UL}$(å $_{i_k}^{DL}$) is the aggregate interference-plus-noise terms at the user i_k in the uplink (downlink) channel.

By reformulating this nonconvex problem as an equivalent multi-convex optimization problem with the addition of two auxiliary variables similar to [29], we propose a low complexity alternating algorithm which converges to a local optimum point.

Note that our scenario, i.e., full-duplex base-stations serving full-duplex users also cover the scenario full-duplex base-station serving half-duplex users, because the additional interference paths introduced with the full-duplex operation of the users can be set to zero in half-duplex user case, and thus the full-duplex scenario comes down to half-duplex scenario. In this regard, the algorithms proposed above is readily applicable to full-duplex base-stations serving half-duplex users in a multi-cell scenario.

5. RELAYING IN FULL-DUPLEX

5.1. Multiple HD UEs per Relay FD BS in Single/Multiple Cell Deployment Scenario

FD is also a viable solution to boost performance of cooperative systems once it overcome the issue of multiplexing loss inherent of HD cooperative schemes [5], [10]-[14]. Additionally, in [5], [10]-[14] it is shown that FD relays can still achieve good performance even in the presence of strong self-interference levels.

5.1.1. Three node relaying case

We assume a Nakagami-m fading scenario, the performance of dual-hop FD decode-and-forward relaying schemes subject to co-channel interference (CCI), self-interference at the relay, and noise at the relay and destination is investigated. Some recent works examined the performance of dual-hop cooperative networks under CCI, but the analysis was performed in a HD relaying context. Figure 15 illustrates a 3-node relaying network, where UE1 communicates with UE2 with help of the FD BS, which acts as a relay and implements relaying protocols [5], [10]-[14].

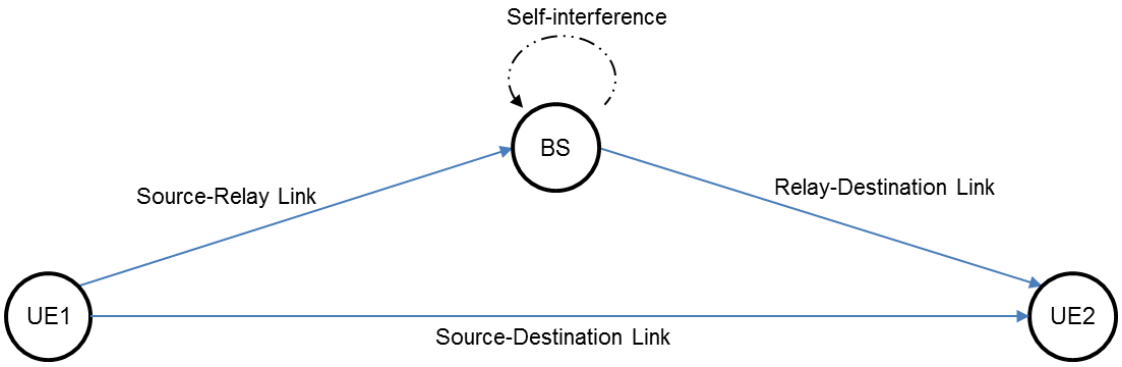

Figure 15: 3-node relaying setup: UE1 acts as a source and communicates to the destination, UE2, with help of a FD BS, which acts as a relay node.

Herein, differently from previous works two main scenarios are considered. In the first scenario, the direct link between the source and destination is seen as interference and a conventional FD dual-hop (FDDH) cooperative protocol is employed. On the other hand, in the second scenario the direct link is seen as useful information at the destination and a FD joint decoding (FDJD) cooperative scheme is adopted. In both schemes, the effect of self-interference at the relay (due to its full-duplex nature) is taken into account. Moreover, all channels are assumed to be quasi-static, independent and non-necessarily identically Nakagami-m distributed, with m_{ij} being the Nakagami-m fading parameter pertaining to the link between $i \in \{S,R\}$ and $j \in \{R,D\}$, while h_{ij} denotes the Nakagami-m channel coefficient and $\Omega_{ij} = E\left[\left|h_{ij}\right|^2\right]$ represents the corresponding average fading power, and κ_{ij} represents the path loss coefficient. We consider perfect channel state information at the receivers. Moreover, we assume that the interference comes from K interferers in a Nakagami-m fading environment. Each interferer has average powerP_k, and fading coefficient $\{h_{kj}\}_{k=1}^{K}$, satisfying and $\Omega_{kj} = E[\left|h_{kj}\right|^2]$ and m_{kj}.

Further, three distinct scenarios are considered with respect to which node perceives CCI, thus

- (Scenario 1): CCI at R with noisy D;

- (Scenario 2): CCI at D with noisy R;
- (Scenario 3): independent sources of CCI at R and D (both noisy)

Moreover, we assume the effect of the direct link at D in two different ways: i) we either assume that the direct link is seen as interference at D (FDDH scheme); or ii) we assume that the direct link is seen as useful signal and joint decoding is applied between the signals received from S and R (FDJD scheme)

5.1.1.1. Outage probability of FD dual-hop (FDDH) cooperative protocol

We suppose that R and D suffer from CCI, R suffers from self-interference, and D suffers from the interference coming from the direct link. Then, assuming unitary bandwidth and Gaussian inputs, the mutual information of source-relay and relay-destination links can be written, respectively, as

$$I_{SR} = \log_2\left(\frac{|h_{SR}|^2 P_S \kappa_{SR}}{|h_{RR}|^2 P_R + \sum_{k=1}^{K}|h_{kR}|^2 P_k \kappa_{kR} + 1}\right) \quad (5.1.1.1.1)$$

$$I_{RD} = \log_2\left(\frac{|h_{RD}|^2 P_R \kappa_{RD}}{|h_{SD}|^2 P_S \kappa_{SD} + \sum_{k=1}^{K}|h_{kD}|^2 P_k \kappa_{kD} + 1}\right) \quad (5.1.1.1.2)$$

The general outage probability expression is then defined as follows

$$P_{\text{FDDH}} = \Pr[I_{SR} < \mathcal{R}] + \Pr[I_{SR} > \mathcal{R}] \Pr[I_{RD} < \mathcal{R}] \quad (5.1.1.1.3)$$

Then, we apply this expression to each scenario. For instance in Scenario 1 we assume that the interference at the destination, if exists, is at the noise floor. Therefore, the CCI component from I_{RD} can be neglected except for the direct link. Then, in Scenario 2 we assume henceforth that the CCI at the relay, if exists, is at the noise floor while the CCI at the destination cannot be neglected. Thus, the term regarding the CCI in I_{SR} cancels out except for the self-interference which cannot be completely removed. The third scenario, accounts for CCI in both relay and destination. Closed-form expressions for each scenario are introduced in [14].

5.1.1.2. Outage probability of FD joint decoding (FDJD) cooperative protocol

In the FDJD cooperative scheme, the direct link is seen as useful information at the destination [5]. In the broadcast phase, the message is transmitted from source to both relay and destination as in FDDH. However, in the FDJD scheme the source splits the message into L blocks. While the relay receives the l-th block, $l \in \{1,2,\dots,L\}$, it simultaneously forwards to the destination the previous block. Then, at the destination, after the transmission of all blocks, the signals coming from source and relay are jointly decoded. In order to do so, as the transmissions from S and R interfere with each other, the destination employs an iterative process based on block decoding. For instance, backward decoding is employed in [16], [17], while in [18] the authors propose that S and R use block-Markov encoding associated with superposition coding. Bearing this in mind, the overall mutual information of FDJD is $I_{\text{FDJD}} = \min\{I_{SR}, I_{RD}\}$ [5], where

$$I_{RD} = \log_2\left(\frac{|h_{SD}|^2 P_S \kappa_{SD} + |h_{RD}|^2 P_R \kappa_{RD}}{\sum_{k=1}^{K}|h_{kD}|^2 P_k \kappa_{kD} + 1}\right) \quad (5.1.1.2.1)$$

Then, the overall outage probability is defined as

$$P_{\text{FDJD}} = \Pr[I_{\text{FDJD}} < \mathcal{R}] = \Pr[I_{SR} < \mathcal{R}] + \Pr[I_{RD} < \mathcal{R}] - \Pr[I_{SR} < \mathcal{R}] \Pr[I_{RD} < \mathcal{R}] \quad (5.1.1.2.2)$$

Accurate, closed-form expressions for the outage probability are derived for the general case, in which CCI and noise are assumed at both the relay and destination. Based on these expressions, which are found in [14] we address special cases assuming CCI only at the relay and assuming CCI only at the destination. It is shown that CCI at the relay is more harmful for the system performance than CCI at the destination.

Numerical results and discussion is introduced [14] as well as in Deliverable D4.1.2.

5.1.2. FD relaying: network level analysis

Reactive relay selection mechanisms have received a lot of attention as evidenced by recent papers. In this work, a semi-Markov process is used to model relay selection procedure for cooperative diversity protocols in full-duplex networks. We investigate the impact of the loop interference on the network performance. A dynamic relay selection procedure is considered where a suitable relay is selected at each hop and the cost of this selection procedure is incorporated into the achievable rate. Stochastic geometry is used to model network deployments. We consider a fixed and reactive relay schemes. In the reactive relay schemes, two distinct relay selection algorithms are used: the standard binary and a novel auction-based algorithm.

Following the settings of **Section 4.2.1** and following the steps 1 to 4 from **Procedure 1** we can determine the statistics of the perceived CCI at the user of interest, and then the SIR at the user of interest. We define the CCI at tagged FD receiver as

$$Z_0^{FD} = \delta\, p_{00} x_{00} + \sum_{(\varphi_i, x_i) \in \tilde{\Phi}_{BS}} Y_{i0} + \sum_{(\varphi_i, x_i) \in \tilde{\Phi}_{UE}} Y_{j0} \qquad (5.1.2.1)$$

where p_{00} and δ represent the self-interference component and the corresponding attenuation factor, respectively. To account for the aggregate CCI from multiple interfering tiers we employ the cumulants additivity property. Since BSs and UEs are assumed to be independently deployed, the resulting process from each such tier is also independent. Note that the tagged receiver perceives, not only the interference from the neighboring BSs (first summand in Z_0^{FD}), but also the interference for the neighboring UEs (second summand in Z_0^{FD}), and self-interference.

Then we can attain the SIR at the receiver as Γ and then define the outage probability as $\Pr[\Gamma < \gamma_{th}]$ where γ_{th} the corresponding SIR threshold. Then, by following the steps 1 until 4 from **Procedure 1** we attain the parameters of the approximated distribution, namely V0, which is a Normal RVs (in logarithmic scale) representing the power received from the desired transmitter and V the CCI at the user of interest. With those results at hand, we can then determine the SIR at the receiver, which can be represented as $\Gamma \sim \text{Normal}\left(\mu_{V_0} - \mu_V, \sigma_{V_0}^2 + \sigma_V^2\right) \sim \text{Normal}(\mu_\Gamma, \sigma_\Gamma)$, which lead us to the an outage probability given as

$$\Pr[\Gamma < \gamma_{th}] = Q\left[\frac{\mu_\Gamma - \gamma_{th}}{\sigma_\Gamma}\right]. \qquad (5.1.2.2)$$

In what follows, we denote p_{SD} the probability that power level of the source received signal is above the interference level. In this work, the interference is represented by the interference component from the nearest interferer. We approximate this value by matching the moments of the actual distribution to a approximating lognormal.

5.1.2.1. Relay selection protocol and steady-state throughput

A dynamic relay selection procedure is considered where a suitable relay is selected at each hop and the cost of this selection procedure is incorporated into the achievable rate. Stochastic geometry is used to model network deployments, following the step presented in [1]-[2].

We consider a fixed and reactive relay schemes. In the reactive relay schemes, two distinct relay selection algorithms (RSA) are used: the standard binary and a novel auction based algorithm. First, a totally random approach based solely on the Standard Tree Algorithm (STA) is used to implement the RSA. We summarize its behavior as follows: the source sends a Request to Send (RTS) packet to initiate the relay selection procedure. Nodes that listen to this request reply with a Clear To Send (CTS) packet based on the probability of accessing the channel. If a collision occurs, nodes that have transmitted in previous slot retransmit or not through random process similar to a Q-

sided coin. The source node should receive the replies from all the candidate relays so as to select the next relay greedily, i.e. the closest node to the destination whether there is one available.

Them in order to implement this protocol we introduce a semi-Markov process (depicted in Figure 16), which models the relay selection procedure for cooperative diversity protocols in full-duplex networks. We investigate the impact of the self-interference on the network performance.

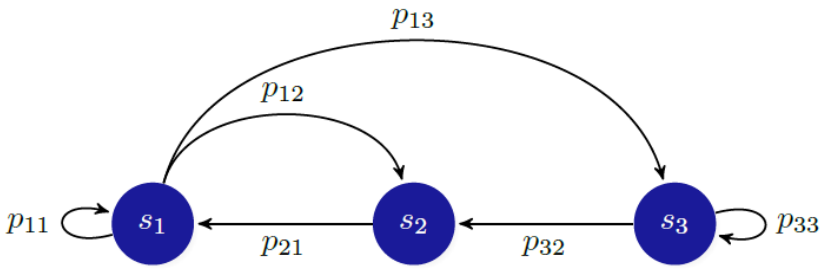

Figure 16: Semi-Markov process: At transition instants the semi-Markov process behaves as a Markov process, though the transition instants follow a distinct probabilistic mechanism. Each state is related to an outage event.

We consider a general class of process where the elapsed time between transitions may take several unit intervals, as well as it depends on the transition that occurred [15]. At transition instants the semi-Markov process behaves as a Markov process, though the transition instants follow a distinct probabilistic mechanism. Then, we can define the state transition matrix as

$$P = \begin{bmatrix} p_{11} & p_{12} & p_{13} \\ p_{21} & p_{22} & p_{23} \\ p_{31} & p_{32} & p_{32} \end{bmatrix} \quad (5.1.2.1.1)$$

which is a function of the outage probabilities of each link, for instance,

$$p_{11} = p_{SD} \quad (5.1.2.1.2)$$

$$p_{12} = (1 - p_{SD})\, p_{SD} \quad (5.1.2.1.3)$$

$$p_{13} = (1 - p_{SD})\,(1 - p_{SR}) \quad (5.1.2.1.4)$$

where p_{SD} and p_{SR} yield the probability that the source message is correctly received by the final destination and relay, respectively.

A message is successfully delivered to the destination node when the process returns to the state s_1. The reward function $R(\tau)$ corresponds to the cumulative reward after a period τ and yields the total number of rewards, namely the correct number of receptions. According to the fundamental renewal-reward theorem, the long-term throughput is given by the following value,

$$\eta = \lim_{\tau \to \infty} \frac{R(\tau)}{\tau} \quad (5.1.2.1.5)$$

$$= \frac{\sum_{i=1}^{K} \pi_i \bar{R}_i}{\sum_{i=1}^{K} \pi_i \bar{D}_i} \quad (5.1.2.1.6)$$

where K yields the number of states, $\bar{R} = \sum_j^K p_{ij} R_{ij}$ is the mean rewarding, and $\bar{D} = \sum_j^K p_{ij} D_{ij}$ is the mean waiting time.

Further discussion and numerical results are introduced in Deliverable D4.1.2.

6. MANET PROTOCOLS FOR FULL-DUPLEX

In this section, we describe the different protocols developed for use in a full duplex Mobile Ad hoc Network (MANET). We focus on 802.11 MANETs and use the OMNET++ simulator in order to implement and test the described protocols.

6.1. Introduction to OMNET++

OMNET++ is a discrete event - all purpose - simulator. Used in conjunction with the INET framework - which provides an extensive set of networking related protocols (a non-exhaustive list includes 802.11 b/g, 802.3, ARP, RIP, BGP, OLSR, AODV, TCP, UDP) – it is possible to construct a network of nodes communicating using either wired or wireless communication technologies (e.g. IEEE 802.11g) and study the behaviour of different protocols and/or mobility patterns etc.

6.2. MAC protocol

6.2.1. Introduction

Currently standardized MAC protocols are not designed with full duplex in mind. This means that using readily available MAC protocols (e.g. 802.11 protocols) would result in underutilization of the capabilities of full duplex devices as well as wasted bandwidth.

There are two possible approaches to full duplex MAC protocols:

- Bidirectional full duplex, where 2 nodes are involved and exchange messages between themselves (see Figure 17)
- Relay full duplex, where 3 nodes are involved (source, relay and destination) and the relay receives from the source while transmitting to the destination (see Figure 18).

Bidirectional FD is first studied in [91] where transmission start in HD mode and later continues in DF mode when possible. Relay full duplex is discussed in [92] and [93], where traffic monitoring is used to identify possible FD relaying opportunities by populating neighbour tables.

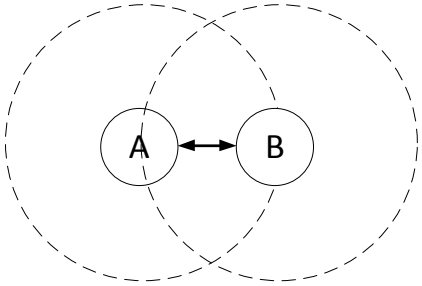

Figure 17: Bidirectional Full Duplex

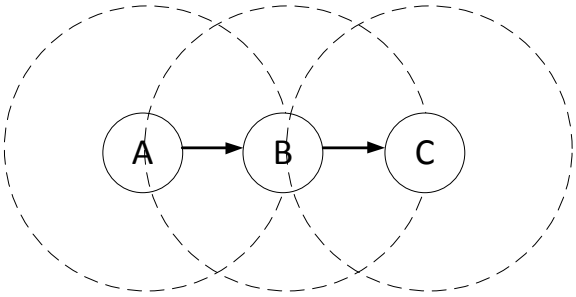

Figure 18: Relay full duplex

Relay full duplex seems more adapted to MANETs as more nodes are involved in the communication but the biggest drawback of this solution is the lack of channel reservation mechanisms. Indeed, it is

impossible to implement a RTS/CTS mechanism that would be efficient in this kind of networks and because of the nature of the transfer, we can't rely on the channel occupation and the "listen before send" mechanism of neighbouring nodes to avoid collisions.

6.2.2. Protocol description

6.2.2.1. General overview

Because the available solutions were not satisfying regarding the previously mentioned requirements, we decided to develop our own MAC protocol that would comply with those requirements. Our protocol is a bidirectional full duplex MAC protocol based on the IEEE 802.11g protocol. By focusing on the bidirectional case, we can ensure that the channel around both nodes involved in the full duplex transmission is reserved such that no communication from neighbouring nodes can start and produce interference.

In order to achieve successful channel reservation, two new frame types have been introduced in our MAC protocol:

- RTS_FD frame
- CTS_FD frame

Both of these frames contain the same fields as their half duplex counterparts. The difference lies in the Frame Control subtype field (see Figure 19) where two new frame types have been introduced without affecting existing ones. Using these two new control messages, our MAC protocol allows the sender and the receiver to negotiate their full-duplex capabilities as well as the size of exchanged frames. At the end of our handshake process, and in case both nodes possess full duplex capabilities, the channel is reserved for a duration that matches the size of the biggest frame exchanged. Note that all other MAC frames remain unchanged.

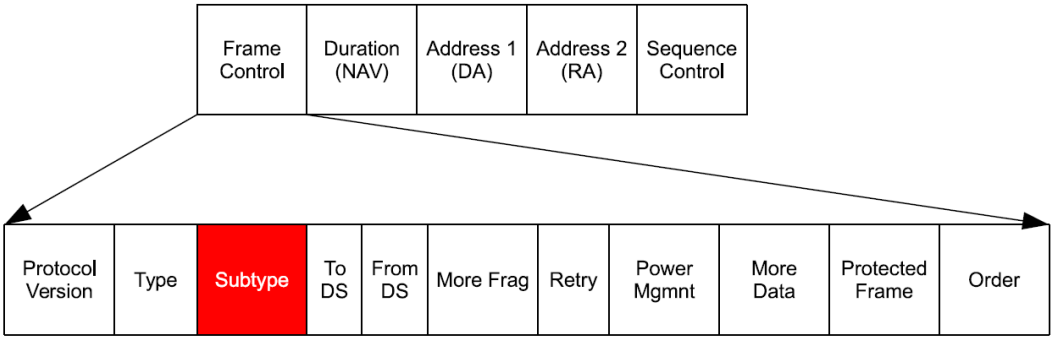

Figure 19: RTS_FD frame format

6.2.2.2. Detailed description

Upon reception of a RTS_FD frame, a node will either reply with a CTS or a CTS_FD frame. The choice is based on the current frame in the head of its queue (lines 5 to 7 of ALGORITHM 7):

- If the first frame in the head of the queue is to be sent to the emitter of the RTS_FD frame, then a CTS_FD frame is sent.
- Otherwise, the node responds with a usual CTS frame.

In the case where a frame is available in the head of the queue, then we compare the sizes of the two frames based on the NAV in the RTS_FD frame:

- If the frame to be sent is smaller than the RTS_FD NAV, then the receiver pads its frame in order to match the size of the sender message (lines 10-11 of ALGORITHM 7)

- Otherwise, the original transmitter will pad its frame based on the NAV in the received CTS_FD frame (lines 20-23 of ALGORITHM 8)

After transmission/reception of the CTS_FD frame, both nodes send their data frames (with padding if necessary) and send an acknowledgement upon successful reception as defined in the classical IEEE 802.11 scheme.

Padding is meant for channel reservation purposes. Indeed, when sending the RTS_FD frame, a node cannot know whether the data frame to be sent by the receiver will be larger than its own data frame. Because nodes in the vicinity of the source node will stop transmitting for a period defined by the NAV of the RTS, these nodes may wake up before the end of the full duplex transmission and sense the channel as free in some cases. In order to avoid these nodes from interfering with the reception of the data frame, we add zero padding to the shorter frame. This makes the channel busy from the point of view of neighbouring nodes and therefore prevents interference from these nodes.

Zero padding is analogous to bit stuffing as it does not add any useful information in the frames to transmit. Instead of bit stuffing we could have tried to add meaningful information. One idea is to look in the queue and see if any packet meant for the other node may fit in the padding space. This, however, questions the fairness of the MAC protocol as some nodes may get a greater number of frames transmitted. Another idea is to use the leftover space to do forward error correction (FEC). While this idea seems very interesting to us, we did not have time to investigate the implications and the feasibility of such a scheme.

```
1:  LISTEN_FOR_FRAME()
2:  rcv_frame ← RECEIVE()
3:  rts_nav ← GET_NAV(rcv_frame)
4:  frame ← POP_QUEUE()
5:  if TYPE(rcv_frame) == RTS_FD then
6:      if DST(frame) == SRC(rcv_frame) then
7:          cts_fd ← BUILD_CTS_FD(frame, rcv_frame)
8:          cts_nav ← GET_NAV(frame)
9:          SEND(cts_fd)
10:         if rts_nav ≥ cts_nav then
11:             PAD_FRAME(rts_nav − cts_nav)
12:         end if
13:         SEND(next_frame)
14:         RECEIVE()
15:         WAIT_FOR_ACK()
16:         SEND(ack)
17:     end if
18: else if TYPE(rcv_frame) == RTS then
19:     cts ← BUILD_CTS(rcv_frame)
20:     SEND(cts)
21:     RECEIVE()
22:     SEND(ack)
23: end if
```

ALGORITHM 7. Receiver Algorithm

```
Require: max_trials
get_frame:
frame ← POP_QUEUE()
rts_nav ← LENGTH(frame)
rts_fd ← BUILD_RTS(frame)
trials ← 0
send_rts_fd:
SEND(rts_fd)
wait_for_reply:
if Timeout then
    if trials ≤ max_trials then
        trials ← trials + 1
        BACKOFF()
        go to send_rts_fd
    else
        go to get_frame
    end if
else
    reply ← RECEIVE()
end if
if TYPE(reply) == CTS_FD then
    cts_nav ← GET_NAV(reply)
    if cts_nav ≥ rts_nav then
        PAD_FRAME(cts_nav − rts_nav)
    end if
    SEND(frame)
    RECEIVE()
    WAIT_FOR_ACK()
    SEND(ack)
else if TYPE(reply) == CTS then
    SEND(frame)
    WAIT_FOR_ACK()
end if
```

ALGORITHM 8. Emitter Algorithm

6.2.2.3. Backwards compatibility

We have also tried to keep in mind backwards compatibility as a goal for this protocol in order to ensure easy integration between currently available half duplex UEs and full duplex UEs. This can be made possible if half duplex UEs handle the RTS_FD frame as a regular RTS frame. We can therefore use the RTS_FD and RTS frames as indicators of full duplex capabilities of a station as described below and summarized in Table 4 and Table 5:

- Full duplex devices only send RTS_FD frames but can respond to both RTS_FD and RTS frames with either a CTS or CTS_FD frame depending on the frame received, the sender and the current state of the buffer.
- Half duplex equipment only send RTS frames but can respond to both RTS_FD and RTS frames exclusively with a CTS.

Table 4: Response to a RTS_FD frame

Receiving node	Frame in queue	No Frame in queue
Full duplex	CTS_FD	CTS
Half Duplex	CTS	CTS

Table 5: Response to a RTS frame

Receiving node	Frame in queue	No Frame in queue
Full duplex	CTS	CTS
Half Duplex	CTS	CTS

We have therefore successfully modified the existing HD implementation in order to make it compatible with the RTS_FD messages and therefore were able to have co-existence of HD and FD UEs.

6.3. Routing solutions

From the results available in D4.1.2 section 6.2.3 [68], it is clear that currently available routing solutions in MANETs may not be good enough to leverage efficiently the additional bandwidth offered by full duplex technology. These results also show that a better knowledge of the topology and of traffic patterns may help reaching that goal.

In this section we discuss the possible routing mechanisms to put into place in order to leverage the full duplex gains in these types of networks. In order to obtain a better knowledge of traffic patterns, we believe that it is necessary to adopt a cross layer approach. Indeed, by leveraging information at the MAC layer about overheard transmissions, we can already aggregate traffic pattern information in the vicinity of each node.

A full duplex ad-hoc routing protocol would have to communicate with the MAC layer in order to get information about the traffic pattern and forward those traffic patterns to neighbouring nodes in order to derive larger scale information.

We can then combine this information with traditional routing metrics in order to derive a new metric that promotes bidirectional traffic over the full duplex network.

Another aspect to take into account is the co-existence of HD and FD UEs in the network. Indeed, presence of HD UEs in the network changes the routing metric as these nodes cannot process as much traffic and our routing metric is based on traffic pattern evaluation. Therefore HD UEs need to be treated as a special case by any FD routing protocol.

6.4. Control Plane Design

The problem with the requirements discussed in the previous section is that the overall signalling overhead they need in order to provide meaningful results may be a lot for the network to handle and might in the end reduce the bandwidth available for data communication.

This is the reason why we propose a control plane design capable of reducing the amount of bandwidth necessary for signalling purposes by merging together information from several layers.

The proposed design shown in Figure 20 revolves around a neighbour database and an external dissemination protocol. In this design, the control plane communicates with both the routing and MAC layers which provide information to fill the neighbour database.

The role of the neighbour database is to aggregate information about traffic patterns from the MAC layer as well as routing measurements. The control plane could also take into account PHY layer aspects such as CSI, signal strength to derive more precise metrics. All this information would make it possible to assess the FD capabilities of neighbours prior to the RTS_FD/CTS_FD handshake. It also enables the routing protocol to derive metrics based on more precise/timely data coming from the MAC layer.

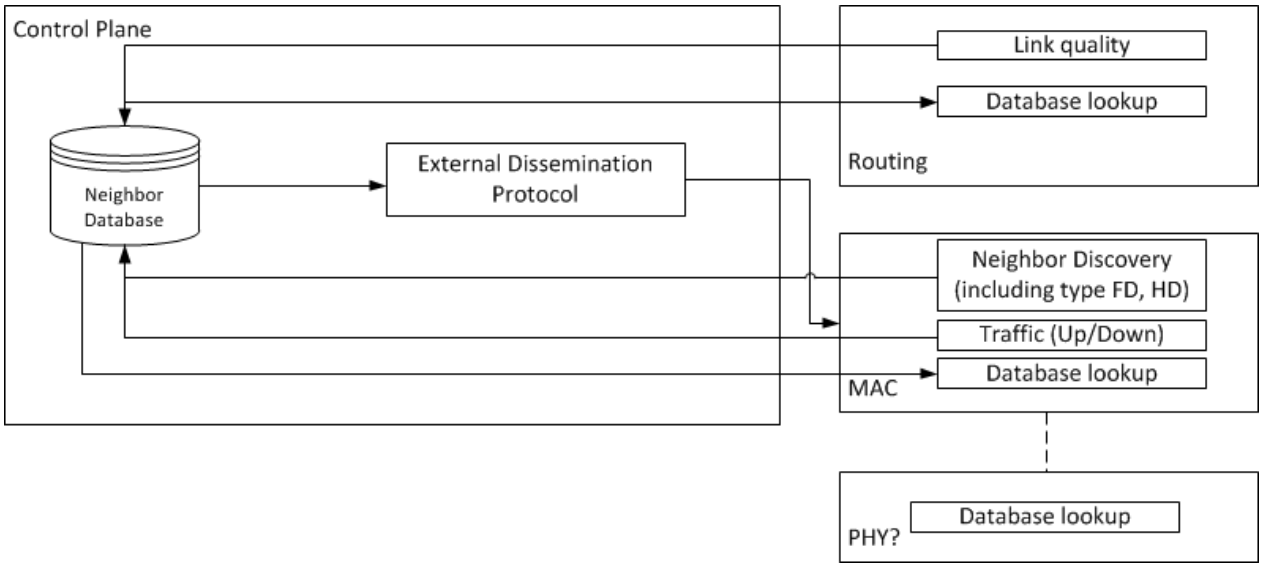

Figure 20: Control plane design

Table 6 describes the fields contained for each entry in the neighbour database.

Table 6: Neighbour table entry format

MAC address	IP address	Type (FD/HD)	Signal Strength	Traffic To XX	Traffic from XX	Traffic to YY	Traffic from YY

The external dissemination protocol would then act as a proxy to the routing protocol. It uses the neighbour database in order to decide when is an appropriate time to send routing control messages. It can even prevent some messages from being sent as data from lower layers updates the neighbour database, thus rendering the routing message redundant.

Another role of the external dissemination protocol is to generate control messages of its own in order to propagate traffic pattern information throughout the network in a controlled manner. By controlled, we mean that it aggregates information before sending it and schedules the information transfer in reasonable time intervals in order to avoid congestion and/or saturate the network.

By aggregating control information we make it possible to achieve the requirements of a FD routing protocol for MANETs without overloading the network with dissemination of control information coming from several layers at the same time.

7. SUMMARY AND CONCLUSIONS

This section summarizes the work provided throughout the document on a chapter by chapter basis and provides conclusions and further work possibilities for FD systems.

Chapter 2 focused on the single FD bidirectional link case. The achievable rate region was analysed by taking into account the transceiver's non-idealities via EVM modelling. Algorithms for rate maximization were derived with either uniform or non-uniform power allocation. The study of power allocation policies made it possible to derive an algorithm that maximizes data rates.

Chapter 3 introduced methods and algorithms for single cell deployment. A beamformer design solution for spectral efficiency maximization was introduced. The importance of scheduling algorithms and power control algorithms is underlined as well as the necessity for co-channel interference management. Since co-channel-interference (CCI) is a critical factor that needs to be controlled for successful deployment of full-duplex systems, a CCI aware user scheduling scheme which can control the CCI is a good solution to the full-duplex systems which we will tackle. This allows us to exploit the multiuser diversity gain in both uplink and downlink directions. Furthermore, since the uplink performance of the full-duplex system is significantly reduced due to a large amount of self-interference, a mechanism to control the fairness among users needs to be proposed by imposing a rate constraint on the sum-rate of the uplink channel. Lastly, we have proposed a hybrid scheduler for single-cell systems, the future research can also include an efficient hybrid algorithm to switch between full-duplex and half-duplex systems for multi-cell systems. Chapter 3 also considered multiple antennas systems and D2D scenarios. In the latter, outage probabilities were derived for the cellular user selection in hybrid-duplex D2D cellular networks.

Chapter 4 analysed multi-cell deployment scenarios both in the SISO and MIMO case where all UEs operate in a FD fashion. As in chapter 3, radio resource management appears as a very important factor in optimizing FD system performance. Multi-cell scenarios have only been considered in very specific cases (e.g. not considering HD and FD UE coexistence, etc.). With the adoption of FD and the increase of small cell deployments, the necessity to study radio resource management in this context will be crucial. Further work will need to assess inter-cell interference and co-channel interference in denser networks as well as coexistence of HD and FD UEs.

Chapter 5 addressed full-duplex relaying. FD relaying overcomes the spectral inefficiency of its HD counterpart, and additionally enhances performance. In what regards to the design of cooperative networks with FD relays, DUPLO provides theoretical benchmark and guidelines. Therefore, practical protocols and implementation need to be assessed.

Chapter 6 provided an analysis of full duplex in MANETs. A bidirectional FD MAC protocol was developed and described using a modified RTS/CTS scheme in order to provide FD channel reservation. Routing solutions and a control plane design in order to limit control information exchanges are also discussed. Further work can still be done to optimize the MAC, notably in regards to the padding aspects where padding bits could be replaced by either useful payloads or even forward error correction in order to improve the performance. A study of heterogeneous networks (containing both HD and FD UEs) may also be interesting in regard of performance and behaviour of FD protocols. Routing solutions could be further tested and the control plane design could be put into practice in large scale simulations in order to test the scalability and the performance gains obtained.

8. REFERENCES

[1] C. H.M. de Lima, H. Alves, P. H.J. Nardelli, and M. Latva-aho, “Hybrid Half- and Full-Duplex Communications Under Correlated Lognormal Shadowing,” VTC-2015 Work., 2015, pp. 1-5.

[2] C. H. M. de Lima, P. H. J. Nardelli, H. Alves, and M. Latva-aho, Full-duplex communications in interference networks under composite fading channel, in 2014 Eur. Conf. Networks Commun., 2014, pp. 1-5.

[3] H. Alves, C. H. M. De Lima, P. H. J. Nardelli, R. D. Souza, and M. Latva-aho, On the Average Spectral Efficiency of Interference-Limited Full-Duplex Networks, in 9th Int. Conf. Cogn. Radio Oriented Wirel. Networks, Oulu, 2014, pp. 1-5.

[4] M. Duarte, C. Dick, and A. Sabharwal, “Experiment-driven characterization of full-duplex wireless systems,” IEEE Trans. Wireless Commun., vol. 11, no. 12, pp. 4296–4307, 2012.

[5] T. Riihonen, S. Werner, and R. Wichman, “Mitigation of loopback self-interference in full-duplex mimo relays,” IEEE Trans. Signal Process., vol. 59, no. 12, pp. 5983–5993, 2011.

[6] H. Alves, D. da Costa, R. Souza, and M. Latva-aho, “Performance of block-Markov full duplex relaying with self -interference in Nakagami-m fading,” IEEE Wireless Commun. Letters, vol. 2, no. 3, pp. 311–314, 2013.

[7] C. H. M. de Lima, P. H. J. Nardelli, H. Alves, and M. Latva-aho, Full-duplex communications in interference networks under composite fading channel, in 2014 Eur. Conf. Networks Commun., 2014, pp. 1-5.

[8] M.-S. Alouini and A. J. Goldsmith, “Area spectral efficiency of cellular mobile radio systems,” IEEE Trans. Wireless Commun., vol. 48, no. 4, pp. 1047–1066, Jul. 1999.

[9] C. H. M. de Lima, M. Bennis, and M. Latva-aho, “Coordination mechanisms for self-organizing femtocells in two-tier coexistence scenarios,” IEEE Trans. Wireless Commun., vol. 11, no. 6, Jun. 2012.

[10] S. Weber, J. Andrews, and N. Jindal, “An overview of the transmission capacity of wireless networks,” IEEE Trans. Commun., vol. 58, no. 12, pp. 3593–3604, Dec. 2010.

[11] T. Kwon, S. Lim, S. Choi, and D. Hong, “Optimal duplex mode for DF relay in terms of the outage probability,” IEEE Trans. Veh. Technol., vol. 59, no. 7, pp. 3628–3634, Sep. 2010.

[12] T. Riihonen, S. Werner, and R. Wichman, “Hybrid full-duplex/halfduplex relaying with transmit power adaptation,” IEEE Trans. on Wireless Commun., vol. 10, no. 9, pp. 3074–3085, 2011.

[13] P. K. Sharma and P. Garg, “Outage analysis of full duplex decode and forward relaying over nakagami-m channels,” in 2013 National Conference on Communications (NCC), 2013, pp. 1–5.

[14] T. Baranwal, D. Michalopoulos, and R. Schober, “Outage analysis of multihop full duplex relaying,” IEEE Commun. Letters, vol. 17, no. 1, pp. 63–66, 2013.

[15] H. Alves, R. D. Souza, and M. Latva-aho, Full-Duplex Relaying Systems Subject to Co-channel Interference and Noise in Nakagami-m, in VTC-2015 Work., 2015, pp. 1-5.

[16] R. A. Howard, Dynamic Probabilistic Systems, Volume II: Semi-Markov and Decision Processes. Dover Publications, 2007.

[17] S. Goyal, P. Liu, S. Panwar, R. DiFazio, R. Yang, J. Li, and E. Bala,“Improving small cell capacity with common-carrier full duplex radios,” in *Proc. IEEE Int. Conf. Commun. (ICC 2014)*, pp. 4987-4993, June 2014.

[18] X. Shen, X. Cheng, L. Yang, M. Ma, and B. Jiao, “On the design of the scheduling algorithm for the full duplexing wireless cellular network,” in *Proc. IEEE GLOBECOM*, pp. 4970-4975, Dec. 2013.

[19] A. C. Cirik, K. Rikkinen, Y. Rong, “A subcarrier and power allocation algorithm for OFDMA full-duplex systems”, accepted to EuCNC2015 conference, July 2015.

[20] A. C. Cirik, K. Rikkinen, M. Latva-aho, “Joint subcarrier and power allocation for sum-rate maximization in OFDMA full-duplex systems”, accepted to IEEE Vehicular Technology Conference (VTC2015-Spring), May 2015.

[21] A. C. Cirik, K. Rikkinen, R. Wang, and Y. Hua, “Resource allocation in full-duplex OFDMA systems with partial channel state information," accepted to IEEE China Summit and Int. Conf. Signal and Inf. Process. (ChinaSIP), July 2015.

[22] R.Wang and V. K. N. Lau, “Cross layer design of downlink multiantenna OFDMA systems with imperfect CSIT for slow fading channels”, *IEEE Trans. Wireless Commun.*, vol. 6, no. 7, pp. 2417-2421, July 2007.

[23] A. C. Cirik, R. Wang, Y. Hua, and M. Latva-aho, “Weighted sum-rate maximization for full-duplex MIMO interference channels," *IEEE Trans. Commun.*, vol. 63, no. 3, pp. 801-815, March 2015.

[24] A. C. Cirik, “Fairness considerations for full duplex multi-user MIMO systems," *IEEE Wireless Communications Letters*, in press, April 2015.

[25] A. C. Cirik, R. Wang, Y. Rong and Y. Hua, “MSE based transceiver designs for full-duplex MIMO cognitive radios," *IEEE Trans. Commun.*, in press, May 2015.
[26] D. Nguyen, L. Tran, P. Pirinen, and M. Latva-aho, “On the spectral efficiency of full-duplex small cell wireless systems,” IEEE Trans. Wireless Commun., vol. 13, no. 9, pp. 4896-4910, Sept. 2014.
[27] D. Nguyen, L.-N. Tran, P. Pirinen, and M. Latva-aho, “Precoding for full duplex multiuser MIMO systems: Spectral and energy efficiency maximization,” IEEE Trans. Signal Process., vol. 61, no. 16, pp. 4038-4050, 2013.
[28] S. Li, R. Murch, and V. Lau, “Linear transceiver design for full-duplex multi-user MIMO system,” IEEE Int. Conf. Commun. (ICC), pp. 4921-4926, June 2014.
[29] S. S. Christensen, R. Agarwal, E. Carvalho, and J. M. Cioffi, “Weighted sum rate maximization using weighted MMSE for MIMO-BC beamforming design,” *IEEE Trans. Wireless Commun.*, vol. 7, pp. 4792-4799, Dec. 2008.
[30] H. Al-Shatri, et al, "Multi-convex optimization for sum rate maximization in multiuser relay networks," *IEEE 24th Int. Symp. Personal Indoor and Mobile Radio Communications (PIMRC),* pp. 1327-1331, Sept. 2013.
[31] S. Sadr, A. Anpalagan, and K. Raahemifar, “Radio resource allocation algorithms for the downlink of multiuser OFDM communication systems,” IEEE Communications Surveys and Tutorials, vol. 11, no. 3, pp. 92–106, 2009.
[32] E. Yaacoub and Z. Dawy, “A survey on uplink resource allocation in OFDMA wireless networks,” IEEE Communications Surveys and Tutorials, vol. 14, no. 2, pp. 322–337, Second Quarter 2012
[33] W. Yu, G. Ginis, and J. Cioffi, “Distributed multiuser power control for digital subscriber lines,” IEEE Journal on Selected Areas in Communications, vol. 20, no. 5, pp. 1105–1115, Jun. 2002.
[34] W. Yu, W. Rhee, S. Boyd, and J. Cioffi, “Iterative water-filling for Gaussian vector multiple-access channels,” IEEE Transactions on Information Theory, vol. 50, no. 1, pp. 145–152, Jan. 2004.
[35] F. Boccardi, R. W. Heath, A. Lozano, T. L. Marzetta, and P. Popovski, “Five disruptive technology directions for 5G,” IEEE Commun. Mag., vol. 52, no. 2, pp. 74–80, Feb. 2014.
[36] H. Wang, J. Lee, S. Kim, and D. Hong, “Capacity enhancement of secondary links through spatial diveristy in spectrum sharing,” IEEE Trans. Wireless Commun., vol. 9, no. 2, pp. 494–499, Feb. 2010.
[37] K. Doppler, M. Rinne, C. Wijting, C. B. Ribeiro, and K. Hugl, “Device-to-device communication as an underlay to LTE-Advanced networks,” IEEE Commun. Mag., vol. 47, no. 12, pp. 42–49, Feb. 2009.
[38] C. H. Yu, O. Tirkkonen, K. Doppler, and C. Ribeiro, “Power optimization of Device-to-Device communication underlaying cellular communication,” in Proc. IEEE International Conference on Communications (ICC), Dresden, Germany, June 2009.
[39] X. Chen, L. Chen, M. Zeng, X. Zhang, and D. Yang, “Downlink resource allocation for Device-to-Device communication underlaying cellular networks,” in Proc. IEEE International Symposium on Personal Indoor and Mobile Radio Communications (PIMRC), Sydney, Australia, June 2012.
[40] H. Ju, E. Oh, and D. Hong, “Improving efficiency of resource usage in two-hop full duplex relay systems based on resource sharing and interference cancellation,” IEEE Trans. Wireless Commun., vol. 8, no. 8, pp. 3933–3938, Aug. 2009.
[41] T. Riihonen, S. Werner, and R. Wichman, “Optimized gain control for single-frequency relaying with loop interference,” IEEE Trans. Wireless Commun., vol. 8, pp. 2801–2806, June 2009.
[42] S. Ali, N. Rajatheva, and M. Latva-aho, “Full-Duplex Device-to- Device communication in cellular networks,” in Proc. European conference on Networks and Communications (EuCNC), Bologna, Italy, June 2014.
[43] K. T. Hemachandra, N. Rajatheva, and M. Latva-aho, “Sum-rate analysis for full-Duplex underlay Device-to-Device networks,” in Proc. IEEE Wireless Communications and Networking Conference (WCNC), Istanbul, Turkey, April 2014.
[44] A. Ghasemi and E. S. Sousa, “Fundamental limits of spectrumsharing in fading environment,” IEEE Trans. Wireless Commun., vol. 6, no. 2, pp. 649–658, Feb. 2007.
[45] K. Hamdi, W. Zhang, and K. B. Letaief, “Power control in cognitive radio systems based on spectrum sensing side information,” IEEE Intl. Conf. Commun., Glasgow, UK, June 2007.
[46] A. Goldsmith, S. A. Jafar, I. Maric, and S. Srinivasa, “Breaking spectrum gridlock with cognative radios: an information theoretic perspective,” Proceedings of the IEEE, vol. 97, no. 5, pp. 894–914, May 2009.
[47] M. Jain, J. Choi, T. M. Kim, D. Bharadia, S. Seth, K. Srinivasan, P. Levis, S. Katti, and P. Sinha, “Practical, real-time, full duplex wireless,” in Proc. IEEE MobiCom, Las Vegas, Nevada, USA, Sep. 2011.
[48] G. Santella and F. Mazzenga, “A hybrid analytical-simulation procedure for performance evaluation in M-QAM-OFDM schemes in presence of nonlinear distortions,” IEEE Trans.Veh. Technol., vol. 47,

no. 1, pp. 142-151, Feb. 1998.
[49] H. Suzuki, T. V. A. Tran, I. B. Collings, G. Daniels, and M. Hedley, "Transmitter noise effect on the performance of a MIMO-OFDM hardware implementation achieving improved coverage," IEEE J. Sel. Areas Commun., vol. 26, no. 6, pp. 867-876, Aug. 2008.
[50] W. Li and J. Lilleberg, "Full-Duplex Link Performance Under Consideration of Error Vector Magnitude", In Proc. on IEEE Wireless Communications and Networking Conference WCNC 2014, pp. 654 – 659,Istanbul, Turkey, April 2014.
[51] W. Li, J. Lilleberg, and K. Rikkinen, " On Rate Region Analysis Of Half- and Full-Duplex OFDM Communication Links", IEEE Journal on Selected Areas in Communications (JSAC), Vol. 32, No. 9, pp.1688 - 1698, Sept. 2014.
[52] 3rd Generation Partnership Project, TS 36.104 V10.2.0, LTE; Evolved Universal Terrestrial Radio Access (E-UTRA); Base Station (BS) radio transmission and reception (Release 10).
[53] V. Tapio, "System Scenarios and Technical Requirements for Full-Duplex Concept", INFSO-ICT-316369 DUPLO - Report D1.1, April 2013.
[54] H. Weingarten, Y. Steinberg, and S. Shamai, "The capacity region of the Gaussian multiple-input multiple-output broadcast channel," *IEEE Trans. Inf. Theory*, vol. 52, no. 9, pp. 3936-3964, Sep. 2006.
[55] D. Tse and P. Viswanath, Fundamentals of Wireless Communication. Cambridge University Press, 2005.
[56] N. Sidoropoulos, T. Davidson, and Z.-Q. Luo, "Transmit beamforming for physical-layer multicasting," IEEE Trans. Signal Process., vol. 54, no. 6, pp. 2239-2251, Jun. 2006.
[57] A. Gershman, N. Sidoropoulos, S. Shahbazpanahi, M. Bengtsson, and B. Ottersten, "Convex optimization-based beamforming," *IEEE Signal Process. Mag.*, vol. 27, no. 3, pp. 62-75, May 2010.
[58] Z.-G. Luo, W.-K. Ma, A.-C. So, Y. Ye, and S. Zhang, "Semidefinite relaxation of quadratic optimization problems," *IEEE Signal Process. Mag.*, vol. 27, no. 3, pp. 20-34, May 2010.
[59] A. Wiesel, Y. Eldar, and S. Shamai, "Zero-forcing precoding and generalized inverses," *IEEE Trans. Signal Process.*, vol. 56, no. 9, pp. 4409-4418, Sep. 2008.
[60] L.-N. Tran, M. Juntti, M. Bengtsson, and B. Ottersten, "Beamformer designs for MISO broadcast channels with zero-forcing dirty paper coding," *IEEE Trans. Wireless Commun.*, vol. 12, no. 3, pp. 1173-1185, Mar. 2013.
[61] L.-N. Tran, M. Juntti, M. Bengtsson, and B. Ottersten, "Weighted sum rate maximization for MIMO broadcast channels using dirty paper coding and zero-forcing methods," *IEEE Trans. Commun.*, vol. 61, no. 6, pp. 2362-2373, Jun. 2013.
[62] M. Bengtsson and B. Ottersten, "Optimal and suboptimal transmit beamforming," in *Handbook of Antennas in Wireless Communications*, L. C. E. Godara, Ed., CRC Press, 2001.
[63] M. Frank and P. Wolfe, "An algorithm for quadratic programming," *Naval Research logistics Quarterly*, vol. 3, no. 1-2, pp. 95-110, 1956.
[64] A. Beck, A. Ben-Tal, and L. Tetruashvili, "A sequential parametric convex approximation method with applications to nonconvex truss topology design problems," *Journal of Global Optimization*, vol. 47, no. 1, pp. 29-51, 2010.
[65] L.-N. Tran, M. F. Hanif, A. Tölli, and M. Juntti, "Fast converging algorithm for weighted sum rate maximization in multicell MISO downlink," *IEEE Signal Process. Lett.*, vol. 19, no. 12, pp. 872-875.
[66] L.-N. Tran, "An iterative precoder design for successive zero-forcing precoded systems," *IEEE Commun. Lett.*, vol. 16, no. 1, pp. 16-18, Jan. 2012.
[67] D. Nguyen, L.-N. Tran, P. Pirinen, and M. Latva-aho, "On the spectral efficiency of full-duplex small cell wireless systems," ," IEEE Trans. Wireless Commun., vol. 13, no. 9, pp. 4896-4910, Sept. 2014.
[68] H.Alves, "Performance of Full-Duplex Systems", INFSO-ICT- 316369 DUPLO - Report D4.1.2, May 2015.
[69] F. Gomez-Cuba, R. Asorey-Cacheda, and F. J. Gonzalez-Castano, "A survey on cooperative diversity for wireless networks," IEEE Communications Surveys Tutorials, vol. 14, no. 3, pp. 822-835, Third 2012.
[70] H. A. Ngo and L. Hanzo, "Hybrid automatic-repeat-request systems for cooperative wireless communications," IEEE Communications Surveys Tutorials, vol. 16, no. 1, pp. 25-45, First 2014.
[71] G. Kramer, M. Gastpar, and P. Gupta, "Cooperative strategies and capacity theorems for relay networks," IEEE Transactions Information Theory, vol. 51, no. 9, pp. 3037-3063, Sep. 2005.
[72] H. Alves, G. Fraidenraich, R. D. Souza, M. Bennis, and M. Latva-aho,"Performance analysis of full duplex and selective and incremental half duplex relaying schemes," in IEEE Wireless Communications and Networking Conference (WCNC), April 2012, pp. 771-775.
[73] H. Alves, R. D. Souza, and G. Fraidenraich, "Outage, throughput and energy efficiency analysis of some half and full duplex cooperative relaying schemes," Transactions on Emerging

Telecommunications Technologies, 2014.
[74] M. Khafagy, A. Ismail, M. S. Alouini, and S. Aissa, “On the outage performance of full-duplex selective decode-and-forward relaying,” IEEE Communications Letters, vol. 17, no. 6, pp. 1180-1183, June 2013.
[75] Y. Y. Kang, B. Kwak, and J. H. Cho, “An optimal full-duplex AF relay for joint analog and digital domain self-interference cancellation,” IEEE Transactions on Communications, vol. 62, no. 8, pp. 2758-2772, Aug 2014.
[76] Y. Zhu, Y. Xin, and P.-Y. Kam, “Outage probability of Rician fading relay channels,” IEEE Transactions Vehicular Technologies, vol. 57, no. 4, pp. 2648–2652, Jul. 2008.
[77] Y. Zhu, Y. Xin, and P.-Y. Kam, “Optimal transmission strategies for Rayleigh fading relay channels,” IEEE Transactions on Wireless Communications, vol. 7, no. 2, pp. 618-628, feb. 2008.
[78] H. Alves, D. B. da Costa, R. D. Souza, and M. Latva-aho, “Performance of full duplex relaying under co-channel interference and Nakagami-m fading,” in VTC-2015 DUPLO Work., Glasgow, Scotland, April. 2015, pp. 1-5.
[79] D. Moya Osorio, E. Benitez Olivo, H. Alves, J. Santos Filho, and M. Latva-aho, “Exploiting the direct link in full-duplex amplify-and-forward relaying networks,” IEEE Signal Processing Letters, vol. PP,po. 99, pp. 1–1, 2015.
[80] I. Krikidis, H. A. Suraweera, P. J. Smith, and C. Yuen, “Full-duplex relay selection for amplify-and-forward cooperative networks,” IEEE Transactions on Wireless Communications, vol. 11, no. 12, pp. 4381-4393, December 2012.
[81] I. Krikidis, H. A. Suraweera, S. Yang, and K. Berberidis, “Full-duplex relaying over block fading channel: A diversity perspective,” IEEE Transactions on Wireless Communications, vol. 11, no. 12, pp. 4524-4535, December 2012
[82] A. Sabharwal, P. Schniter, D. Guo, D. Bliss, S. Rangarajan, and R. Wichman, “In-Band Full-Duplex Wireless: Challenges and Opportunities,” IEEE Journal on Selected Areas in Communications, vol. 32, no. 9, pp.1637-1652, Sept 2014.
[83] S. Hong, J. Brand, J. Choi, M. Jain, J. Mehlman, S. Katti, and P. Levis, “Applications of self-interference cancellation in 5G and beyond,” IEEE Communications Magazine, vol. 52, no. 2, pp. 114-121, February 2014.
[84] Z. Zhang, X. Chai,K. Long, A.V. Vasilakos, L. Hanzo, "Full duplex techniques for 5G networks: self-interference cancellation, protocol design, and relay selection," Communications Magazine, IEEE , vol.53, no.5, pp.128,137, May 2015
[85] M. Heino, D. Korpi, T. Huusari, E. Antonio-Rodriguez, S. Venkatasubramanian, T.; Riihonen, L. Anttila, C. Icheln, K. Haneda, R. Wichman, M. Valkama, "Recent advances in antenna design and interference cancellation algorithms for in-band full duplex relays," Communications Magazine, IEEE , vol.53, no.5, pp.91,101, May 2015.
[86] D. Kim, H. Lee, D.Hong, “A Survey of In-band Full-duplex Transmission: From the Perspective of PHY and MAC Layers”, IEEE Communications Survey & Tutorials, 2015.
[87] S.Boyd, L. Vandenderghe, Convex Optimization, Cambridge University Press, 2004.
[88] B. Di, S. Bayat, L. Song, and Y. Li, “Radio resource allocation for full-duplex ofdma networks using matching theory,” in IEEE Conference on Computer Communications Workshops (INFOCOM WKSHPS). IEEE, 2014, pp. 197–198.
[89] S. Shao, D. Liu, K. Deng, Z. Pan, and Y. Tang, “Analysis of carrier utilization in full-duplex cellular networks by dividing the co-channel interference region,” IEEE Communications Letters, vol. 18, no. 6, pp. 1043–1046, June 2014.
[90] H.-H. Choi, “On the design of user pairing algorithms in full duplexing wireless cellular networks,” in International Conference on Information and Communication Technology Convergence (ICTC), Oct 2014, pp. 490–495.
[91] A. Sahai, G. Patel, and A. Sabharwal, “Pushing the limits of full-duplex: Design and real-time implementation”, July 2011
[92] R. Ari, T. Kenta, S. Yusuke, B. Masaki, S. Shunsuke, and W. Takashi, “Full duplex media access control by monitoring traffic on adjacent nodes for wireless multi-hop networks”, 2012
[93] K. Tamaki, H. Raptino, Y. Sugiyama, M. Bandai, S. Saruwatari, T. Watanabe et al., “Full duplex media access control for wireless multi-hop networks,” in Vehicular Technology Conference (VTC Spring), 2013